Royal Netherlands
Meteorological Institute
Ministry of Infrastructure and the Environment

Final Report of WP1 of the WTI2017-HB Wind Modelling project

Peter Baas

De Bilt, 2014 | KNMI Scientific Report; WR 2014-02

Royal Netherlands Meteorological Institute
Ministry of Infrastructure and the Environment

Final report of WP1 of the WTI2017-HB Wind Modelling Project

Final

August 2014

Final Report of WP1 of the WTI2017-HB Wind Modelling project

Peter Baas
Royal Netherlands Meteorological Institute

25 August, 2014

Abstract

For the derivation of the Hydraulic Boundary Conditions (HBCs), information on extreme winds over open-water areas is required. To this end, a new method is developed that will answer the need for a description of not only the storm's peak impact but also the spatial and temporal characteristics of extreme storms. The method relies on using high-resolution atmospheric model simulations rather than on using spatial interpolation of sparse point measurements of wind speed. The HARMONIE model, which has a grid spacing of 2.5 km, has been selected to perform the simulations.

The present report is the final report of Work Package 1 (WP1) of the WTI2017 - Wind Modelling project. WP1 describes the assessment of the high-resolution model, in particular the spatial and temporal structures of the modelled wind fields. To this end, HARMONIE simulations of 16 historical storms were performed. Based on a verification with the available wind measurements, we conclude that the wind fields produced by the model are realistic in time and space. The temporal correlation between modelled and observed wind speed is 0.95 over sea. The model represents spatial characteristics of the storms well. Over sea, modelled wind speeds have a positive bias of about 0.5 m/s; for most stations the root mean square (rms) difference is between 1.5 and 2.0 m/s. The bias in wind direction is a few degrees, the rms difference is in the order of 10° for winds of 8 Bft and higher. For these high-wind conditions, modelled wind speeds over Lake IJssel are generally too high. Overall, the modelled wind speeds over the lake are 5-10% higher than observed. Over land, extreme wind speeds are underestimated.

The added-value of high-resolution modelling is most pronounced in coastal areas and for large inland water bodies like Lake IJssel. In those areas, wind and surface-stress values of models with a coarser resolution become less accurate. This is shown in a comparison of HARMONIE wind fields with output from the ERA-Interim model dataset, which has a resolution of approximately 80 km. Storm surge calculations with the WAQUA model indicate that the water levels predicted from HARMONIE output are consistently closer to observed water levels than when output from the much coarser resolution ERA-Interim model is used. To avoid mismatches between drag relations used by the different models, we use the surface stress to drive the WAQUA model rather than the wind speed.

Overall, we rate the model results as good. As such, we conclude that, although at some points further evaluation can be done, the model is suitable to be used as it is in Work Packages 2 and 3 of the Wind Modelling project and that it provides a strong basis for further use in the WTI program.

Keywords
High-resolution modelling, HARMONIE, model evaluation, extreme wind, stability, hydraulic boundary conditions

Executive Summary

General

According to the Dutch Water Act (Waterwet, 2009) the safety of the Dutch primary water defences must be assessed periodically. The water defences must offer protection against water levels and wave conditions at normative conditions, known as Hydraulic Boundary Conditions (HBCs). To obtain reliable HBCs, accurate wind fields are required. To ensure that the quality of the HBCs will meet future needs, Rijkswaterstaat has funded a long-term R&D project, WTI2017-Hydraulics Loads. The goal of the WTI2017-Wind Modelling subproject is to improve on existing methodologies by making use of numerical atmospheric model simulations.

Problem statement and goals

For the determination of the HBCs, information on open-water surface winds is required for driving hydrodynamic models. The presently used wind fields are based on spatial interpolation of point measurements from the network of KNMI wind stations. Unfortunately, most of the measurement locations are located on land. Although the current interpolation methods to convert land-based observations to open-water winds are based on well-established theories, contradictory results were obtained for extreme winds (e.g. Caires *et al.* 2009).

Given the limitations of the applied method, the Hydraulic Review Team advised the use of atmospheric models instead. These models should produce more realistic spatial and temporal patterns since fewer simplifying assumptions are made compared to the current method. The WTI2017-Wind Modelling project was initiated to set up a new method based on high-resolution atmospheric model simulations for estimating extreme surface wind fields. To perform the simulations, the HARMONIE model (www.hirlam.org) was selected. Since 2012 HARMONIE has been used by KNMI for high-resolution weather forecasting. It is run with a grid-spacing of 2.5 km.

The present report is the final report of Work Package 1 (WP1) of the Wind Modelling project. WP1 deals with assessing the high-resolution model with specific attention to the spatial and temporal structures of the modelled wind fields. As such, the aim of this report is to establish how well the high-resolution atmospheric model (i.e. HARMONIE) is capable of simulating realistic (open water) wind fields, including their variations in time and space.

Approach

To gain confidence in the high-resolution wind fields produced by the model, a test-set of 17 historical storms that occurred between 1979-2007 has been composed. Several model experiments were performed to establish the optimal modelling strategy for the purpose of the Wind Modelling project. The resulting model set-up was used to perform hindcasts of the 17 test-set storms. The model results were compared with available

station observations from KNMI, with satellite winds from a scatterometer, and with tall mast observations. Apart from the spatial and temporal evolution of the wind and surface stress fields, the models ability to represent land-water transitions and the influence of atmospheric stability has been examined. The added-value of high-resolution modelling is determined from a comparison with a much coarser atmospheric model. Since the modelled wind and stress fields will be used as input for hydrodynamic models, we also investigate the added value of the high-resolution model for the prediction of storm surges along the coast.

Because HARMONIE is run on finite domain, information on the state of the atmosphere must be provided at the boundaries. To this end, we use the ERA-Interim reanalysis dataset from the ECMWF (European Centre for Medium-Range Weather Forecasts, www.ecmwf.int). The strength of the ERA-Interim data set is that it combines one of the leading numerical weather prediction models (the ECMWF model) with an advanced data assimilation system (Dee *et al.* 2011). The resulting analyses can be considered a best-estimate of the state of the atmosphere given the model information and the observations. The grid-spacing of ERA-Interim is approximately 80 km. ERA-Interim analyses are available from 1979 onwards.

Conclusions

Based on verification with observations, we conclude that the wind fields produced by the HARMONIE model are realistic. Temporal and spatial characteristics of the storms are generally well-captured. Discrepancies with observations are largest for small and quickly developing storm depressions that pass close to The Netherlands.

Over sea, modelled wind speeds show a positive bias of about 0.5 m/s. For most stations, the root mean square (rms) difference between model and observations is between 1.5 and 2.0 m/s. For wind speeds over 17.2 m/s (8 Bft or higher) these values are almost the same. The bias in wind direction is a few degrees, rms differences range from 15° when all data are taken into account to about 10° for winds of 8 Bft and higher. These numbers are rather similar to those derived in operational practice. Note that the error in the observations is about 1 m/s in the wind speed and 10° in wind direction. Bias and rms scores based on satellite winds over open water from Quikscat agree with scores derived from station observations.

Over land, the wind speed bias is mostly close to zero with rms differences between 1.0 and 1.5 m/s. However, for wind speeds over 8 Bft generally a negative bias of about 2 m/s is identified with rms differences varying from 1.5 to 4 m/s. Temporal correlation between modelled and observed wind speed is 0.95 over sea. Spatial characteristics are generally well-captured. Spatial correlation between observations valid at the same time amounts to 0.87 on average. HARMONIE represents spatial gradients in 10-m wind speed between a selection of stations rather well. As over sea, the modelled wind speed over Lake IJssel and the Wadden Sea is higher than observed. This conclusion is based on a comparison of model output with data from measuring locations operated by Rijkswaterstaat. For wind

speeds of 8 Bft and higher, modelled wind speeds over Lake IJssel are 5-10% higher than observed. For the Wadden Sea this difference is 0-5%.

The spatial patterns of the wind speed over Lake IJssel are accurately reproduced by the model. Cross-section of modelled and observed wind speed show that the model reproduces transitions from land to water realistically, including the impact of stability on the near-surface wind speed .

For different areas, the Figure below summarizes the improvement on the wind (reduction of the rms difference between modelled and observed wind speeds and more realistic spatial patterns) by using a high-resolution model like HARMONIE instead of a coarse resolution model product like the ERA-Interim dataset. Because of the much better representation of the land-sea mask, the largest improvement is reached in coastal areas and for large inland water bodies like Lake IJssel. In these areas, wind and surface stress values of ERA-Interim become less accurate due to the coarse resolution. Even smaller water bodies (Frisian Lakes, Veluwse Randmeren, rivers) are too small to be explicitly resolved by the 2.5 x 2.5 km HARMONIE grid.

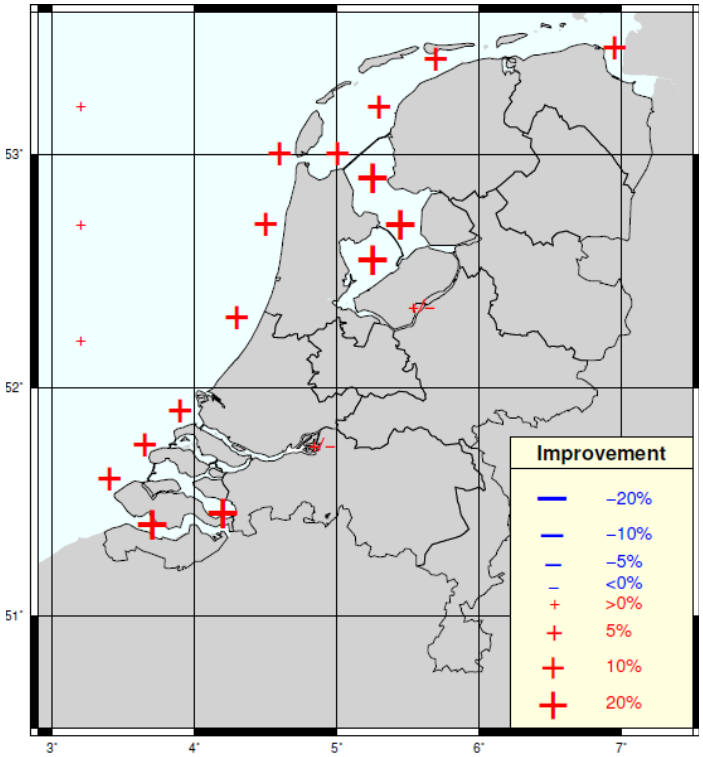

The improvement on the wind by using HARMONIE instead of ERA-Interim for different areas.

Storm surge calculations with the WAQUA model indicate that the water levels predicted with HARMONIE output are consistently closer to observed water levels than when model output from ERA-Interim is used. To avoid mismatches between drag relations used by the different models, we use the surface stress to drive the WAQUA model rather than the wind speed.

Currently applied methods rely on the transformation of wind speeds over land to open water locations by only considering the difference in roughness length. However, here we demonstrate that for westerly winds the observed wind speed ratio between IJmuiden (sea) and Schiphol (land) show a significant daily and yearly cycle. Around noon, this ratio between the wind speed over sea and over land varies by as much as 25% between its minimum in April and its maximum in November. This suggests that the current methodology is prone to errors as it does not take into account variations in atmospheric stability. Observed IJmuiden to Schiphol wind speed ratios were compared to those produced by HARMONIE and by a simple two-layer model (2LM). The agreement between HARMONIE and the measurements is better than the agreement between 2LM and the measurements.

Overall, we rate the model results as good. As such, we conclude that, although at some points further evaluation can be done, the model is suitable to be used as it is in Work Packages 2 and 3 of the Wind Modelling project and that it provides a strong basis for further use in the WTI program.

Recommendations

To establish the value of the high-resolution model for the determination of the HBCs in more detail, we suggest the following:

- The HARMONIE model is suitable to be used as it is in Work Packages 2 and 3 of the Wind Modelling project. It provides a solid basis for further work.
- When using the HARMONIE wind fields to drive hydrodynamical models, special attention should be paid to the consequences of the overestimation of the wind speed over Lake IJssel.
- By means of a statistical upscaling technique, HARMONIE wind fields will be transformed to the normative conditions that are needed for deriving the hydraulic boundary conditions. In the end-phase of the project a comparison of the thus obtained wind fields with those derived from the current practice of interpolating point measurements is needed.
- The underestimation of extreme wind speeds over land remains an intriguing topic for further research. Model development, focusing on the representation of the boundary layer and the air-surface interaction, is needed to better understand the causes of this general model problem.
- In many cases, differences exist in the modelling of the air-sea interaction of hydro-dynamic models and atmospheric models that are used to drive those. This mismatch may lead to ambiguous results. It would be more consistent to drive the hydro-dynamic models with the surface-stress of the atmospheric models rather than with the 10-m wind. In the end, we advocate the use of coupled models in which the interaction between the atmosphere and the water surface is explicitly taken into account.

Contents

1 Introduction

In compliance with the Dutch Water Act (Waterwet, 2009) the strength of the Dutch primary water defences must be assessed periodically[1] for the required level of protection, which, depending on the area, may vary from 250 to 10000 year loads; see Figure 1.1. These loads are determined on the basis of Hydraulic Boundary Conditions (HBC).

The HBC and the Safety Assessment Regulation ("Voorschrift op Toetsen op Veiligheid", VTV), play the crucial role in the assessment of the primary water defences. Until 2011, the safety assessment was based on the failure probability of a dike section. In the future, assessments will be based on the probability of flooding of a dike ring, or dike ring trajectories. The corresponding normative return periods still have to be established. This means that not only the values in Figure 1.1 will change, but also the interpretation of the normative values. These will be related to probabilities of failure, rather than to the probability of exceedance of hydraulic loads as in the present methodology. The knowledge underlying the presently available HBC and VTV will be incorporated in the new instrumentation to assess the safety of dike rings, or at least parts of a dike ring. Most probably the new instrumentation will be Hydra-Ring.

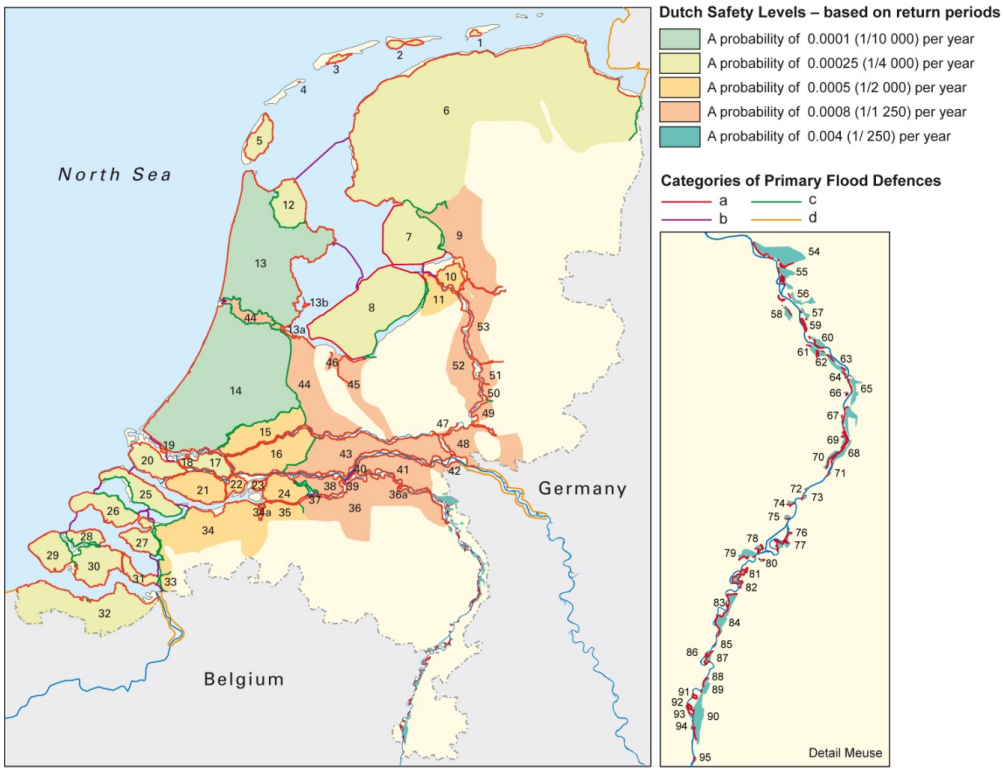

Figure 1.1. The safety standards of the Dutch primary water defences.

[1] Previous assessments took place in 1996, 2001 and 2006. The date of the next assessment is 2017 and for the period after 2017 the assessment will be on a continuous basis.

1.1 WTI 2017

With the aim of delivering legal assessment instruments for the fourth assessment period, starting in 2017, *Rijkswaterstaat – Dienst Water, Verkeer en Leefomgeving* is funding the long-term project WTI 2017. The WTI ("*Wettelijk Toets Instrumentarium*": legal assessment instruments) project provides the HBC and other necessary instruments for the assessment of the primary sea defences. Insights have changed over the years and many developments have triggered improvements to the instrumentation. The research project Strengths and Loads of Water Defences ("*Sterkte en Belastingen Waterkeringen*", SBW) started ten years ago with the aim to provide expertise and instruments for WTI.

1.2 WTI2017-Wind Modelling

To obtain reliable HBCs, accurate (especially open-water) wind fields are required. Recently, following the advice of the Hydraulic Review Team, the KNMI-Deltares "WTI2017-Wind Modelling" project was initiated to set up a new method based on high-resolution atmospheric model simulations for estimating extreme surface wind fields. An overview of the WTI2017-Wind Modelling project is given in Groeneweg *et al.* (2011; 2012a).

The project is divided into three Work Packages:

1. Assessment of how well high-resolution atmospheric models can represent storm wind fields, including their spatial and temporal characteristics.
2. Production of a long-term (of the order of 30 years) storm dataset that can be used for deriving the extreme wind statistics needed for the determination of HBC.
3. Extreme value analysis of the surface wind and stress fields, including a proper time and space dependence.

The present report is the final report of Work Package 1 (WP1) of the Wind Modelling project, summarizing all relevant findings and conclusions of the interim reports that have been published before. WP1 deals with assessing the high-resolution model including the spatial and temporal structures of the modelled wind fields. Before a decision whether to use the new method can be made, it is important to gain confidence in the new method, and to establish how the results of the new method relate to current practice. This is done by simulating a suite of historical storm periods and comparing the high-resolution model results with available observations. In WP1 the following activities have been defined (Groeneweg *et al.* 2011, 2012a):

1. Set-up of the high-resolution model;
2. Identification, description and high-resolution modelling of a test-set of relevant historical storms;
3. Evaluation of the model results with available measurements;
4. Investigation of the added-value of the high-resolution model in view of determining hydraulic loads;

5. Comparison of storm wind fields from model simulations with storm wind fields from interpolating measurements.

Here we report on the results and conclusions of each of these activities. Most of the presented material has been published before in one of the WP1 Interim Reports (Groen and Caires, 2011; Baas and De Waal, 2012; Van den Brink *et al.* 2013; Baas, 2013; Baas and Van den Brink, 2014). In addition, relevant new results will be presented, for example, a first verification of the long-term 'production runs' that are performed in Work Package 2.

1.3 Motivation

Current methodologies to derive open-water wind fields at normative conditions rely on spatial interpolation of point measurements from the network of KNMI wind stations (De Waal, 2010; Lopez de la Cruz *et al.* 2010). Unfortunately, most of the measurement locations are located on land. Although the methods to convert land-based observations to open-water winds are based on well-established theories, the following drawbacks have been identified:

- For many water systems the extreme wind fields are uniform in space or with a fixed spatial gradient.
- For several water systems the temporal evolution of storm events is neglected. For other water systems it is included, albeit strongly schematized.
- Sufficiently long observational records are virtually absent.
- For extreme wind speeds contradictory results were obtained (e.g. Caires *et al.* 2009).

To improve on existing methodologies, we explore the use of an atmospheric model (cf. Tammelin *et al.* 2011; Weisse *et al.* 2009). Such a model should produce more realistic spatial and temporal patterns since fewer simplifying assumptions are made compared to the current practice of spatial extrapolation of point measurements. This facilitates the wish to include time-dependency in the calculations on failure mechanisms.

In this report we make use of the ERA-Interim dataset from the European Centre of Medium-Range Weather Forecasting (ECMWF, www.ecmwf.int). The ERA-Interim data set combines one of the leading numerical weather prediction models (the ECMWF model) with an advanced data assimilation system (Dee *et al.* 2011). The resulting global analyses can be considered a best-estimate of the state of the atmosphere given the model information and the observations. However, with a resolution of approximately 80 km, the ERA-Interim model itself is too coarse for our application. For example, coastal water bodies like Lake IJssel and the Wadden Sea are not resolved at all.

Instead, we apply dynamical downscaling of the ERA-Interim dataset using the high-resolution HARMONIE model. Since 2012, HARMONIE has been used by KNMI for weather forecasting. It is run with a grid-spacing of 2.5 km. Dynamical downscaling of a coarse resolution model by using a model with a much finer resolution is frequently

applied in the literature, for example in Frank and Majewski (2006), Reistad *et al.* (2011), Winterfeldt and Weisse (2009), Winterfeldt *et al.* (2010) and Feser *et al.* (2011).

Before HARMONIE wind fields can be used as a basis for estimating extreme winds with return periods of up to 10,000 years (Groeneweg *et al.* 2012b), an assessment has to be made of the quality of the modelled wind fields in observed extreme conditions. As such, the present report provides a comprehensive verification of the model simulations of 17 historical storms against observations. Since most of the knowledge gaps in the various techniques and methods that are needed to derive the HBC are related to the 'time' and 'space' dimension, special emphasis is given to the temporal and spatial characteristics of the storms.

1.4 Objectives

The aim of this report is to establish how well the high-resolution HARMONIE model represents storm wind fields, including their variations in time and space. By hindcasting historical storm periods and comparing the model results with available observations, an assessment is made of the quality of the modelled wind fields. A brief analysis of predicted water levels along the Dutch coast is added to ensure the quality of the intermediate steps between the atmospheric model and the output of the hydrodynamic model(s).

Specific objectives of this report include:

- Document the set-up of the high-resolution model
- Validate simulated wind fields of a test-set of selected historical storms against observations, with special focus on the spatial and temporal characteristics of the storms.
- Document the model's ability to represent land-water transitions. Special attention will be given to the representation of Lake IJssel.
- Document the model's ability to capture the influence of atmospheric stability on surface wind fields.
- Assess the added-value of the modelled wind and stress fields of the high-resolution model versus a much coarser model.
- Identify possible situations in which the model behaves problematically.
- Document how modelled sea-to-land wind speed ratios relate to those obtained from a simple two-layer model.
- Assess the predicted water levels along the Dutch coast when using output from the high-resolution atmospheric model.

1.5 Criteria

The HARMONIE wind fields should meet the following criteria:

- In contrast to the presently used wind fields, they should have realistic temporal and spatial patterns.

- Bias and root mean square difference should be comparable to those obtained in operational weather forecasting practice. This seems a sensible criterion, since wind fields produced by operational models give satisfactory results when used to drive hydrodynamic models.
- Water levels obtained from WAQUA simulations driven by HARMONIE output should be closer to observed water levels than water levels from WAQUA simulations driven by ERA-Interim output.

1.6 Report outline

Section 2 provides details on the HARMONIE high-resolution model and describes the model set-up. Section 3 gives an overview of the simulated storm periods. Section 4 assesses the quality of the HARMONIE wind fields in a comparison to available observations. Section 5 discusses the added-value of the high-resolution model wind and stress fields in comparison to a much coarser atmospheric model. Section 6 compares sea to land wind speed ratios derived from HARMONIE model output and from a simple two-layer model. Conclusions and recommendations are presented in Section 7.

1.7 Acknowledgements

I thank my KNMI colleagues Henk van den Brink, Reinout Boers, Fred Bosveld, Ine Wijnant, Jan Barkmeijer, and Gerrit Burgers for their support, the discussions we had and their constructive comments on this report. Also thanks to Sofia Caires, Hans de Waal, Jacco Groeneweg, and Joana van Nieuwkoop from Deltares for the fruitful discussions during our KNMI-Deltares progress meetings and for carefully reading earlier versions of this report.

Jur Vogelzang and Ad Stoffelen from the KNMI satellite wind group are acknowledged for the discussions on the use of scatterometer data and for making these data available for a selection of the storms studied in this report.

The Bundesambt für Seeschifffahrt und Hydrographie is acknowledged for providing data from the FINO measurement tower in the North Sea.

Observations from Lake IJssel and the Wadden Sea were kindly provided by Hans Miedema (Rijswaterstaat).

Han Dolman (VU University) is acknowledged for reviewing our work.

2 Set up of the high-resolution model

This Section is based on the report 'Towards an approved model set-up for HARMONIE' by Van den Brink *et al.* (2013).

2.1 The HARMONIE model

HARMONIE (HIRLAM ALADIN Research On Mesoscale Operational NWP in Euromed) is the operational Numerical Weather Prediction model of KNMI. It is a limited-area model, that has been developed in a consortium involving many European countries. HARMONIE is the successor of the HIRLAM and the ALADIN models. Major differences are that HARMONIE is intended to run on a very high resolution (typically with a grid spacing of 2.5 km) and that is a so-called non-hydrostatic model. The latter means that instead of employing the hydrostatic approximation, which often breaks down in severe-weather events, the vertical momentum equation is solved explicitly. The HIRLAM-ALADIN consortium has extensively tested the model. HARMONIE is also known as the AROME model. More details on HARMONIE / AROME are given by Seity *et al.* (2011), see also the documentation on www.hirlam.org.

The interactions between the atmosphere and the surface and soil processes are handled by the SURFEX model (Le Moigne, 2012). Among others, this involves the calculation of the fluxes at the air-surface interface, which serve as lower boundary condition for the atmospheric part of the model. The stress parameterizations over sea is discussed separately in Section 2.2. Part of SURFEX is the 1-D column model CANOPY, which aims for a more accurate coupling between the atmosphere and the surface (Masson and Seity, 2009). This is done by adding 6 additional levels between the lowest model level and the surface. In fact the surface scheme is driven by the lowest level of the CANOPY model (i.e. 0.5 m) instead of by the lowest level of the atmospheric model (10 m). Over land, the impact of canopy on the air in the surface layer is explicitly modelled. In case of very large vertical gradients of wind and temperature the CANOPY model has a beneficial effect. Over sea, the impact of the model is generally small.

Here, we use HARMONIE CY37h1.1 that was released at 13 June 2012.

2.2 Surface-drag modelling over water

HARMONIE makes a distinction between 'sea' and 'inland water bodies'. The latter includes lakes and rivers. First, we review the drag formulation over sea. The interaction between the sea surface and the atmosphere is calculated by the Exchange Coefficients from Unified Multi-campaigns Estimates (ECUME) module. Being part of the SURFEX model, ECUME is a bulk iterative parameterization developed in order to obtain optimal exchange coefficients for a wide range of atmospheric and oceanic conditions (Weill *et al.* 2003). ECUME is based on the ALBATROS database that consists of data from five flux measurement campaigns. From this database, the relation between the 10-m wind and

the surface fluxes was derived. The observations cover a wide range of atmospheric conditions in terms of atmospheric stability and wind speed (up to 29 m/s). In ECUME, the drag coefficient for momentum is calculated directly from the 10-m wind speed using a fourth-order ordinary polynomial. ECUME drag relation flattens off for wind speeds over 30 m/s. This a more realistic behaviour than obtained in the traditional Charnock formulation (Charnock, 1955), where the drag continuously increases even for very high wind speeds. The effect of atmospheric stability is included using Monin-Obukhov similarity theory.

The left-hand side of Figure 2.1 presents the drag relation modelled by HARMONIE using the default ECUME settings, that is used in the SBW Wind Modelling project. For reference, the solid red lines indicate three versions of the well-known Charnock relation with different Charnock constants (complemented with viscous effects for low wind speeds). For wind speeds between 15 and 30 m/s the ECUME relation corresponds to a Charnock relation with a Charnock constant of approximately 0.020. For comparison, the right-hand side of Figure 2.1 presents the drag relation that is used in the ERA-Interim reanalysis dataset of ECMWF. Especially for high wind speeds, the modelled drag coefficients are substantially higher than in the case of HARMONIE. The impact of this difference is discussed in Section 5.

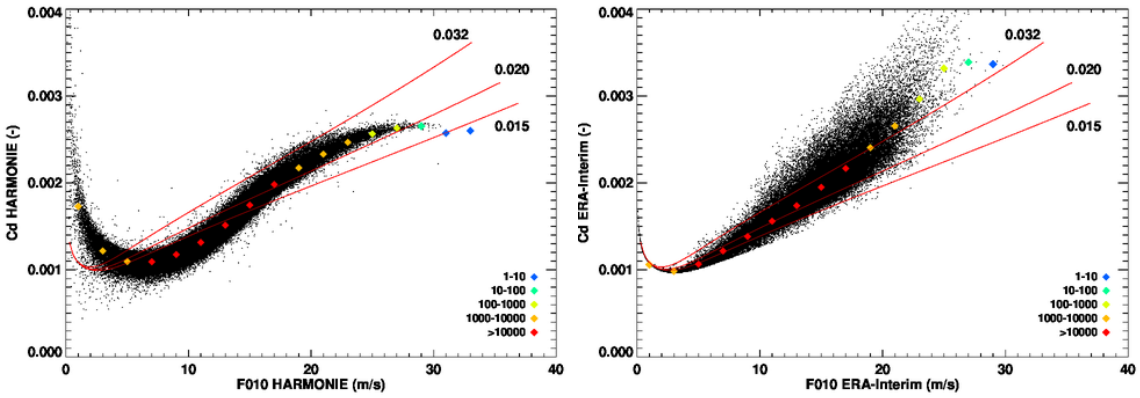

Figure 2.1. The drag relation used by HARMONIE (left) and ERA-Interim (right) over sea. The solid lines indicate a Charnock relation with Charnock parameters of 0.015, 0.020, and 0.032. Diamonds indicate average values for 2 m/s bins. Colours indicate the number of points for each bin.

For the 'inland waters bodies' (e.g. the Lake IJssel), HARMONIE uses a Charnock formulation by default. The value of the Charnock constant is set to 0.015. These setting are adopted in the SBW Wind Modelling project.

For details on the HARMONIE drag modelling over land can we refer to Van den Brink *et al.* (2013).

2.3 Grid configuration and domain

HARMONIE runs on a regular grid with a grid spacing of 2.5 km. The vertical grid contains 60 levels, 15 of which are located below 1000 m of height. The lowest model levels are located at about 10, 30, 60, 90, 130, 180, and 240 m above ground level.

HARMONIE is a limited-area model, meaning that is covers only a part of the globe. As such, before starting a simulation, a suitable domain must be selected. We use a domain size of 500 x 500 grid point (1250 x 1250 km), centred at 54°N 2°E (domain B in Figure 2.2). Sensitivity tests with two other domain configurations were performed. Van den Brink *et al.* (2013) show that wind and pressure fields are best represented when using domain B. An important part of the hydraulic boundary conditions are related to large surges at the Dutch coast. These large surges are caused by North-Westerly winds over the North Sea, implying a northerly track of the depressions. These northerly depressions are better captured by domain B than by domains A and C. This is because the centre of the depression is within the HARMONIE domain during the timespan of high winds over The Netherlands. For the more southerly storm tracks, domains A and B behave similarly (not shown).

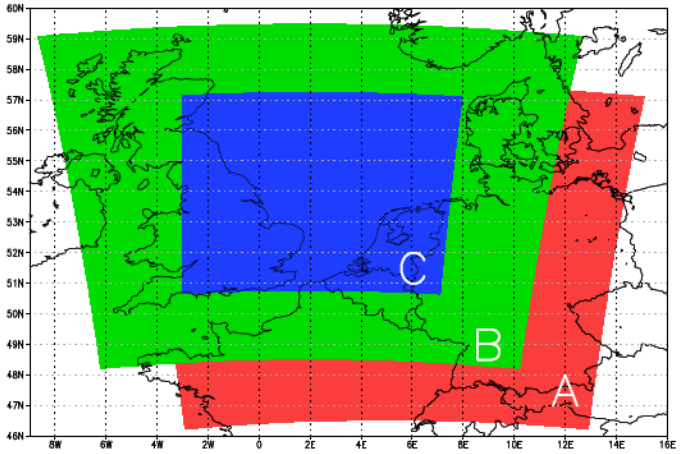

Figure 2.2. Overview of tested HARMONIE domains. Domain B is selected for use in the Wind Modelling project.

2.4 Boundary Conditions and ERA-Interim

Because HARMONIE is run on finite domain, information on the state of the atmosphere must be provided at the boundaries. The lateral boundary conditions are provided by the ERA-Interim reanalysis dataset from the ECMWF (European Centre for Medium-Range Weather Forecasts, www.ecmwf.int). The strength of the ERA-Interim data set is that it combines one of the leading numerical weather prediction models (the ECMWF model) with an advanced data assimilation system (Dee *et al.* 2011). The resulting analyses can be considered a best-estimate of the state of the atmosphere given the model information and the observations. ERA-Interim comprises a full 3D analyses of the global atmosphere

at a spectral resolution T255, corresponding to a grid resolution of approximately 80 km. The data set that has been used for the HARMONIE runs was sampled at 0.5°. The temporal resolution of the ERA-Interim analyses is 6 h. ERA-Interim analyses are available from 1979 onwards.

While HARMONIE uses the ECUME drag relation, ERA-Interim applies the well-known Charnock relation (Charnock, 1955) complemented with viscous effects for low wind speeds,

$$z_0 = \alpha \frac{u_*^2}{g} + 0.11 \frac{\upsilon}{u_*}, \qquad (2.1)$$

with z_0 the roughness length, u_* the friction velocity, g the acceleration due to gravity, ν the kinematic viscosity of air, and α the Charnock constant. However, in ERA-Interim the value of α is not constant but it is a function of the sea state (Bidlot *et al.* 2007), which is determined by the underlying wave model. The resulting drag relation is show in the right panel of Figure 2.1. For increasing wind speeds, the Charnock constant becomes larger.

Starting from each available ERA-Interim analysis (at 0, 6, 12, and 18 UTC) a forecast is performed with HARMONIE. Initial condition of the atmosphere and the surface are prescribed from the ERA-Interim analysis. The model time-step is 1 minute.

2.5 Spin-up

Every 6 h a new HARMONIE simulation is started, initialized from the ERA-Interim analysis. At the start of each simulation, the model fields consist of ERA-Interim fields which are interpolated to the HARMONIE grid. Consequently, small-scale structures are lacking: the HARMONIE model needs some spin-up time in order to reach a new equilibrium and to develop its own structures. Van den Brink *et al.* (2013) demonstrate that small-scale structures over water need 5-10 hours to develop, although the majority is already present after 1 hour. However, shorter spin-up times give better comparisons with wind and pressure observations. They found the best match for a 1 hour spin-up time. Therefore, this was chosen as an appropriate spin-up time. As the model output frequency is one hour, an individual forecast length of 6 hours is needed. Longer time-series are obtained by concatenating the output from the +1 to the +6h lead times of consecutive runs.

2.6 Model output

The model output frequency is once per hour. The provided fields represent the model state at the indicated hour for the complete HARMONIE domain.

Table 2.1 presents the list of variables that have been archived. Besides surface winds and pressure fields, also variables that are needed for the calculation of the drag

coefficient or the atmospheric stability are stored (e.g. T at various levels and H, see Table 2.1 for the abbreviations). For surface stress, both instantaneous fields and accumulated fields[2] are stored. The latter provides an integrated measure of the stress that also includes sub-hourly variations.

The variables that define the thermodynamic state of the atmosphere, i.e. u, v, T and q, are stored at multiple levels. The selected levels are listed in Table 2.2. The dense sampling close to the surface allows a comparison with atmospheric masts (e.g. FINO, OWEZ, Cabauw). These data can also be used to study internal boundary layer development, for instance in the vicinity of land-sea transitions. The thermodynamic fields are also stored at few typical pressure levels higher-up in the atmosphere that are frequently used in meteorology. These can be relevant for distinguishing between air masses or for analysing the synoptic development of storm depressions. The 850, 500 and 300 hPa levels are approximately located at 1500, 5000 and 7000 m above the surface, respectively.

Table 2.1. Overview of output variables. For variables indicated with an asterisk, multiple level output is provided.

Variable name	**Symbol**	**Units**
Mean sea level pressure	*mslp*	Pa
Surface pressure	p_s	Pa
Pressure * (only at z levels)	p	Pa
Geopotential height * (only at p levels)	Φ	m
Zonal wind speed *	u	m / s
Meridional wind speed *	v	m / s
10m Gust speed	f_{max}	m / s
Temperature *	T	K
Surface temperature	T_0	K
2m Temperature	T_{2m}	K
Specific humidity *	q	kg / kg
2m Specific humidity	q_{2m}	kg / kg
Zonal surface stress	τ_x	kg / (m s^2)
Meridional surface stress	τ_y	kg / (m s^2)
Accumulated zonal surface stress	$\sum\tau_x$	kg / (m s)
Accumulated meridional surface stress	$\sum\tau_y$	kg / (m s)
Sensible heat flux	H	W / m^2
Latent heat flux	LvE	W / m^2
Boundary layer height	h	m
Precipitation intensity	P	kg / (m^2 s)
Accumulated precipitation	$\sum P$	kg / m^2

[2] Accumulated fields represent the sum over all preceding time steps of a hindcast run for a particular variable. For example, for precipitation the accumulated fields represent the total amount of rain that has fallen from the start of a hindcast run to the indicated hour. Hourly values can be obtained by subtracting values from subsequent hours. The same is true for surface stress.

Table 2.2. Vertical levels at which *u*, *v*, *T* and *q* are stored. P is stored at height levels, Φ at pressure levels.

Height (m)										**Pressure levels (hPa)**		
10	20	40	60	80	100	150	200	500	1000	850	500	300

2.7 Model simulations

In order to assess the quality of the HARMONIE wind fields, Groen and Caires (2011) composed a test-set of 17 historical storms (Section 3). Most results presented in this report are based on model simulations of these storms. Generally, the HARMONIE simulations start 4 days ahead of the main event and continue to two days after the main event.

In the framework of Work Package 2 of the Wind Modelling project, long-term production runs are being produced with HARMONIE that can be used for deriving the extreme wind statistics needed for the determination of HBC. These simulations consist of the 20% most relevant days of the period 1979-2013 including the full year of 2007. The strategy for selecting the most relevant events is described in Van den Brink (2014). In this report we present a first analysis of the available simulations to confirm that their quality is similar to that of the test-set storms.

3 Selection of the test-set storms

The quality of the HARMONIE wind and stress fields is assessed using simulations from a test-set of historical storms, which were selected and described by Groen and Caires (2011). In this Section we summarize their selection procedure and give an overview of the selected storms.

3.1 Selection procedure

The ERA-Interim dataset, which is used a boundary conditions for the HARMONIE simulations, is available from 1979 onwards. This defines the period from which the storms can be chosen.

The following criteria have been defined to select approximately 15 storms to be simulated by HARMONIE. For a proper evaluation, the test-set should contain sufficient variety in storm characteristics.

The entire set of selected storms should:

- Be relevant in terms of hydraulic loads (waves and water level at each water system). I.e., storms that result in extreme hydraulic loads.
- Contain high wind speeds from different sectors.
- Contain a range of stability characteristics above land and water.
- Consist of a range of small to large storms.
- Consist of a range of slowly to rapidly moving storms.
- Consist of a range of paths followed by storms.
- Contain variety in season (stability, land roughness).
- Contain variety in the role/presence of fronts in the weather system.

In order to select storms according to these criteria, wind, wave and water level measurements available to the WTI project were used. As such, an inventory of the storms was made yielding the highest three (independent) peaks of

1. U_p: potential wind speed at each of the 21 KNMI wind stations for which long term measurements are available,
2. SWH: significant wave height measured by the nine North Sea buoys,
3. SWL: still water level, and
4. Surge (=skew high water offset): surge measured at six locations along the coast.

This procedure yielded a list of 28 storms. To ensure the presence of at least one storm for every wind direction, which is especially relevant in terms of hydraulic loads in Lake IJssel, the storms with the highest potential wind speed values for each 30° directional sector at Schiphol were inventoried. This yielded 6 additional potential storm events.

By expert judgement of the KNMI and Deltares team members, the list of 34 storms was reduced to 15 storms. The storm of 31 January 1953 was added for historical reasons (although it is not included in the ERA-Interim dataset), the storm of 28 May 2000 for its

impact on Lake IJssel. Thus, in total 17 storms were selected to be simulated with HARMONIE.

3.2 The test-set of 17 historical storms

The resulting list of 17 selected storms includes a large variation in relevant characteristics: from small to large, from slow to fast moving, includes almost all wind directions, sometimes with rapid shifts in time of wind speed and wind direction and with variations in atmospheric stability during several seasons. Four examples are given in Figure 3.1. A list of the 17 storms with their characteristics is provided in Table 3.1. The list of selected 17 storms aims at providing an optimal combination of the defined hydraulic and meteorological criteria, tries to avoid duplication of similar situations and aims at covering the broad range of events. The resulting test-set of storms provides a good basis for the validation of the HARMONIE model wind fields.

Table 3.1. Overview of simulated storms (adopted from Groen and Caires (2011), their Table 3.1). Columns show case numbers (1), dates of the main storm events (2), the maximum potential wind speed (3), the number of locations (out of 21) for which the event is ranked in the top-3 in terms of potential wind speed and hydraulic parameters (4), the prevailing wind direction (5), the width of the major wind field (6), the length of the major wind field (7), the displacement of the storm centre in 24 hours (8), the estimated change in the 850 hPa temperature (9), and a yes/no indication of the passage of frontal system or trough with a marked shift in wind (direction and/or speed) around the main event (10). The last two columns indicate the start date and end date of the HARMONIE simulations.

Nr.	Max. wind date	Max. U_p (m/s)	Nr. U_p/ Nr. Hydr. peaks	Sector	Grad. width (° lat)	Field length (° lat)	Track (° lat)	Delta T850 (°C)	Shift (Y/N)	Hindcast start date	Hindcast end date
1	1953 02 01	25.7	not available	NNW	8	20	8	10	Y	1953 01 26	1953 02 04
2	1979 02 14	24.7	1/0	ENE	5	12	5	5	N	1979 02 10	1979 02 17
3	1983 02 01	24.1	1/4	SW-NW	10	13	10	2	Y	1983 01 27	1983 02 04
4	1983 11 27	24.6	7/0	SW-NW	5	20	11	6	Y	1983 11 23	1983 11 29
5	1984 01 14	26.3	4/0	SW-WNW	16	30	16	5	Y	1984 01 10	1984 01 19
6	1989 02 14	19.3	0/5	NW	7	10	10	3	N	1989 02 10	1989 02 17
7	1990 01 25	27.0	17/2	SW	9	25	15	12	Y	1990 01 21	1990 02 03
8	1990 02 26	24.9	4/4	W-NW	20	25	16	5	Y	1990 02 22	1990 03 02
9	1990 12 12	20.4	0/7	S-NW	5	10	11	4	Y	1990 12 07	1990 12 14
10	1993 11 14	22.5	0/5	SW-NW	4	7	8	5	Y	1993 11 10	1993 11 16
11	1994 01 28	19.4	0/6	NW	7	15	11	5–12	N(5)-Y(12)	1994 01 24	1994 01 30
12	1996 02 19	14.5*	0/0	NE	13	25	12	5	Y	1996 02 15	1996 02 22
13	2000 05 28	22.7	0/0	W	10	20	9	7	Y	2000 05 24	2000 05 30
14	2002 10 27	25.7	12/2	SW-NW	10	10	10	10	Y	2002 10 23	2002 10 29
15	2006 11 01	22.1	0/6	NW-W	12	16	11	14	Y	2006 10 28	2006 11 03
16	2007 01 18	23.5	6/0	SSW-NW	6	25	6	2	Y	2007 01 10	2007 01 20
17	2007 11 09	18.7	0/8	NW	6	25	6	5	N	2007 11 05	2007 11 11

The reasoning for the selection of these particular storms was as follows:

1. The 1953, 1990 (both January and February), 2002, 2006 and 2007 (November) storms were chosen for their relevance in terms of hydraulic loads (resp. numbers 1, 7, 8, 14 and 17).
2. The May 2000 storm for its effect in Lake IJssel (number 13).
3. The 1979 and 1996 storms for their apparent (north-)eastern characteristics. The 1993 storm also due to its directional changes in time, including a period of strong northeasterly wind.

The remaining storms all had at least four peaks in terms of wind, wave or water level.

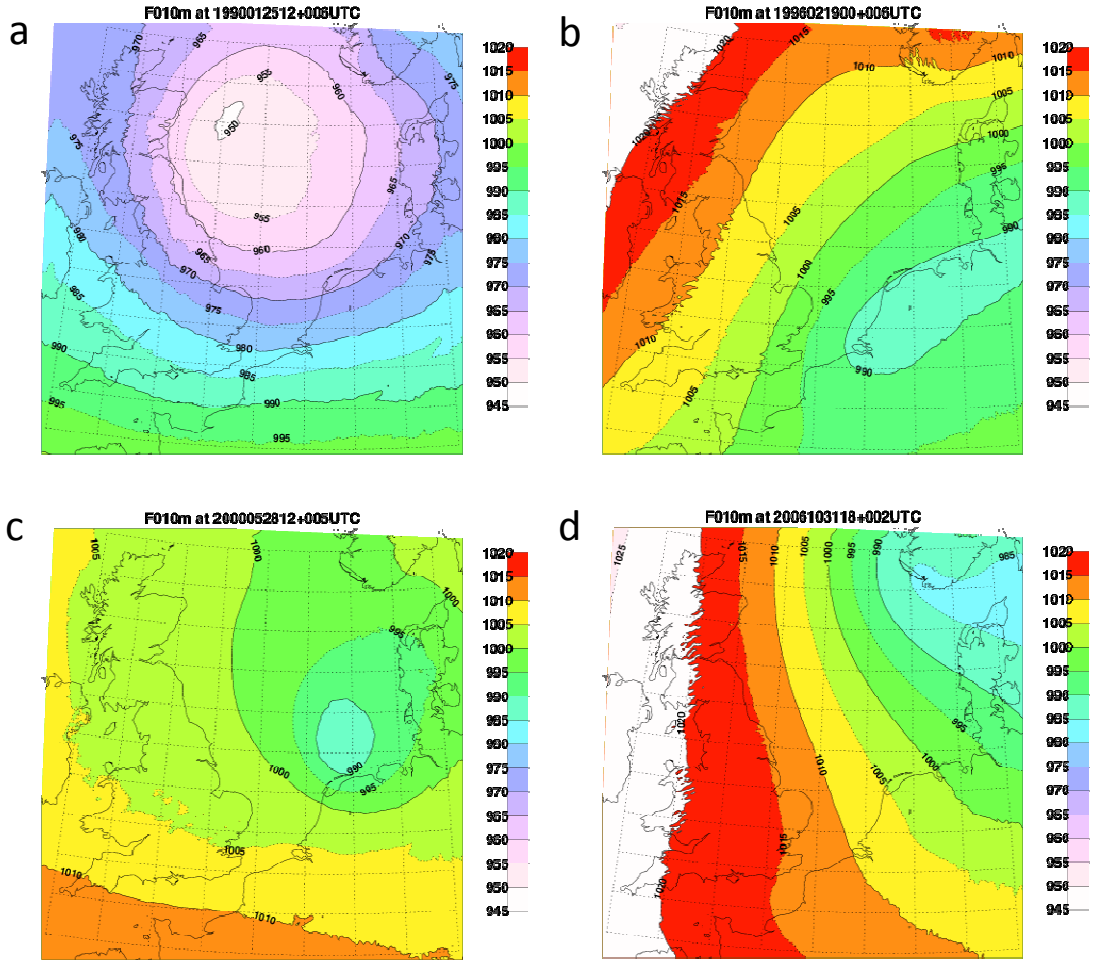

Figure 3.1. Examples of four different storm types. a) Baroclinic wave in the polar front, b) Strong easterly wind in a southward moving through, c) Small, quickly developing secondary low, d) Cold-air development causing a long NW fetch over the North-Sea. The Figures show the mean sea level pressure in hPa.

4 Evaluation of HARMONIE wind fields

Baas (2013) presented a comprehensive evaluation of HARMONIE simulation of the test-set storms with available observations. The most important results and conclusions will be reproduced here. As motivated in Baas (2013), the 1953 storm is left out of the evaluation study, mainly because of observational issues. As such, the evaluation of the wind fields is based on 16 storm events.

In the meantime, the long-term HARMONIE simulations have become available. In this Section we also present a first evaluation of these production runs to ensure that their quality is the same as the model simulations of the test-set storms.

4.1 Observations

4.1.1 KNMI stations

The cornerstone of the evaluation are the observations made at the operational network of KNMI stations. The station locations are indicated in Figure 4.1. Data availability varies between the stations. For each of the 16 storms of the test-set, APPENDIX A indicates for which stations data are available. Per storm, the number of available stations increases from 15 in 1979 to over 50 for the most recent storms.

For the evaluation, data from the KNMI climatological database have been used. Detailed information on measurement systems, procedures and algorithms can be found in the *Handboek Waarnemingen* (Royal Netherlands Meteorological Institute, 2001). For wind speed, the hourly averaged values are archived, together with the average over the last 10 minutes of each hour and the maximum (3 second average) gust that occurred during the hour. For wind direction, the 10-minute average before the whole hour is archived. Since 1995, 10-minute averaged data are available for some stations, since 2003 for almost all stations (Wever and Groen, 2009). The present evaluation is based on hourly averaged observations, which are, as a matter of course, subjected to a manual quality control which includes filling of gaps.

Until 1 July 1996, wind speed observations were archived in discrete knots (1 knot = 0.514 m/s). Since then, data have been archived in discrete m/s. The standard data accuracy is about 1 m/s, but for some non-standard measuring sites, e.g. at oil platforms, and for some periods the accuracy may be lower due to flow distortions (see Verkaik (2001) and references therein).

WMO regulations require that wind observations must be performed above short grass (if over land), in open terrain, and at a height of 10 m above the surface. While most measurement locations above land meet these criteria, most stations over sea and some coastal stations measure at a different height. Non-standard measuring heights are indicated in APPENDIX A. In accordance with standard KNMI practice, we use the Benschop correction to convert wind speeds from non-standard heights to the 10-m level (Benschop, 1996). The Benschop correction transforms the observed wind at the

measurement height to the reference 10-m level using a logarithmic wind profile and the local roughness. Offshore, a fixed roughness length of 0.0016 m is used to calculate the Benschop correction. This value originates from applying a Charnock relation with a Charnock constant of 0.032 and a 10-m wind of 15 m/s (Benschop, 1996). As demonstrated in APPENDIX B, for our purposes application of the Benschop correction is justified. Associated errors are comparable in size to the errors in the observations.

For temperature, humidity, and pressure the hourly values represent 1-minute averaged values before the whole hour.

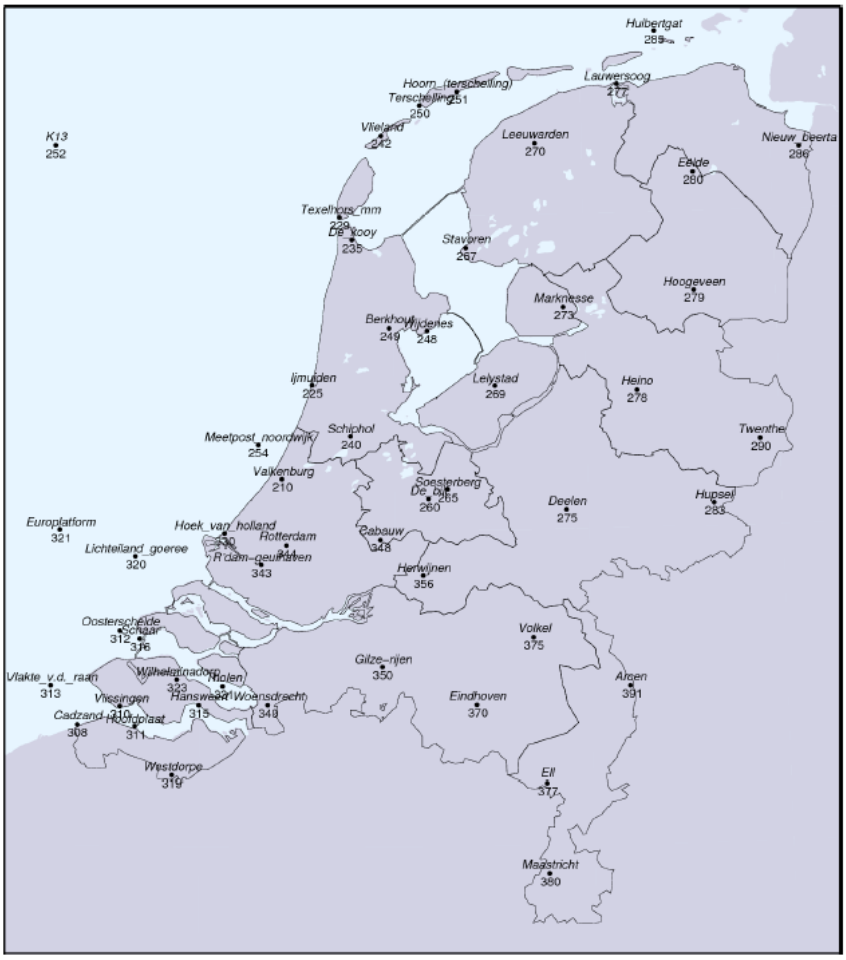

Figure 4.1. Locations of KNMI wind measurement sites (from Wever and Groen, 2009). Numbers indicate station codes. Not shown are the remote platforms F3 (239) and AUK-Alfa (253).

4.1.2 RWS measuring locations

In 1997, Rijkswaterstaat (RWS) started an extensive wind and wave measuring campaign in Lake IJssel and Lake Sloten. In this report, we use wind observations of several

measuring sites. Detailed information about the measuring instruments can be found in Bottema (2007). In 2010, the network of observation was extended with several location in the Northern part of Lake IJssel. In 2008, a measurement program in the Wadden Sea was set-up. The locations of the RWS sites are given in Figure 4.2, data availability for each station is indicated in Figure 4.3. The measurement height for all these stations is 10 m above the (slightly varying) water level. For consistency with the KNMI stations described above, we use hourly averaged values of wind speed.

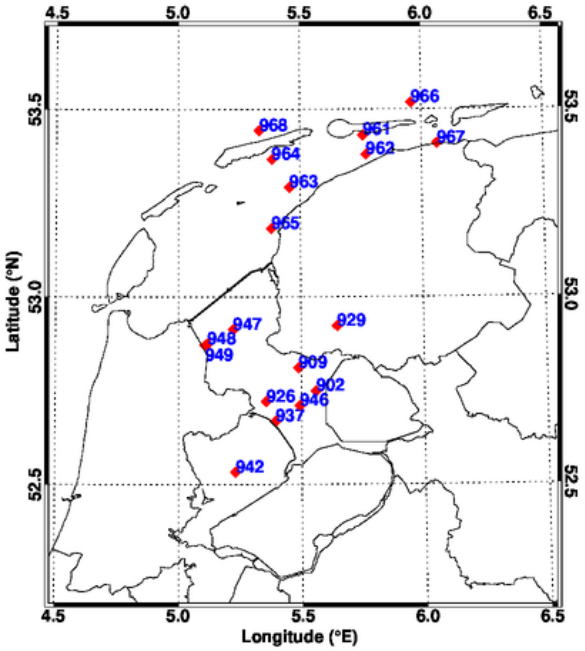

Figure 4.2. Map with RWS measuring location in Lake IJssel and the Wadden Sea. The numbers refer to station codes used in this report, see Figure 4.3 for the full station names.

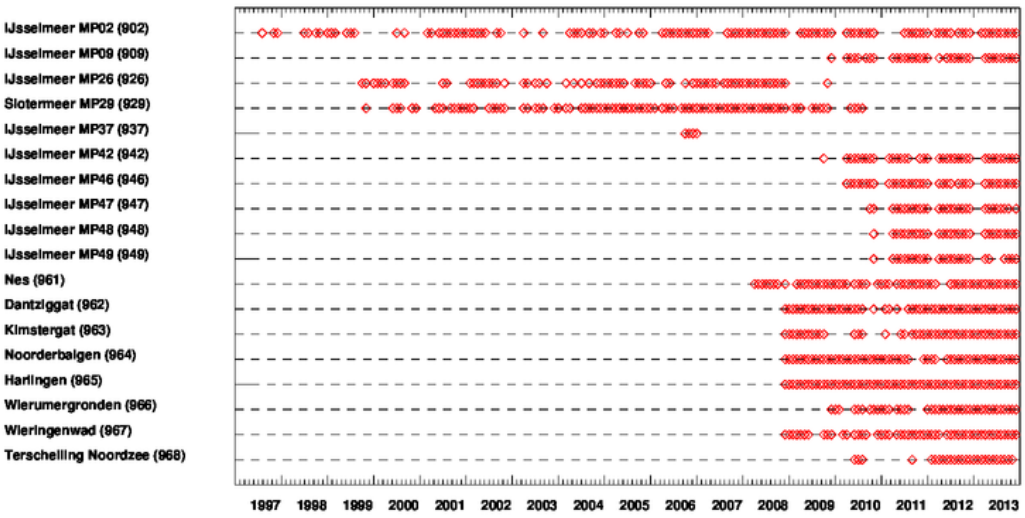

Figure 4.3. Availability of RWS Lake IJssel and Waddenzee measuring location. For each location, the symbols indicate months with at least 80% of the data available.

4.1.3 Quikscat satellite winds

From 2000 onwards, over sea we have satellite wind data from the Quikscat scatterometer at our disposal. They have the advantage of an extensive spatial coverage in an area where station observations are rare. A scatterometer measures the electromagnetic radiation scattered back from ocean gravity-capillary waves (Portabella and Stoffelen, 2009; Vogelzang *et al.* 2011). These are the small-scale surface ripples that are directly related to the wind speed. The backscattered radiation is related to the 10-m wind by a so-called (inverse) Geophysical Model Function (GMF).

We use the Quikscat 25 km product based on a state-of-the-art processing algorithm developed by KNMI. Each Quikscat image is collocated to the HARMONIE wind field from the nearest hour. Each scatterometer point is compared to the average of all HARMONIE grid points over an area of 25x25 km^2. Typically, 2-3 (partial) overpasses over North Sea per day are available.

4.2 Evaluation strategy

4.2.1 Comparing model grid boxes with point observations

As demonstrated by various authors (e.g. De Rooy and Kok, 2004; Verkaik, 2006), comparing point observations with model grid values is not trivial, especially not over land. The model applies gridbox-average roughness lengths, which may differ significantly from local values within the gridbox. For stations in coastal areas a comparison with model data critically depends on the exact station location and the modelled water fraction of the model.

Partly based on earlier work, Baas (2013) developed a method which allows for a fair comparison between model grid boxes and point observations. First it is determined whether a station behaves as a land or a water station using direction dependent roughness information. Therefore 'observed' roughness lengths are used that are derived from the standard deviation of the wind speed for sectors of 20°. If the local upwind roughness length is less than 0.01 m the station is treated as a water station.

In case the station behaves like a water station, the procedure is as follows:

1. Select the grid box with the highest water fraction in a square of 3x3 grid boxes centred on the gridbox in which the observation site is located.
2. If multiple grid boxes with a water fraction of 1 are detected, select the gridbox that is closest to the model upwind direction. For stations located in open water, the nearest gridbox is selected.

In case the station behaves like a land station, the procedure is as follows:

1. Select the gridbox in which the observation site is located.
2. Apply physical downscaling. Using the roughness length applied by the model (derived from the 10-m wind speed and the surface stress), the wind speed at a blending height of 60 m above ground level is calculated using a logarithmic wind

profile. Next, the 10-m wind used for the model evaluation is calculated using the direction dependent roughness length.

Figure 4.4 illustrates the difference between the procedure described above (left panels) and the method that simply compares the observations to the closest gridbox (right panels) for both a coastal station (Vlissingen) and a land station that is located in complex terrain (Soesterberg).

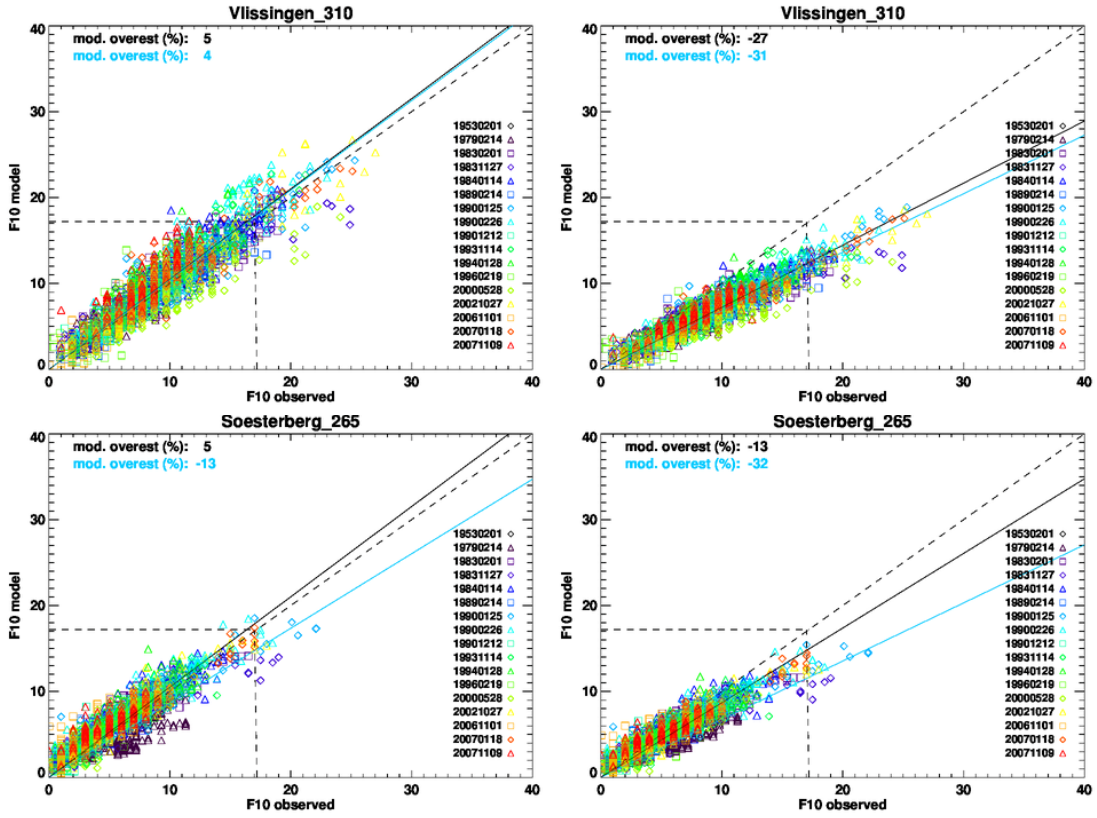

Figure 4.4. Modelled versus observed 10-m wind speed (m/s) for Vlissingen and Soesterberg. The left panels are based on the evaluation method described in the text, the right panels are based on the 'closest gridbox' approach. Black lines represent the best linear fit through all the data points, blue lines through data points which exceed the 8Bft threshold (indicated by the dashed lines) in either the model or the observations. Numbers indicate the modelled overestimation in %.

4.2.2 Temporal resolution of model and observations

For the verification we compare hourly averaged observations with the average of two model wind fields: one valid at the start of the hour, the other at the end. This method is illustrated in Figure 4.5.

Besides hourly averaged observations, also the 10-minute averaged values just before the hour are available. When we base the model evaluation on a comparison of this 10-minute

observations valid just before the hour (available for all storms) with the model wind field valid at the hour, we consistently find larger difference between model and observations than when we apply the method of Figure 4.5. The difference in rms error is typically 0.4 m/s.

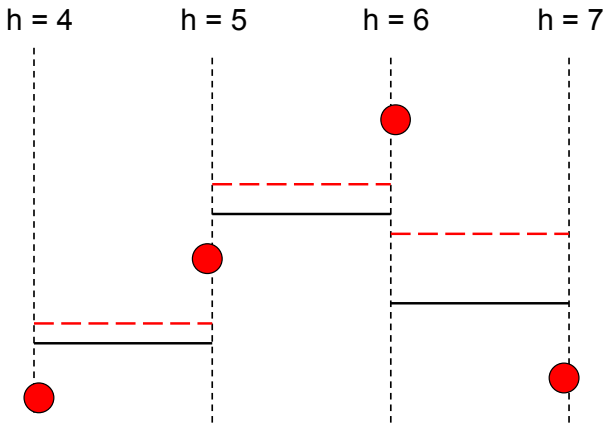

Figure 4.5. Schematic diagram of the method how the model is compared to the observations. Black solid lines: hourly averaged observations, red circles: model states at the hour, red dashes lines: average of two model states at the start and end of each hour.

4.3 Evaluation of wind and pressure fields

4.3.1 Wind distributions

To investigate the general wind climatology of the model, empirical PDFs of the wind speed are considered. Figure 4.6 presents the frequency distribution of the modelled and observed wind speed. It contains the hourly data for all 16 storms for all available stations. Summarized over all storms and all stations 117133 hours of data are included, which is the equivalent of 13 years. In general, the correspondence between model and observations is very good, indicating that the model has a realistic wind climate. The occurrence of extreme wind speeds is slightly too high in the model.

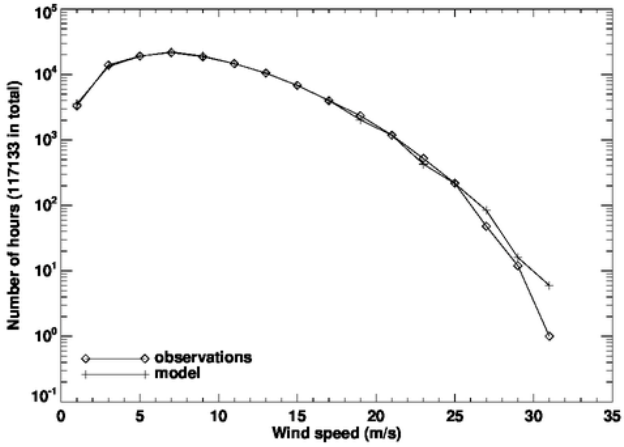

Figure 4.6. Distribution of modelled and observed 10-m wind speed (m/s) for all storms and all stations for bins of 2 m/s.

The occurrence of wind speeds exceeding consecutive Bft thresholds is summarized in Table 4.1. The results are split-up for stations over open water and over land (coastal stations are ignored). As we only consider wind speeds of 6 Bft and higher, the total number of observed and modelled hours is not the same. Absolute numbers between land and water are hard to compare because the number of stations is not the same, but it is clear that extreme wind speeds are much rarer over land than over water. Thus, the tail of the distribution shown in Figure 4.6 consists mostly of water cases, in particular for wind speeds over 10 Bft (24.5 m/s). Over water, the model overestimates the occurrence of extreme wind speeds, over land the number of extreme wind cases is underestimated.

The differences between model and observations may seem larger than they actually are: small shifts in the wind speed distribution lead to significant changes in the number of exceedances of the respective Bft thresholds. This is especially true in the tail of the distribution. For example, the difference over open water between model and observations corresponds to a 5 % overestimation of the modeled wind speed or, alternatively, as a positive bias of 0.5 m/s. The difference in number of occurrences of Bft 9 or higher over land corresponds to a negative bias of 1.5 m/s. See also Figure 4.8, which shows exactly the same data, but represented in a different way.

Table 4.1. Occurrence of observed and modelled wind speeds (number of hours) for consecutive Bft thresholds for stations located over open water and over land.

	Open water #obs | #mod	Land #obs | #mod
Bft 6 or higher	10962 | 11966	6588 | 6404
Bft 7 or higher	6014| 6480	2176 | 1747
Bft 8 or higher	2101 | 2391	578 | 386
Bft 9 or higher	574 | 680	118 | 28
Bft 10 or higher	77 | 153	9 | 0
Bft 11 or higher	5 | 8	0 |0
Bft 12 or higher	0 |0	0 |0

.

4.3.2 Temporal evolution

4.3.2.1 General model scores

For each station the correlation coefficient, *r*, between modelled and observed wind speeds were calculated. For stations over sea *r* is close to 0.95. This value is slightly but consistently higher than over land. The high values indicate that, apart from possible biases, the model captures the temporal evolution of the wind speed observations very well. The fact that differences between the stations are small is encouraging. Hour-to-hour variations in the 10-m wind speed are reasonably captured by the model. Extreme changes of more than 5 m/s per hour are underestimated (Baas, 2013).

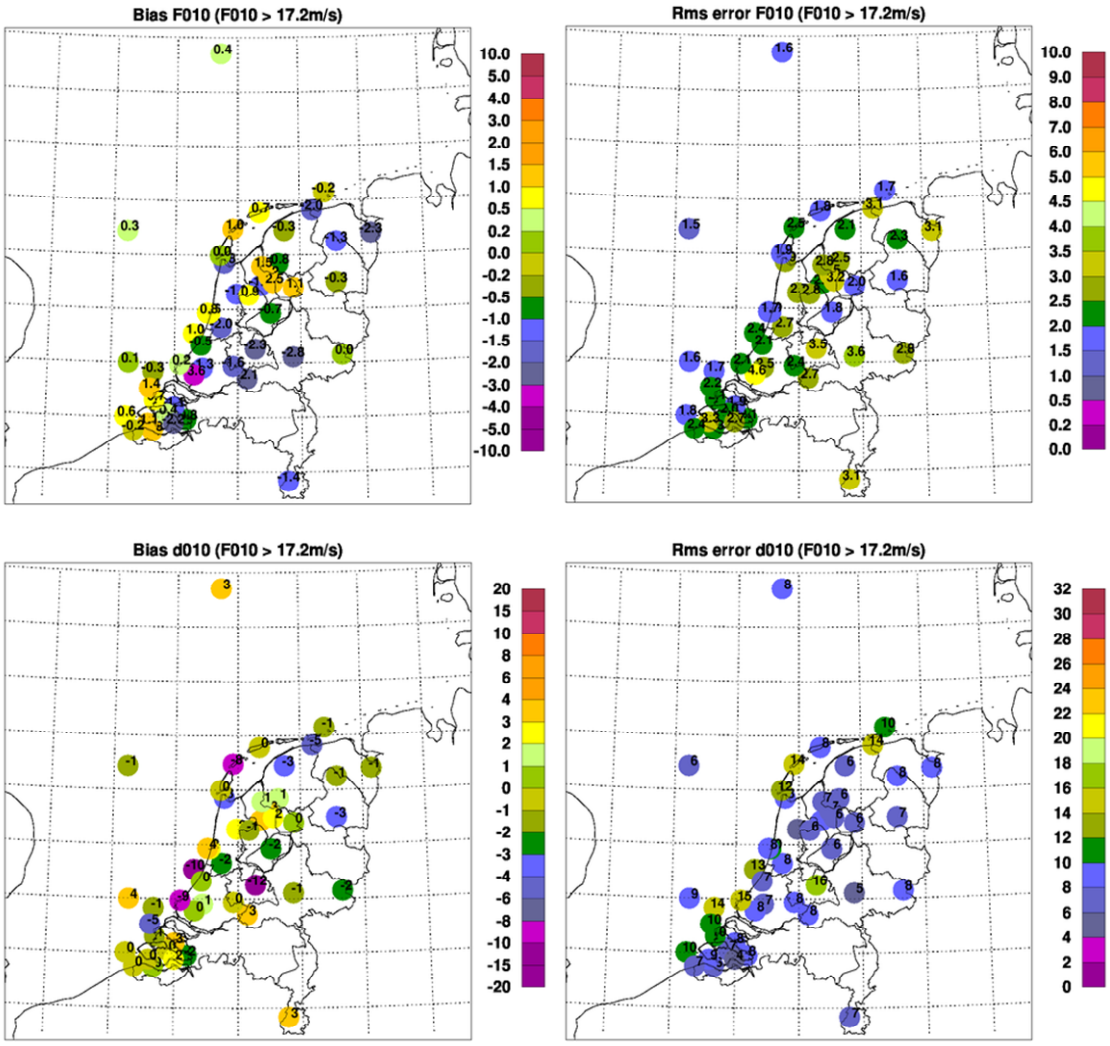

Figure 4.7. Bias (left panels) and rms differences (right panels) for the 10-m wind speed (top panels) and direction (lower panels). Only cases for which the 8 Bft threshold is exceeded in either the observations or the model are included. Only stations with at least 12 hours of data are shown.

Model scores have been determined following the method that has been explained in Section 4.2.1. Figure 4.7 presents bias and root mean square (rms) differences between the model and the observations for 10-m wind speed (upper panels) and direction (lower panels). Only cases for which the modelled or observed hourly exceeds the 8 Bft threshold of 17.2 m/s are included.

For stations over sea, the modelled wind speeds show a small positive bias of about 0.5 m/s, which is nearly independent of the wind speed. The rms difference is between 1.5 and 2.0 m/s, with only small variations between stations. The bias in the wind direction is a few degrees and does not show any trend as a function of wind speed (not shown). Rms differences are in the order of 10°. These numbers are rather similar to those derived in

operational practice. Note that the observational error is about 1 m/s in the wind speed and 10° in wind direction. The model performance over inland waters like Lake IJssel and the Wadden Sea is discussed separately in Section 4.6

Over land, the model performance is worse than over sea. Figure 4.7 shows that for wind speeds of 8 Bft and higher, generally a negative bias of about 2 m/s is identified with rms differences varying from 1.5 to 4 m/s between stations. Averaged over all wind speeds, the bias is close to zero for most of the stations.

Figure 4.8 presents exactly the same data in a slightly different way. It shows the bias in the wind speed over sea (left) and over land (right) as a function of the wind speed. Figure 4.8 clearly shows that over sea the bias in the wind speed is almost independent of the wind speed itself, while over land a serious negative bias develops for increasing wind speeds. The model underestimates the wind speed over land by about 10%.

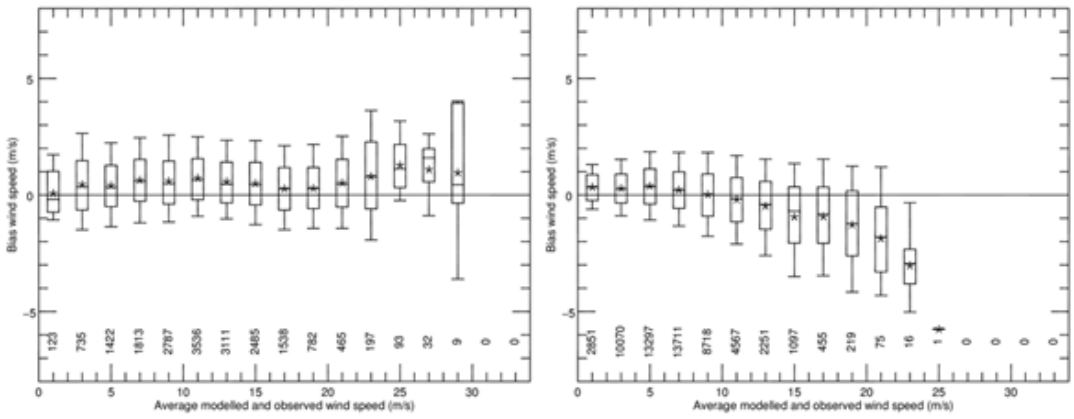

Figure 4.8. Bias (model – observations) in the 10-m wind speed as a function of wind speed for all stations over sea (left) and over land (right).

These findings are in line with other studies that also find that models have difficulties in reproducing extreme winds over land, see e.g. Lindenberg (2011). Although we are primarily interested in extreme wind speeds over water, model performance over land remains an intriguing topic for further research. A preliminary comparison of model output with data from a wind profiler system[3] at Cabauw, suggests that the negative bias is confined to the boundary layer: at heights of 1500 m the bias has disappeared (not shown). This points to a problem in the boundary layer parameterization and/or in the representation of the interaction of the atmosphere with the underlying –heterogeneous-surface.

[3] A wind profiler emits radar pulses to determine vertical profiles of the wind speed. The velocity of the air toward or away from the radar as a function of altitude is calculated from the doppler frequency shift of the backscattered energy.

4.3.2.2 Model scores per storm

Figure 4.9 presents rms differences for pressure (left), wind speed (middle), and wind direction (right) for each of the 16 storms to examine the variations in model performance between storms. We make a distinction between stations over sea, land, and along the coast. The quality of the modelled pressure evolution is rather equal for all storms. There is one notable exception: the storm of 27 Nov 1983. This relatively small, quickly developing system is not accurately captured by the model. In the southwest of The Netherlands large differences of up to 8 hPa between observed and modelled pressure values occur. This bad representation of the surface pressure is reflected in the wind speed scores for this storm. Generally, the quality of the wind speed is rather uniform among the storms with no trend in time (see also Van den Brink *et al.* 2013). There is no clear distinction between different station locations.

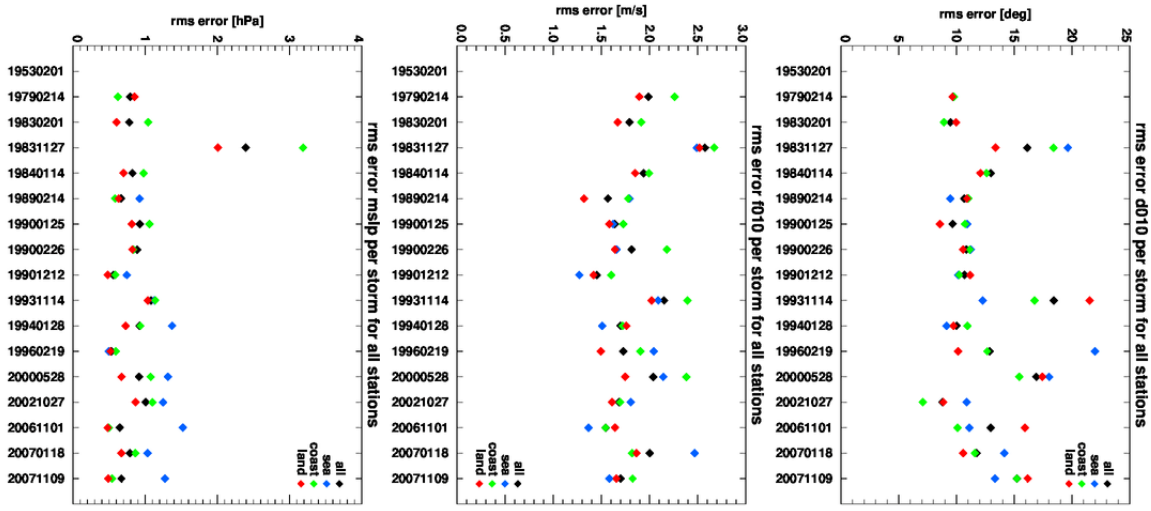

Figure 4.9. Station-averaged rms-error for pressure (left), wind speed (middle), and wind direction (right) for each of the 16 storms. For each station, only data within 12 hours before and 12 hours after the maximum observed wind speed are included. Colors indicate a subset of the stations: sea (blue), coast (green), land (red) and overall (black).

The magnitude of the wind direction error appears to be related to the horizontal dimensions of the storm: for small storms with the centre of low pressure close to The Netherlands the variation in wind direction in time is large. Therefore, it is not surprising that the storms of 27 Nov 1983, 14 Nov 1993, and 28 May 2000 show the highest errors.

4.3.3 Spatial patterns

The correlation between modelled and observed station data valid at the same time, indicates the ability of the model to reproduce spatial patterns. For the 16 test-set storms this spatial correlation between modelled and observed fields is on average 0.87, indicating that in principle the model reproduces the observed spatial patterns. A similar number is obtained from scatterometer data.

HARMONIE represents spatial gradients between a selection of stations in 10-m wind speed and surface pressure rather well. This is shown in Figure 4.10, which shows the differences between K13 and Europlatform (north-south) and between K13 and Huibertgat (west-east). For most of the storms, differences between the stations remain below 5 m/s. However, for several storms the spatial gradients become large. The largest spatial gradients in wind speed occur in the vicinity of the low pressure centre.

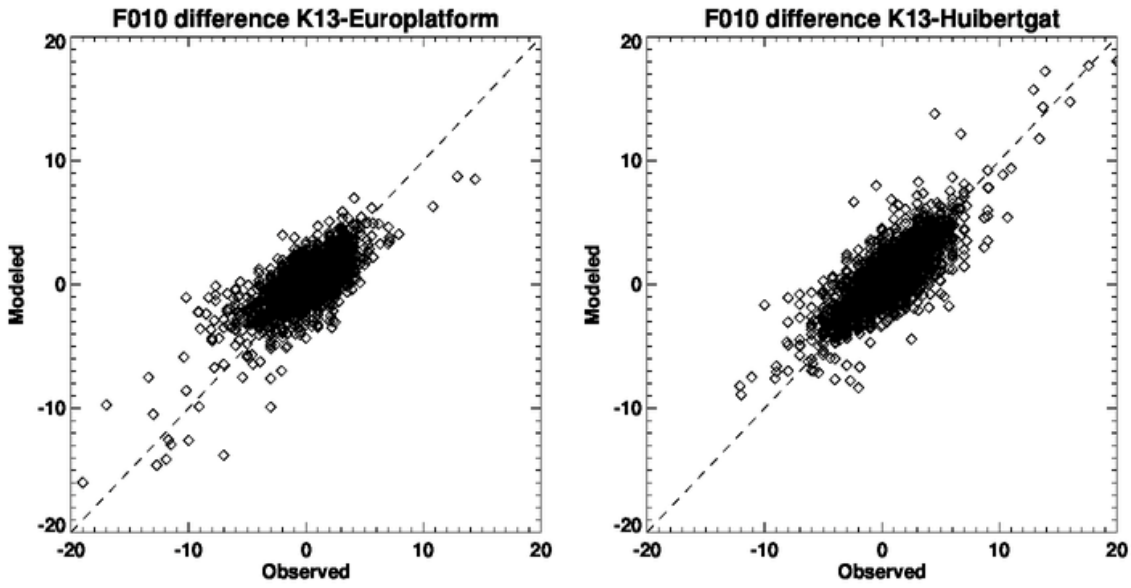

Figure 4.10. Modelled versus observed difference in 10-m wind speed (m/s) between K13 and Europlatform (left) and K13 and Huibertgat (right).

The surface geostrophic wind vector is a measure of the magnitude and the orientation of the mean sea level pressure field. Thus, the ability of the model to reproduce the observed geostrophic wind is an indication of how well the model reproduces pressure patterns. At Cabauw the surface geostrophic wind is monitored on a continuous basis using pressure observations from 16 KNMI stations that are located within a radius of 75 km around the site. For the 16 test-set storm periods geostrophic wind at Cabauw have been calculated from HARMONIE pressure fields following exactly the same procedures as for the observations (pers. comm. Bosveld, 2014).

The correlation (r) between the modelled and observed geostrophic wind speeds amounts to 0.95. The bias is -0.78 m/s, the rms difference is 3.2 m/s, and the scatter index is 0.16. The bias in the direction is 2.2° with a rms difference of 11.5°. These numbers indicate that HARMONIE reproduces the temporal and spatial variations in the surface pressure field very well.

However, Figure 4.11 reveals that a negative bias develops for increasing geostrophic wind speeds. Although scatter is large, this means that the model underestimates the most extreme pressure gradients. (For reference, a difference of 1 hPa over a distance of 100 km, equals a difference in geostrophic wind speed of 7 m/s.) It is tempting to relate the underestimation of extreme geostrophic wind to the underestimation of the 10-m wind over land. The correlation between the bias in the geostrophic wind and the bias in the Cabauw 10-m wind is 0.20. Comparison with data for Lichteiland Goeree, one of the closest open-water stations, yields a correlation of only 0.005. These low correlations suggest that the impact of the bias in the geostrophic wind on the 10-m wind scores is small. Therefore, it is unlikely that it is responsible for the underestimation of the 10-m wind over land.

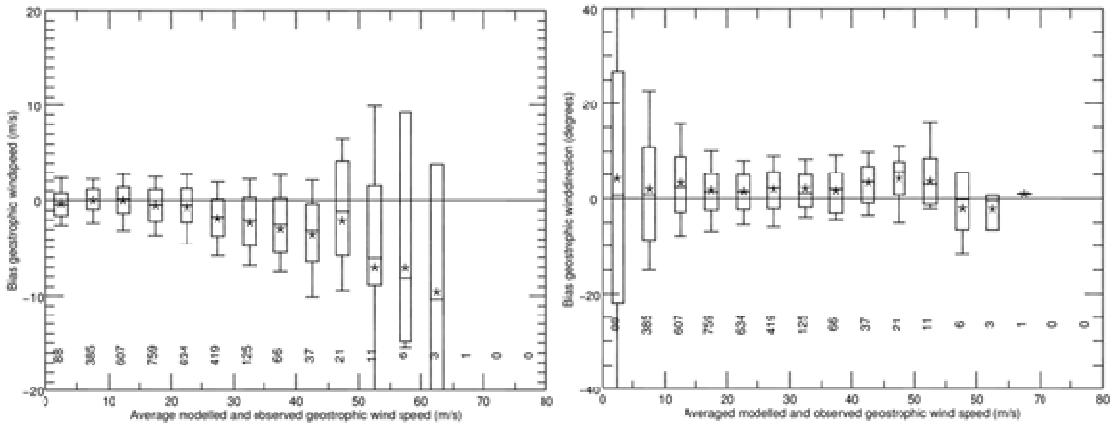

Figure 4.11. Bias (model – observations) in the surface geostrophic wind speed (left) and the direction (right) as a function of the geostrophic wind speed for Cabauw.

4.3.4 Comparison with satellite winds

For open water areas, Figure 4.12 compares wind speed and direction as modelled by HARMONIE to satellite observations from Quikscat. The bias / rms error in the wind speed amounts to 0.57 / 1.65 m/s. In the wind direction the bias / rms error amounts to 0.87 / 15.9°. These numbers agree with scores derived from station observations. For the comparison of wind direction only observations over 5 m/s are taken into account.

For each pair of collocated scatterometer-HARMONIE wind fields the spatial correlation has been calculated. The distribution peaks at values between 0.85 and 0.90. The results indicate high spatial correspondence between the observed and modelled wind fields.

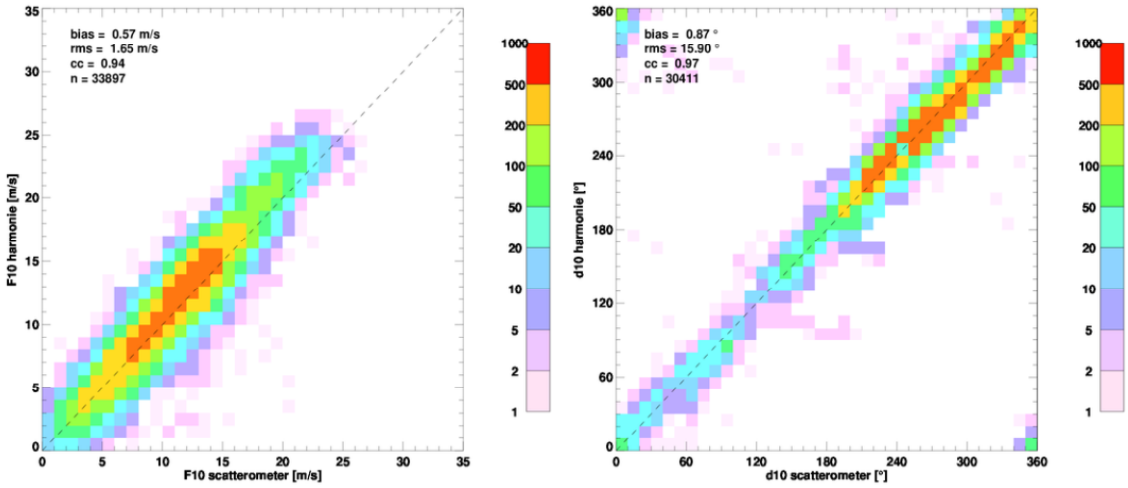

Figure 4.12. Scatter density plots of modelled wind speed (left) and direction (right) versus scatterometer data.

4.4 Production runs

Some basic checks have been performed to verify whether the quality of the production runs equals that of the simulations of the test-set storms. As an example, Figure 4.13 shows scatter plots of modelled versus observed 10 m wind speeds for platforms K13 and Europlatform. Model scores are in line with findings from test-set storms.

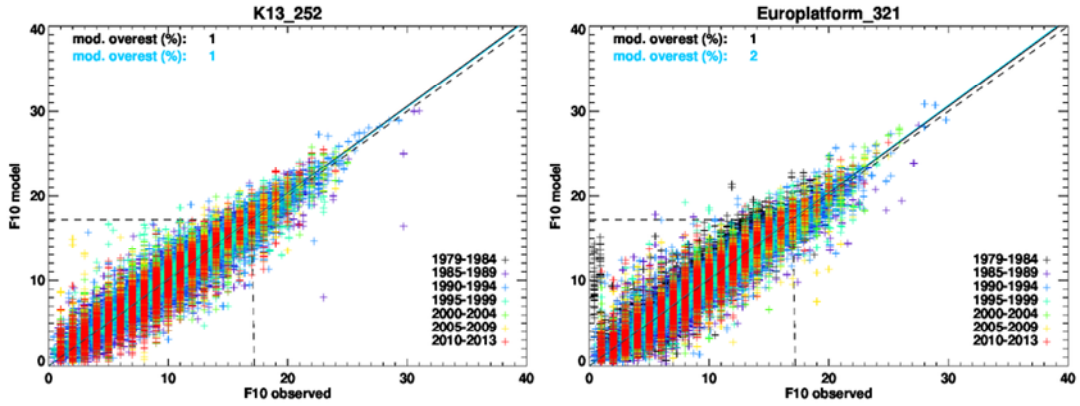

Figure 4.13. Scatter plots of modelled versus observed 10-m wind speeds for the production runs. The model overestimation in % is indicated for the complete dataset (in black) and for only those cases that exceed the 8 Bft threshold value (in blue), which is indicated by the dashed lines.

In addition, for stations over sea Figure 4.14 presents modelled and observed cumulative distributions of the wind speed for the 16 test-set storms and the production runs. For both datasets the modelled frequency distributions follow the observed ones quite closely. The modelled wind speeds are slightly higher than observed. For the production runs the difference is smaller than for the test-set storms. We conclude that the quality of the production runs is equal to those of the test-set storms.

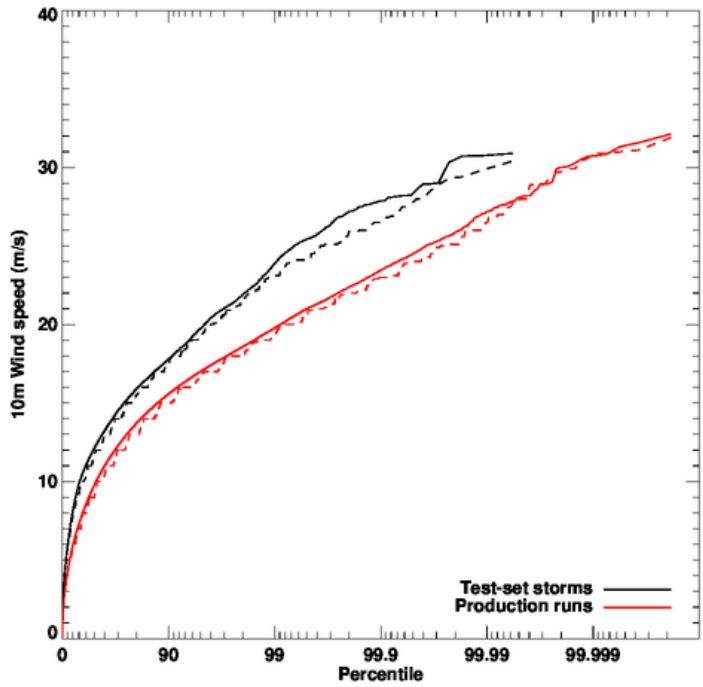

Figure 4.14. Frequency distribution of the modelled (full lines) and observed (dashed lines) wind speed for 16 test-set storms (black) and the production runs (red).

4.5 Comparison with tall mast observations

4.5.1 Representation of the wind profile

To assess the quality of the modelled wind profiles, we compare model output with observed profiles from three tall measuring towers. Two of them are located at sea, one is located on land. The FINO mast is located 50 km north of Schiermonnikoog, the OWEZ mast is located 20 km off the coast of Egmond aan Zee. The Cabauw mast is located in the western part of the Netherlands. As for FINO and OWEZ the observations start only in 2004 and mid 2005, only a limited comparison with model data from the 16 storm periods is possible. Therefore, we choose to base the comparison on model data from the production runs, in particular the simulations from the full year of 2007.

Figure 4.15 presents averaged modelled and observed wind speed profiles for the different towers. Correspondence between modelled and observed profiles is good. For

FINO the observed wind speeds are higher than modelled, but the difference is in the same order as the uncertainty in the observations. Especially for FINO[4] and Cabauw the modelled wind shear is too small. In other words, for these locations the increase of wind speed with height is underestimated by the model. This suggests that the vertical mixing in the model is too large. Model sensitivity experiments indicate that the shape of the wind profile is very sensitive to details in the turbulence parameterization (not shown).

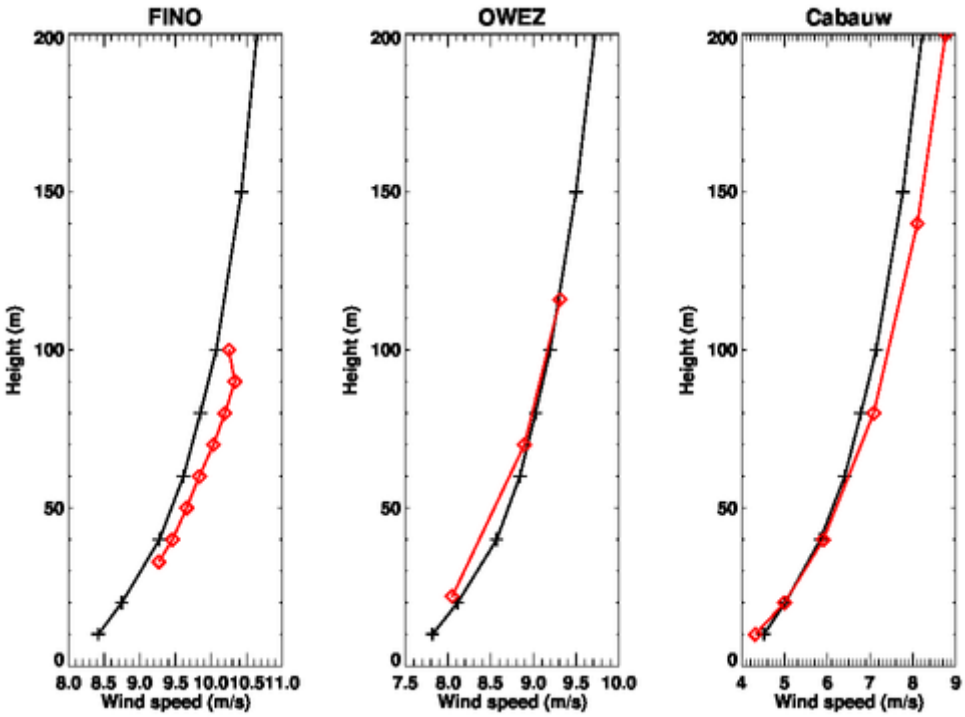

Figure 4.15. Average modelled (black) and observed (red) wind speed profiles for the FINO, OWEZ, and Cabauw masts.

4.5.2 Representation of stability

4.5.2.1 Vertical wind speed ratios

The stability of the boundary layer has a significant impact on the near-surface wind. As shown by Barthelmie (1999) and Sathe *et al.* (2011), for increasing wind speeds the occurrence of significantly stable and unstable conditions decreases. However by analyzing vertical wind speed ratios, Baas *et al.* (2014) demonstrate that also in strong wind conditions stability is important, especially over sea. This is shown in Figure 4.16, which shows the ratio of the wind speed at 116 and 21 m at OWEZ (a) and Cabauw (b) versus stability, represented by the bulk Richardson number,

$$Ri_b = \frac{g}{\overline{\theta_v}} \frac{z\Delta\theta_v}{U^2} \ .$$

[4] The discontinuity in the observed FINO profile is caused by a deviating measurement set-up at 100 m.

Here g is the acceleration due to gravity, $\Delta\theta_v$ is the difference in virtual potential temperature between 22 m and the surface, z is the height above the surface (22 m), U is the wind speed at 22 m, and $\overline{\theta_v}$ is the reference temperature, taken as the 22 m virtual potential temperature. In unstable conditions (Ri_b < 0) the vertical wind speed ratio is relatively constant, while in stable conditions (Ri_b > 0) this ratio increases rapidly with increasing stability. The red symbols represent cases for which the 10-m wind exceeds the 7 Bft threshold value of 13.9 m/s. Over land, scatter is large and no relation with stability can be identified. Apparently, in these strong wind conditions the influence of stability is small. Over sea the opposite is true. Here the wind speed ratio depends systematically on Ri_b also for the strong wind cases. The ratio between the wind speed at 116 and 22 m may vary by 40% depending on the stability. The blue symbols indicate HARMONIE model output for cases of 7 Bft and higher. At OWEZ the model clearly reproduces the observed response of the modelled wind speed ratio to changes in stability for these strong wind conditions, although the response is too weak. For high wind speeds, the modeled variations in Ri_b are much smaller at Cabauw than at OWEZ, in agreement with observations.

An important difference between sea and land is that for the strong wind category the vertical temperature differences span a much wider range over sea than over land. This is related to the different thermal properties of the surface. Due to the large thermal inertia of water, the sea surface temperature does not follow the air temperature closely, which frequently leads to large temperature differences between the air and the underlying sea surface. In contrast, over land the surface temperature and the temperature of the air are tightly coupled.

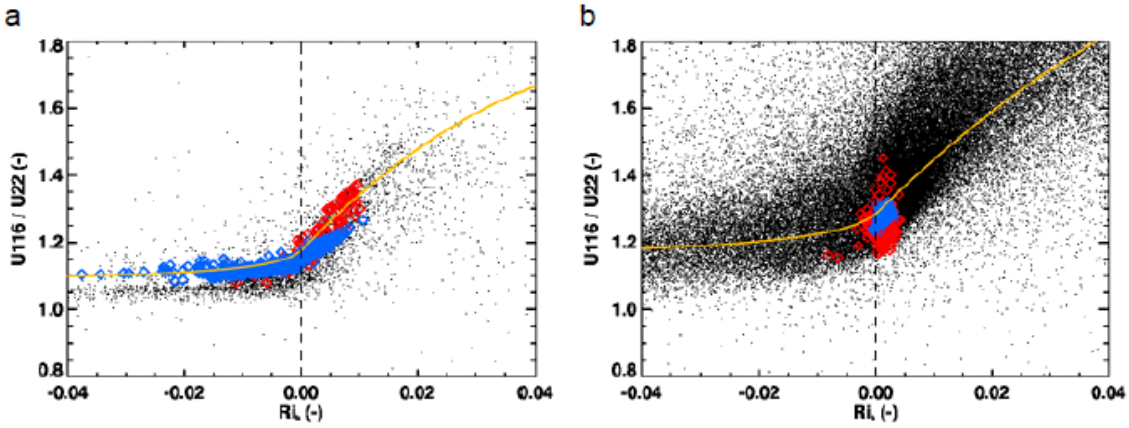

Figure 4.16. Observed vertical wind speed ratios for OWEZ (a) and Cabauw (b) as a function of the bulk Richardson number between 20 m and the surface (black). Data for which the wind speed at 10 m is higher than 13.9 m/s (at least 7 Bft) are indicated in red. Model data (at least 7 Bft) are indicated in blue. The orange line indicates the theoretical relation derived from Monin-Obukhov Similarity Theory.

4.5.2.2 A model sensitivity study

To investigate the impact of stability on the near-surface wind we performed a sensitivity experiment in which we modified the sea-surface temperature (SST) for the severe storm of 25 January 1990. Besides the reference simulation, we did a simulation with the SST increased by 5 K and a simulation with the SST decreased by 5 K. A higher/lower SST results in more unstable/stable conditions (assuming that the air temperature is the same). As a result, the vertical mixing in the boundary layer will be stronger/weaker, leading to an increase/decrease of the wind speed near the surface.

Figure 4.17 shows the impact of modifying the SST on the 10-m wind speed. Figure 4.17a give the average wind speed over the entire day in the reference simulation, the other panels give the difference between the simulations with modified SST and the reference simulation. In the area with the highest wind speed, the difference between the two modified simulations amounts to 2 – 3 m/s, which is 10% of the actual wind speed. Over land differences are small. As the amplitude of our sensitivity run is approximately equal to the yearly SST cycle, this indicates that the sea to land wind speed ratio is not a constant but varies during the year (see also Section 6).

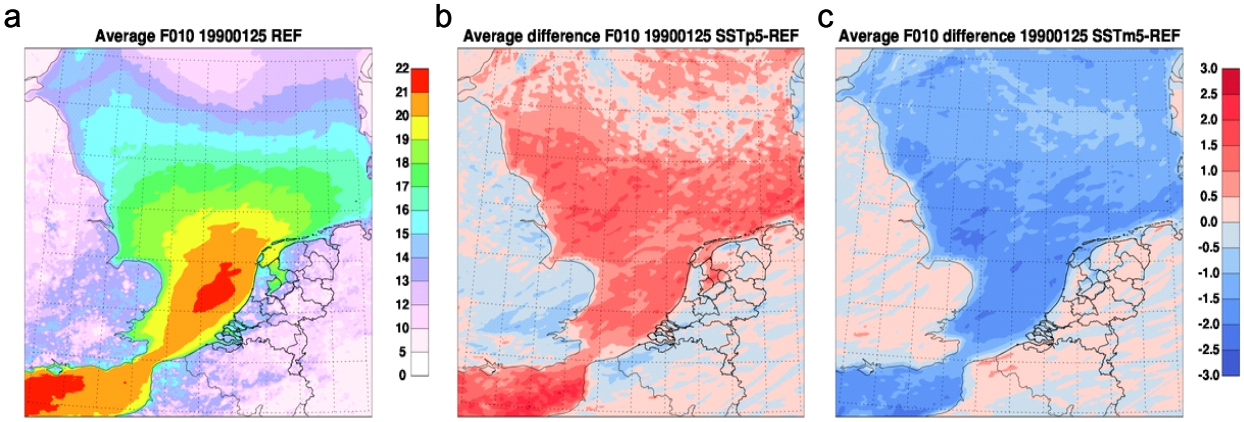

Figure 4.17. Modeled average 10-m wind speed for 25 Jan 1990 for the reference simulation in m s^{-1} (a). Difference in m s^{-1} between SSTp5 and REF (b) and SSTm5 and REF (c).

Figure 4.18 present modelled vertical wind speed profiles for the three simulation averaged over the day. Clearly, stability affects not only the near-surface wind, but modifies the wind profile in the entire boundary layer. For unstable (stable) conditions the wind speed is higher (lower) in the lower part of the boundary layer, but lower (higher) in the upper part of the boundary layer. Above the boundary layer, in the free atmosphere, differences between the model runs are small.

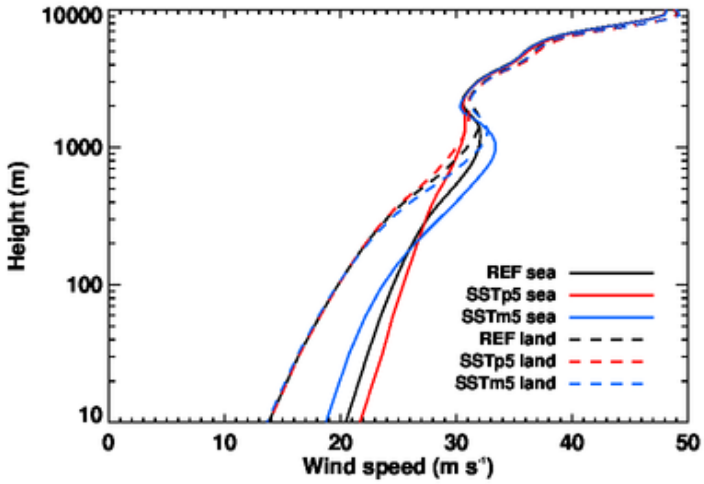

Figure 4.18. Averaged vertical profiles over sea (solid lines) and land (dashed lines) for three simulations of the 25 Jan 1990 storm with different SSTs.

4.6 Model performance over inland waters

4.6.1 Lake IJssel and the Wadden Sea

4.6.1.1 Comparison with RWS observations

Here we discuss the quality of the modelled wind fields over Lake IJssel and the Wadden Sea by comparing model simulations with the available RWS observations. As the number of test-set storms in the period for which these observations are available is limited, we choose to base the evaluation on the production runs.

Model biases for the Lake IJssel and Wadden Sea area given in Figure 4.19. Generally, the modelled wind speeds are too high. When all data are considered, for all RWS stations (except for station 937 in Lake IJssel) the bias is close to zero. When only cases of 8 Bft or higher are considered, both the absolute and relative biases are larger. In that case the largest relative differences are observed for stations 902, 909, 937 for which the modelled winds are too high by 12, 10 and 10%, respectively. Considering all stations, for these high-wind conditions the overestimation of the modelled wind speeds over Lake IJssel is 5-10%. For the Wadden Sea this difference is in the order of 5%. APPENDIX C presents scatter diagrams of modelled versus observed wind speeds for a selection of the Lake IJssel and Wadden Sea stations. These Figures demonstrate that HARMONIE is well capable of representing the temporal variations in wind speed for the different locations.

For stations close to the western shoreline of Lake IJssel the difference between modelled and observed wind speeds is smaller than for stations in the eastern part of the lake. Since the dominant wind direction is from the west, this suggests that the positive bias

over open water is (partly) compensated for by the underestimation of wind speeds over land. Thus, the latter does not lead to an underestimation of the wind speed in Lake IJssel.

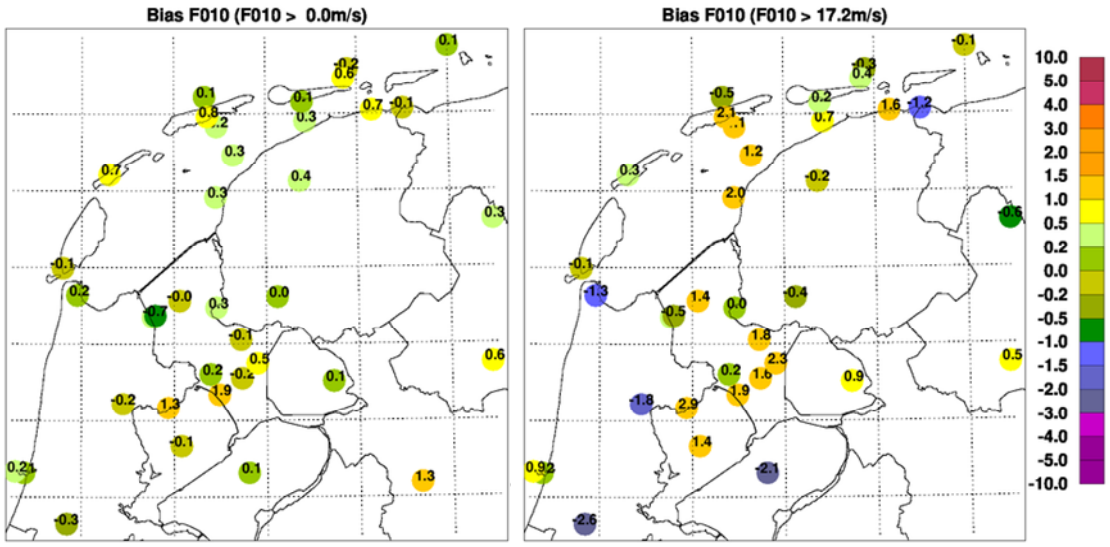

Figure 4.19. Wind speed bias for the Lake IJssel and Wadden Sea area based on the production runs. The left panel is based on all data (at least 240 data points per station), the left panel includes only data which exceeds the 8 Bft threshold (at least 12 data points per station).

4.6.1.2 Wind patterns and stability

Figure 4.20 shows average wind speed fields for the Lake IJssel area over all available HARMONIE forecasts of the test-set storms (Baas, 2013). The left panel shows the average wind field for westerly winds (wind direction at stations 926 and 902 between 240 and 300°), the right panel shows the average wind field for easterly winds (wind direction at stations 926 and 902 between 60 and 120°). The lines of equal wind speed clearly follow the shape of the upstream shoreline. The locations of the stations 902 and 926 are indicated in the Figure.

Baas (2013) demonstrates that the modelled wind speed ratio between stations 926 and 902 increases with an increasing air-water temperature difference (not shown). This agrees with observational findings of Bottema (2007). Figure 4.21 shows the average evolution of the wind speed over a west-east cross-section over Lake IJssel for westerly winds (wind direction between 225° and 315°) for three stability classes. The location of the cross-section is indicated in Figure 4.20. Wind speeds are normalized with the wind speed at the RWS measuring station 902. The black crosses indicate the modelled water fraction. At the location of the cross-section, Lake IJssel is eight grid points wide. It appears that in stable conditions the wind speed increases faster to an equilibrium value than in unstable conditions. Consequently, in stable conditions the wind speed appears to

be more constant over Lake IJssel than during unstable conditions, where a strong east-west gradient is observed. For each stability class, the red asterisks indicate the observed ratio between the RWS measuring stations 926 and 902. Although the impact of stability on the near-surface wind is clearly present in HARMONIE, a comparison with the observations demonstrates that it is too weak.

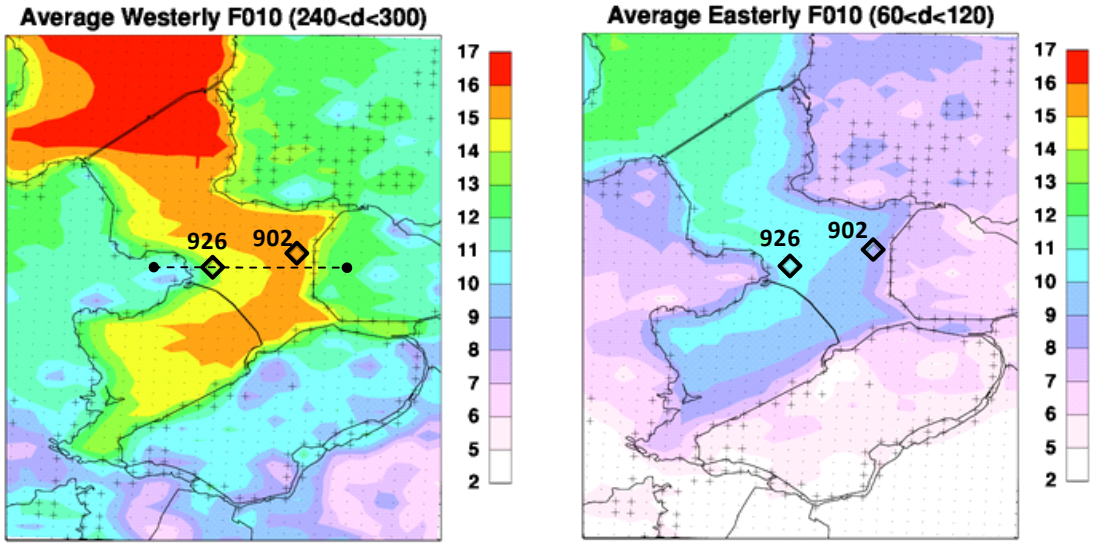

Figure 4.20. Average modelled wind speed over Lake IJssel for westerly (left) and easterly (right) winds (in m/s). Dots indicate the HARMONIE grid, plusses indicate mixed land-water grid points. The diamonds indicate the locations of stations 926 and 902. The dashed line in the left panel indicates the location of the cross-section that is used in Figures 4.21 and 4.22.

Baas and Van den Brink (2014) discuss two-dimensional cross-sections of the thermodynamic state of the boundary layer for a typical stably and a typical unstably stratified case. For both cases the wind comes from the west. Figure 4.22 shows the vertical cross-section for potential temperature (colours) and wind speed (lines) for the lowest 500 m of the atmosphere. The location of the cross section is the same as in Figure 4.21. The location of the shorelines is indicated by vertical dashed lines.

In the stable case, the water temperature is about 4 K *lower* than the air temperature. As a result, as the air flows over the water the air temperature starts to drop. As the increased stability prevents the downward mixing of high-momentum air from above, the wind speed stops increasing already after less than 10 km from the western shore of the lake (*cf.* Figure 4.21). The impact of the land-water transition on the wind speed decreases rapidly with height. Above about 200 m the impact is small.

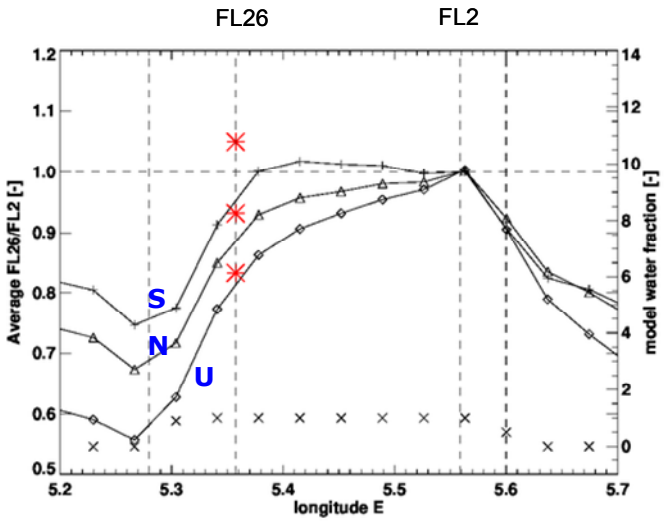

Figure 4.21. Cross-section over Lake IJssel of 10 m wind for three stability classes (right panel) for westerly winds. Diamonds indicate the unstable case, triangles the neutral case, and plusses the stable case. The asterisks indicate the observed wind speed ratio for the three stability classes; the crosses indicate the modelled water fraction (right axis).

In the unstable case, the water temperature is about 5 K *higher* than the air temperature. As a result, as the air flows over the water the air temperature starts to increase. With the fetch becoming larger, the vertical temperature gradient almost vanished. The high temperatures close to the surface promote intense vertical mixing. In this case, the near-surface wind speed keeps increasing until the flow hits the eastern shoreline of the lake (*cf.* Figure 4.21). Initially, the wind speed increases rapidly because of the reduced surface roughness. The slower increase later on is caused by the downward mixing of high-momentum air towards the surface. In this unstable case the wind speed at higher levels decreases significantly. Compared to the stable case, the impact over the surface is felt at higher levels.

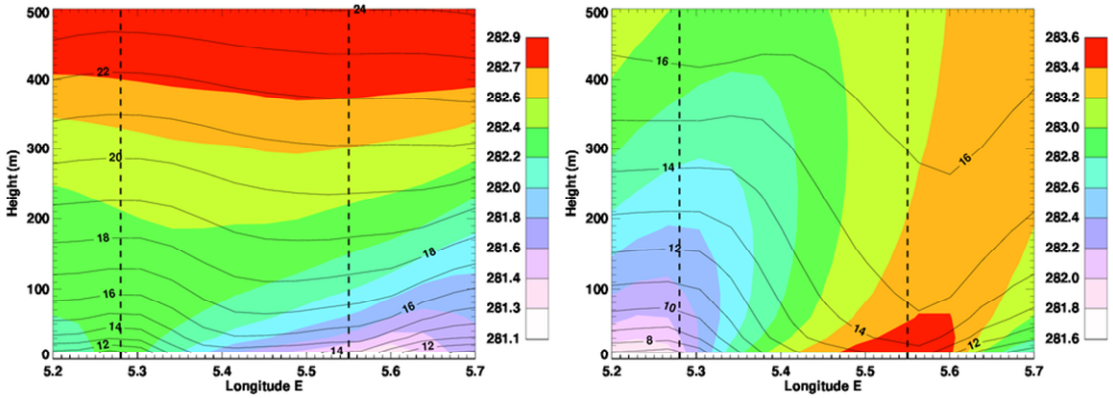

Figure 4.22. Example of a stable (16 Feb 1996, 14UTC) (left panel) and an unstable (24 Oct 2002, 1 UTC) (right panel) case. The colours indicate the potential temperature (in K), the solid black lines indicate the wind speed (in m/s). The vertical dashed lines indicate the western and eastern shorelines of Lake IJssel.

4.6.2 Smaller inland waters

Smaller inland water bodies like the rivers and their estuaries, the Veluwse Randmeren, and the Frisian Lakes are not explicitly resolved in HARMONIE as the 2.5 km grid is too coarse. This is shown in Figure 4.23, which shows the modelled water fraction. Note that the Oosterschelde and the Westerschelde are large enough to be resolved by the model.

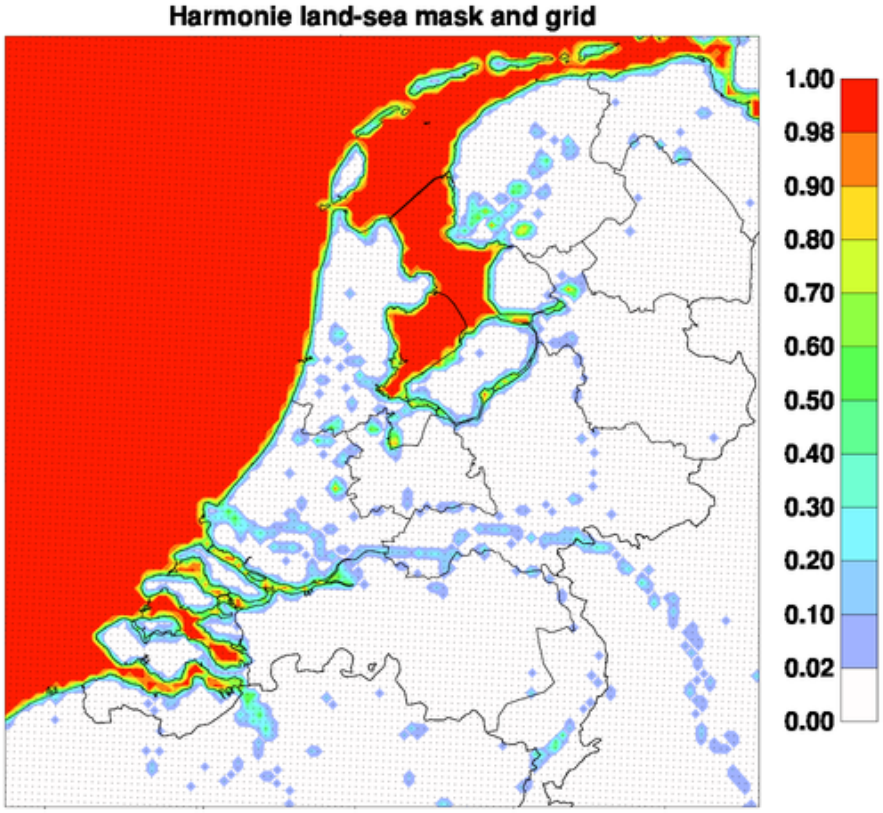

Figure 4.23. HARMONIE water fraction. The grid is indicated by small dots.

To estimate the wind over water bodies that are not explicitly resolved, direct use of the HARMONIE output is not recommended. Instead, we suggest to apply a physical downscaling method that corrects for the difference in modelled and the actual roughness length. The direction-dependent actual roughness length can be estimated from a high-resolution land-use map. This method is essentially similar to the method described in Section 4.2.1.

5 The added-value of the high-resolution HARMONIE model

In this Section the added-value of HARMONIE compared to the ERA-Interim dataset is discussed. The presented material is based on Baas and Van den Brink (2014).

5.1 Comparison of HARMONIE and ERA-Interim wind and stress fields

5.1.1 Comparison of minimum core pressure and maximum wind speed

Figure 5.1 presents the difference in minimum pressure and the maximum wind speed as modelled by HARMONIE and ERA-Interim over the area of the HARMONIE domain. The evaluation is done for all available model data from the 16 simulated storm periods. Every time a +6 h HARMONIE forecast is compared to the ERA-Interim analysis with the same verification time. With about 8 simulation days per storm period and 4 analyses a day, this yields 526 data points in total. Here, we are interested in the large-scale evolution of the storm depressions. Therefore, to enable a fair comparison between the models, the HARMONIE pressure fields were smoothed over an area comparable to the ERA-Interim grid size.

On average, the lowest pressure in the HARMONIE domain is 1.4 hPa lower than in ERA-Interim. This difference can only for a small part be attributed the increased spatial detail: if the HARMONIE pressure fields are averaged to match the ERA-Interim resolution, the resulting average minimum pressure is still 1.1 hPa lower than in ERA-Interim.

For 90% of the cases, the maximum 10-m wind speed in the HARMONIE domain is larger than in the same area in ERA-Interim. The average difference amounts to 1.7 m/s or 9.3%. When no spatial smoothing of the HARMONIE winds is applied, the difference in the 10-m wind increases from 1.7 to 3.2 m/s. The difference between the two numbers indicates to what extent the maximum wind in the domain is increased as a direct result of the difference in resolution between ERA-Interim and HARMONIE. The maximum geostrophic winds are 1.3 m/s larger in HARMONIE than in ERA-Interim (not shown, see Baas and Van den Brink, 2014).

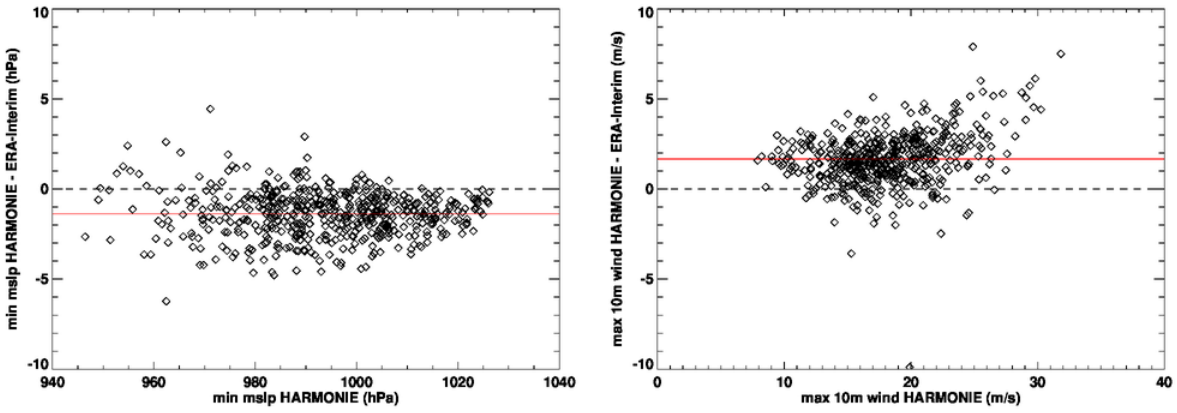

Figure 5.1. Difference between domain-wide minimum pressure (left) and maximum 10-m wind speed (right) as modelled by HARMONIE and ERA-Interim.

5.1.2 Comparison of wind and stress fields

Figure 5.2 compares the 10-m wind speeds and friction velocities of HARMONIE with those obtained from ERA-Interim for ERA-Interim grid points over sea. On average, the HARMONIE wind speeds are 0.80 m/s higher than the ERA-Interim wind speeds. For the highest wind speeds the difference is larger: for HARMONIE the 99th percentile amounts to 23.7 m/s, for ERA-Interim 21.5 m/s, corresponding to a difference of 10%. The differences in friction velocity are smaller than the differences in wind speed, especially for the most extreme cases, for which the HARMONIE 99th percentile is only 4% higher than that of ERA-Interim.

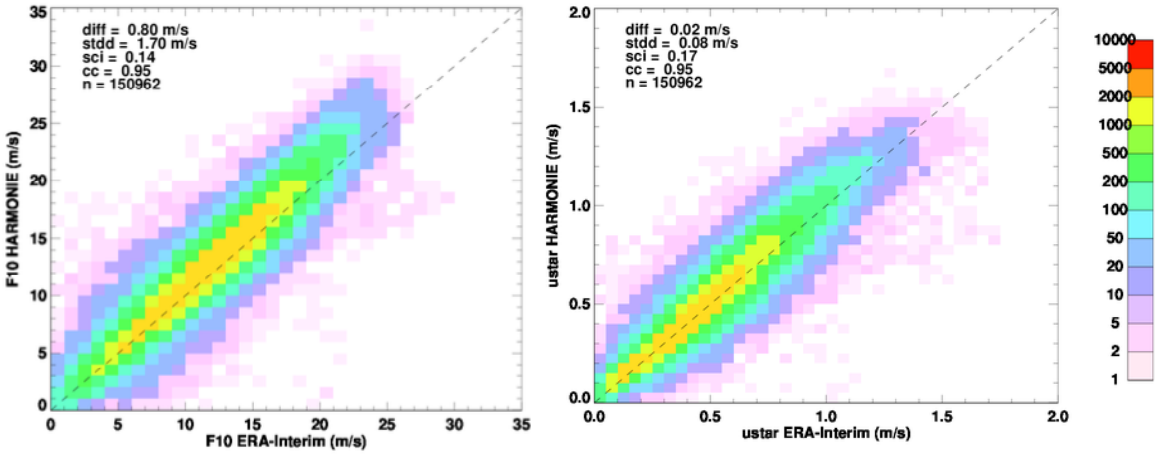

Figure 5.2. HARMONIE versus ERA-Interim 10-m wind speed (left) and friction velocity (right) over sea. The colours indicate the number of occurrences for each bin.

Figure 5.3 shows geographical distribution of the average difference in wind speed and friction velocity for the two models. Focussing on high wind speeds, only data exceeding the 8 Bft threshold value are included. For these cases the difference varies from about 1.7 m/s in the centre of the North Sea to values as high as 5 m/s in some coastal areas. This corresponds to a difference of 7% in open waters. In coastal areas the difference increases to more than 20% in some cases. The relative difference is insensitive to the imposed wind speed threshold. The increased difference close to the coast is a consequence of the coarse resolution of ERA-Interim. More specifically, since the grid spacing of ERA-Interim is 0.5°, the transition from land to water occurs in a broad area of tens of kilometres, while in HARMONIE the transition takes place in a few kilometres.

Over open water the HARMONIE friction velocities are 5-10 % higher than in ERA-Interim. When also lower wind speeds are included, the relative difference between the two model is lower by a factor of two. In coastal areas, the difference increases to more than 20% in some cases. The meridional structures in Figure 5.3 are probably artificial. They originate from the ERA-Interim fields and are likely to be related to the grid configuration.

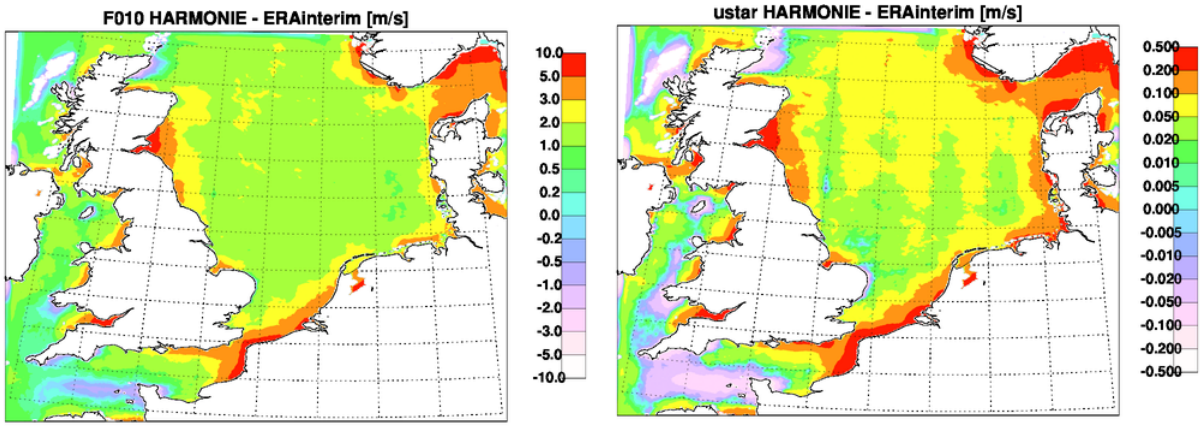

Figure 5.3. Difference in the 10-m wind speed (left) and friction velocity (right) between HARMONIE and ERA-Interim. Only data for 8 Bft and higher are included.

5.1.3 Pseudo-wind

Hydrodynamic models are driven by surface stress. However, in most cases the input for these models consists of 10-m winds that are internally converted to a surface stress by applying a particular drag relation. When wind fields from an atmospheric model are used, this procedure may lead to ambiguous results, in particular when the hydrodynamic model and the atmospheric model apply different drag relations. It would be more transparent if the hydrodynamic model would be driven directly by the surface stress of the atmospheric model.

To correct for the difference in drag relation we introduce the so-called *pseudo-wind*, which is defined as *the 10-m wind that corresponds to the surface stress of the atmospheric model when using the drag relation of the hydrodynamic model.* In other words, the pseudo-wind is a translation of a surface-stress field to a corresponding wind field using a reference drag relation. Driving a hydrodynamic model with pseudo-wind is equivalent to driving this model directly with the surface stress of the atmospheric model (ignoring possible different treatment of the air density).

We motivate the use of the pseudo-wind as follows:

1. Differences in drag relation between a hydrodynamic model and an atmospheric model are corrected for.
2. Results of hydrodynamic model simulations driven by two atmospheric models that apply different drag relations can be compared easier.
3. Pseudo-wind is an intuitive way to interpret differences in surface stress, as most people are more familiar with differences in wind speed than in surface stress.

From a given friction velocity the pseudo-wind is calculated as follows. From the friction velocity, first the roughness length, z_0, is calculated according to the reference drag

relation. In this example we apply a standard Charnock relation (complemented with viscous effects):

$$z_0 = \alpha \frac{u_*^2}{g} + 0.11 \frac{\upsilon}{u_*} . \tag{3.2}$$

The roughness length is then used to calculate the corresponding drag coefficient:

$$C_d = \left(\frac{k}{\ln(z/z_0)} \right)^2 , \tag{3.3}$$

where we combined the logarithmic wind profile with the definition of the drag coefficient. Finally, the latter is also used to calculate the pseudo-wind

$$U = \frac{u_*}{\sqrt{Cd}} . \tag{3.4}$$

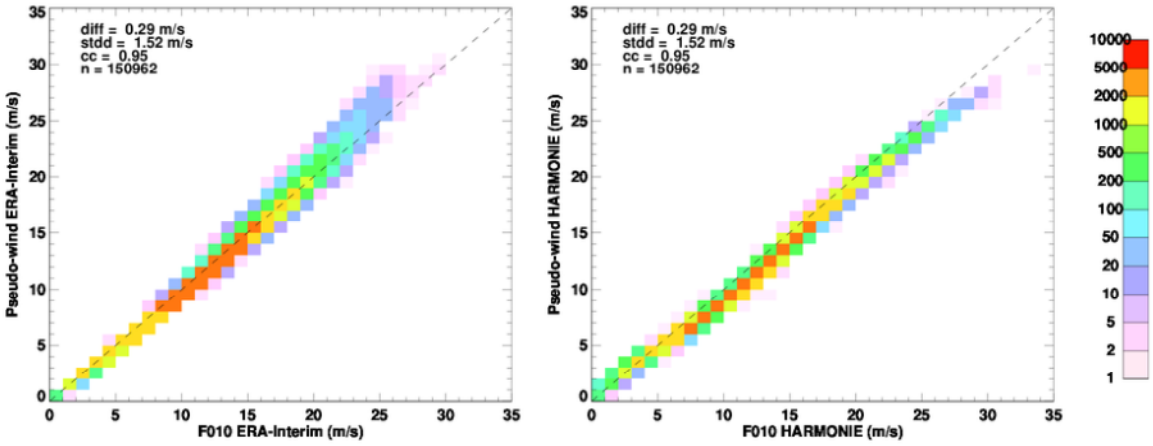

Figure 5.4. Relation between pseudo-wind and real wind for ERA-Interim (left) and HARMONIE (right). The colours indicate the number of occurrences for each bin.

Figure 5.4 shows the relation between the pseudo-wind and the real wind for ERA-Interim and HARMONIE, using a Charnock relation with α=0.032 as a reference drag relation. Clearly, for high wind speeds in ERA-Interim the pseudo-wind is higher than the real wind, while for HARMONIE the opposite is true. This is direct consequence of the different drag relations applied by the models: as can be seen in Figure 2.1, for high wind speeds the ERA-Interim drag relation is *above* the line that represents the Charnock relation with α=0.032, while the HARMONIE drag relation is *below* this line.

Baas and Van den Brink (2014) conclude that differences in wind speed between HARMONIE and ERA-Interim far from the coast can for a large part be explained by

differences in the applied drag relation. Due to the coarse resolution of ERA-Interim, wind speed differences are large in coastal areas and over Lake IJssel. In these areas, ERA-Interim values are contaminated by land surface. For cases of 8 Bft and higher, the difference may increase to 5 m/s both for the real and the pseudo-wind.

5.1.4 Comparison with observations

In Section 4, the HARMONIE wind fields for the 16 test-set storms were compared with available observations. Here, we include ERA-Interim in the comparison. The evaluation is done following similar procedures as in Section 4, except that we now only include HARMONIE forecasts with a lead time of 6 h. For ERA-Interim bilinear interpolation to the station locations has been performed.

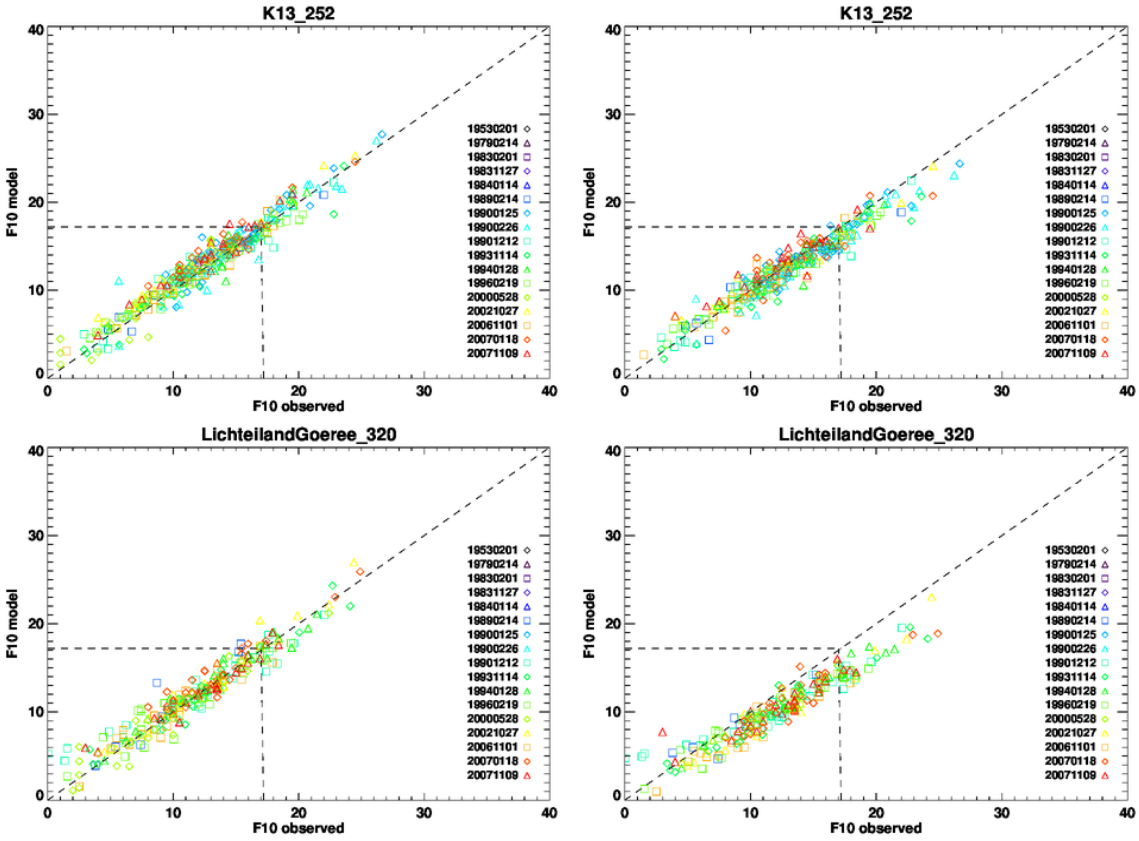

Figure 5.5. Scatter plots of modelled versus observed 10-m wind speed for HARMONIE (left) and ERA-interim (right) for K13 (top) and Lichteiland Goeree (bottom). Dashed lines represent the 1:1 line and the 8 Bft threshold value of 17.2 m/s.

Section 5.1.2 demonstrated that far from the coast the modelled wind speed is slightly higher in HARMONIE than in ERA-Interim and that this difference increases in coastal areas. For both regions we choose a station from the KNMI network to identify which of the two models is closest to reality. As such, Figure 5.5 presents scatter plots of modelled

versus observed wind speeds for two KNMI stations. The top panel shows data for K13, which is located at open sea, while the bottom panels show data for Lichteiland Goeree, which is located close to the coast. For both locations, HARMONIE performs very well. At K13 ERA-Interim performs well up to about 8 Bft. Higher wind speeds are underestimated by ERA-Interim. At Lichteiland Goeree ERA-Interim underestimates the observed wind systematically, which is due to the vicinity of the coast. We conclude that both over open sea as well as in the coastal region HARMONIE performs better than ERA-Interim.

Figure 5.6 presents the overall bias of the 10-m wind speed for stations of the KNMI network for the 16 simulated storm periods. No threshold on wind speed was imposed. This Figure shows that the HARMONIE wind fields have a slightly positive bias. For the open-water stations, the bias in ERA-Interim is generally negative. Variations between stations are larger for ERA-Interim than for HARMONIE, which is a direct consequence of the much coarser land-sea mask. The latter is probably also responsible for the overestimation of the wind speed for some land stations in ERA-Interim. For most of the stations, the rms difference is clearly smaller in HARMONIE than in ERA-Interim. From this we conclude that the high resolution of HARMONIE enables a more direct evaluation with wind observations of individual stations than the coarse resolution ERA-Interim.

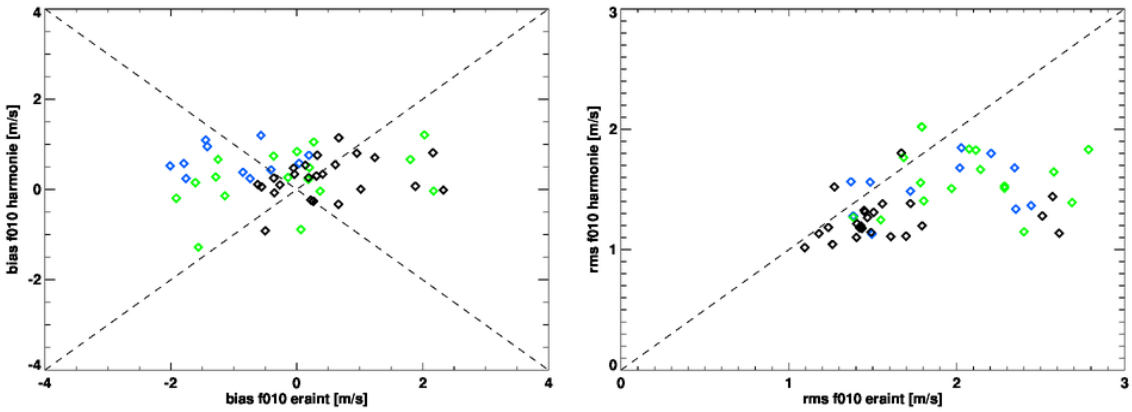

Figure 5.6. Bias (left) and rms error (right) scores of HARMONIE versus ERA-Interim based on station observations for the 16 test-set storm periods. Blue points indicate open-water stations, green point stations located at the coast, and black point station located inland. The dashed lines indicate 1:1 lines (in an absolute sense).

For the 16 test-set storms, Figure 5.7 presents biases for stations of the KNMI network (model – observations) including only data for which or the model data or the observation exceeds the 8 Bft threshold. Only stations with more than five data points are shown. Over land, this criterion is met at only a few station. This comparison makes clear that both at open sea and close to the coast the HARMONIE winds are closer to the observations then the ERA-Interim winds. Note that also over land the extreme winds are higher in HARMONIE than in ERA-Interim.

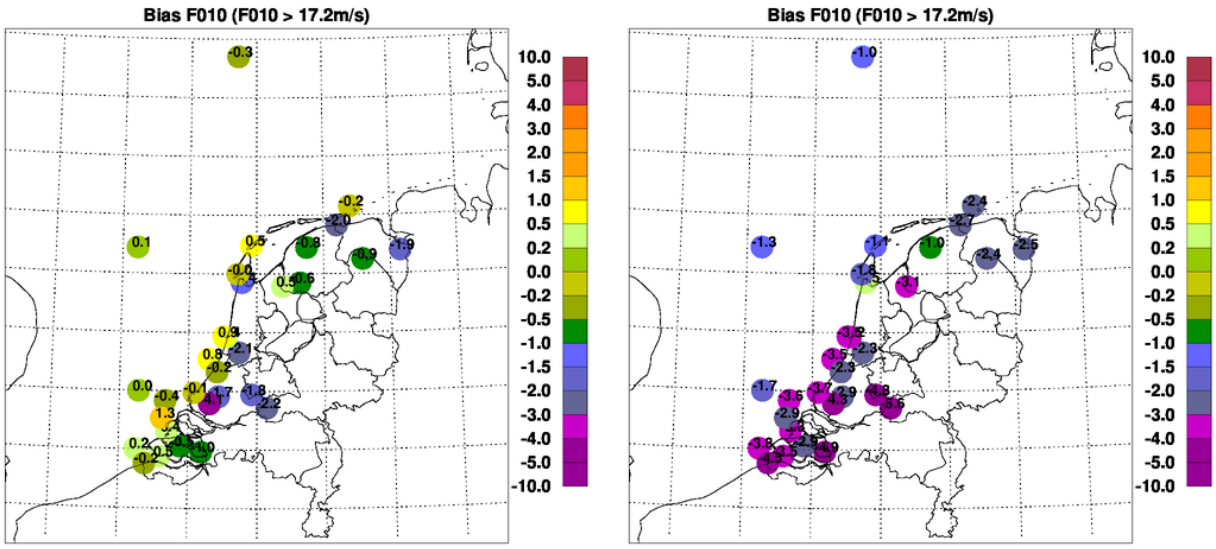

Figure 5.7. Bias (model – observations) between modelled an observed 10-m wind speeds for HARMONIE (left) and ERA-Interim (right) for stations of the KNMI network. Only data of 8 Bft and higher are included.

5.1.5 Identification of areas with highest benefit

Previous Sections have demonstrated that coastal areas benefit most from the increased resolution. These results are in line with what can be expected from inspecting the difference in land sea mask between the two models. Figure 5.8 shows the difference in water fraction between HARMONIE and ERA-Interim. This difference is largest in the coastal zone. The larger the difference, the larger is the improvement of using HARMONIE for wind and stress compared to ERA-Interim. Especially the coastal zone and Lake IJssel will benefit from the high resolution of HARMONIE. For instance, this leads to 25% higher wind in HARMONIE than in ERA-Interim for all wind speed classes. This implies that modelled surges will be order 50% higher (assuming a quadratic relation between the wind and surge).

Avoiding contamination by land points in ERA-Interim is not straightforward. A big advantage of HARMONIE is that we do not need to bother on these issues, at least not at scales larger than a few kilometres.

One could argue that increasing the horizontal resolution is nothing more than refining the land-sea mask. However, by demonstrating that HARMONIE is able to represent a) direction-dependent wind speed patterns over Lake IJssel (see Figure 3.14) and b) the impact of atmospheric stability on the wind field (at least in a qualitative way), Section 4.6 showed that the high resolution of HARMONIE has also a positive impact on the physical and dynamical realism of the model output.

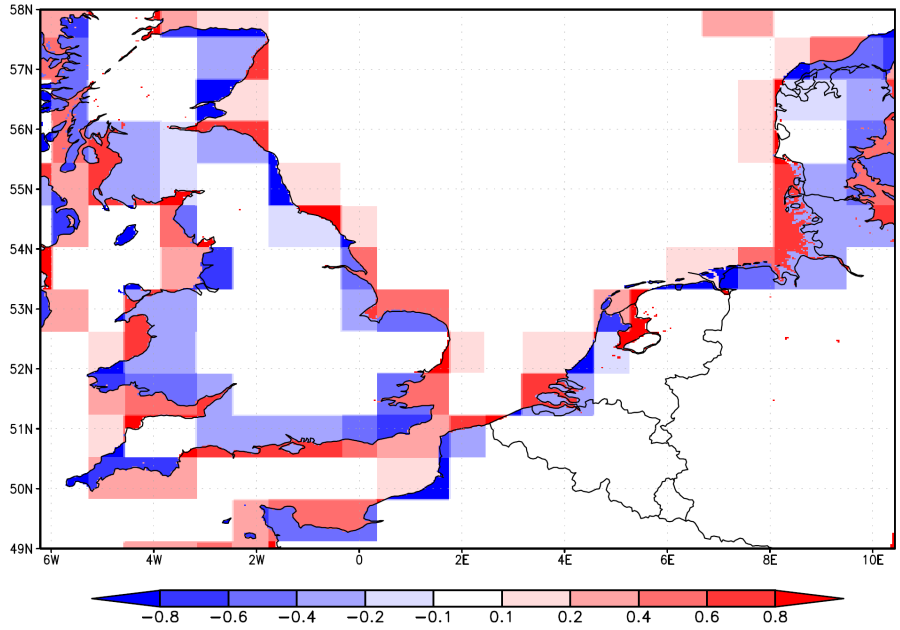

Figure 5.8. Difference in water fraction between HARMONIE and ERA-Interim.

The results presented here are in line with findings of Reistad *et al.* (2011) who performed a dynamical downscaling of the ERA-40 reanalysis dataset using the HiRLAM model. In a comparison against in-situ and satellite observation they found a significant improvement in mean values and upper percentiles of wind vectors and the significant wave height over ERA-40. Apart from the expected improvement in coastal areas, they also showed the low bias in ERA-40 had disappeared in the downscaled simulations. After dynamical downscaling the NCEP-NCAR reanalysis with a higher resolution regional model, Winterfeldt and Weisse (2009) and Winterfeldt *et al.* (2010) found only added value in coastal areas and not in the open ocean. A similar approach as in the present report was followed by Frank and Majewski (2006) who performed hindcasts of 21 historical storms that caused high surges in Northwest Germany. They conclude that high-resolution models add significant value, especially in coastal regions, and that the hindcast simulations are a suitable tool for studying extreme weather events from the past. A general overview of the benefits of using higher resolution models for downscaling global model data is presented by Feser *et al.* (2011).

5.2 Results and discussion of WAQUA runs for the 17 test-set storms

Since the modelled wind and stress fields will be used as input for hydrodynamic models, this report also assesses the added value of the high-resolution model for the prediction of storm surges along the coast. We anticipate that if the high-resolution wind fields have a positive effect on the prediction of such a large-scale quantity as the surge, it is very likely that there will also be a positive impact for smaller water bodies like Lake IJssel. The hydrodynamic model of choice is WAQUA (Verboom *et al.* 1992; De Vries, 2000). For each of the 17 test-set storms the surge along the Dutch coast was calculated using pseudo-winds (effectively the surface stress, see Section 5.1.3) as input for the WAQUA

model. More detail on this model and the simulation strategy can be found in Baas and Van den Brink (2014).

Figure 5.9 shows scatter plots of the maximum modelled skew surges at Vlissingen and Delfzijl against the observed maxima for the 17 selected storms. The scatter plots for some other coastal stations are given in APPENDIX D. Several statistical quantities are summarized in Table 5.1. It shows that for all presented quantities and stations, HARMONIE performs consistently better than ERA-Interim. The best quality is reached for Vlissingen; the worst performing station is Delfzijl.

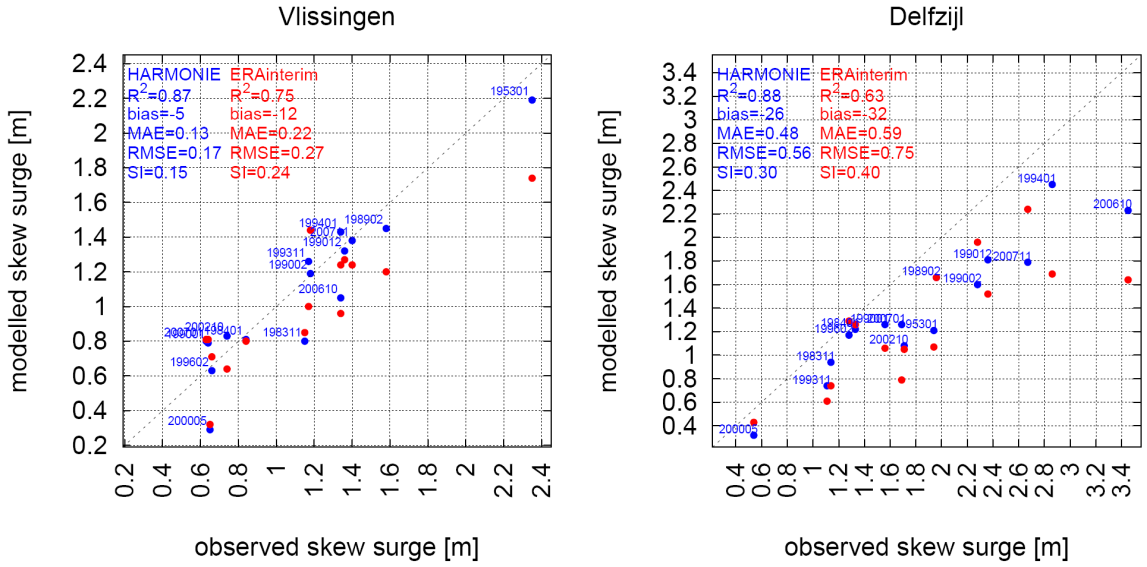

Figure 5.9. Scatter plots of the maximum skew surge at Vlissingen (left) and Delfzijl (right) for the 17 events as modelled by HARMONIE (blue) and ERA (red).

For Delfzijl both HARMONIE and ERA-Interim underestimate the observed skew surges. This is mainly due to the poor performance of WAQUA for Delfzijl, caused by the complex estuary around Delfzijl. The use of the pre-operational, high-resolution version of WAQUA (called DCSMv6) improves only the representation of Delfzijl considerably (Baas and Van den Brink, 2014).

Table 5.1. Comparison of the HARMONIE and ERA-Interim-driven surges as calculated with WAQUA. The left numbers represent the results for HARMONIE, the right numbers for ERA-Interim.

	Hoek van Holland	Vlissingen	IJmuiden	Harlingen	Delfzijl
R^2 [-]	0.91 / 0.87	0.87 / 0.75	0.89 / 0.78	0.87 / 0.77	0.88 / 0.63
Bias [%]	-11 / -18	-5 / -12	-14 / -22	-17 / -23	-26 / -32
MAE [m]	0.20 / 0.26	0.13 / 0.22	0.22 / 0.34	0.33 / 0.44	0.48 / 0.59
RMSE [m]	0.25 / 0.35	0.17 / 0.27	0.30 / 0.43	0.37 / 0.50	0.56 / 0.75
Scatterindex[5] [-]	0.19 / 0.28	0.15 / 0.24	0.22 / 0.31	0.20 / 0.26	0.30 / 0.40

[5] The scatter index is defined as the rms error divided by the mean

6 Analysis of water-land wind speed ratios

In the current WTI practice, extreme wind fields over sea are obtained by converting land-based observation to open water wind by correcting for differences in roughness length. This is done by assuming a logarithmic wind profile (neutral conditions). An overview of the procedures is given by De Waal (2010). In this Section we analyse to what extent stability influences the water to land wind speed ratio including a comparison with HARMONIE model output. Following Baas and De Waal (2012), observed water to land ratios are compared with those modelled by HARMONIE and a simple two-layer model.

6.1 Yearly and diurnal cycles

Inspired by the work of Wieringa and Rijkoort (1983) we first consider the seasonal and daily cycle of the wind speed ratio between IJmuiden and Schiphol. As we include only westerly winds, IJmuiden can be considered an open water location. Figure 6.1 shows the averaged wind speed for every month of the year and for every hour of the day for the two locations. Figure 6.1a shows that over sea the diurnal cycle is virtually absent the whole year. This is a result of the large thermal inertia of the water surface. In winter the wind speeds are larger than in summer because of the enhanced synoptic activity (Coelingh *et al.* 1996). In contrast, over land a clear diurnal cycle is present, which is most prominent in the summer months (Figure 6.1b).

Obviously, the sea-land wind speed ratio varies as a function of time of day and time of year. As shown in Figure 6.1c, it exhibits a maximum during summer nights (when the wind over land is reduced by stable stratification) and a minimum in spring early afternoon. By this time of the year, the SST is still close to its minimum value leading to stably stratified conditions (Coelingh *et al.* 1996). This reduces the near-surface wind speeds over sea. In contrast, as the land surface warms much faster than the sea surface, convective mixing enhances the early spring wind speeds over land. In autumn the opposite is true. Then the combination of high SST and a cooling atmosphere lead to relatively high wind speeds over sea. We conclude that around noon the ratio between the wind speed over sea and over land varies by as much as 25% between its minimum in April and its maximum in November.

As we are primarily interested in strong winds, we also calculated the sea to land wind speed ratio including only those cases for which the wind speed over sea was larger than 13.9 m/s (at least 7 Bft). The result is presented in Figure 6.1d. The difference with Figure 6.1c, which includes all data, is surprisingly small. Apparently, even for high wind speed cases the sea-land wind speed ratio shows clear diurnal and yearly variations.

These results indicate that large errors are introduced in the conversion of land-based winds to open water when stability is ignored.

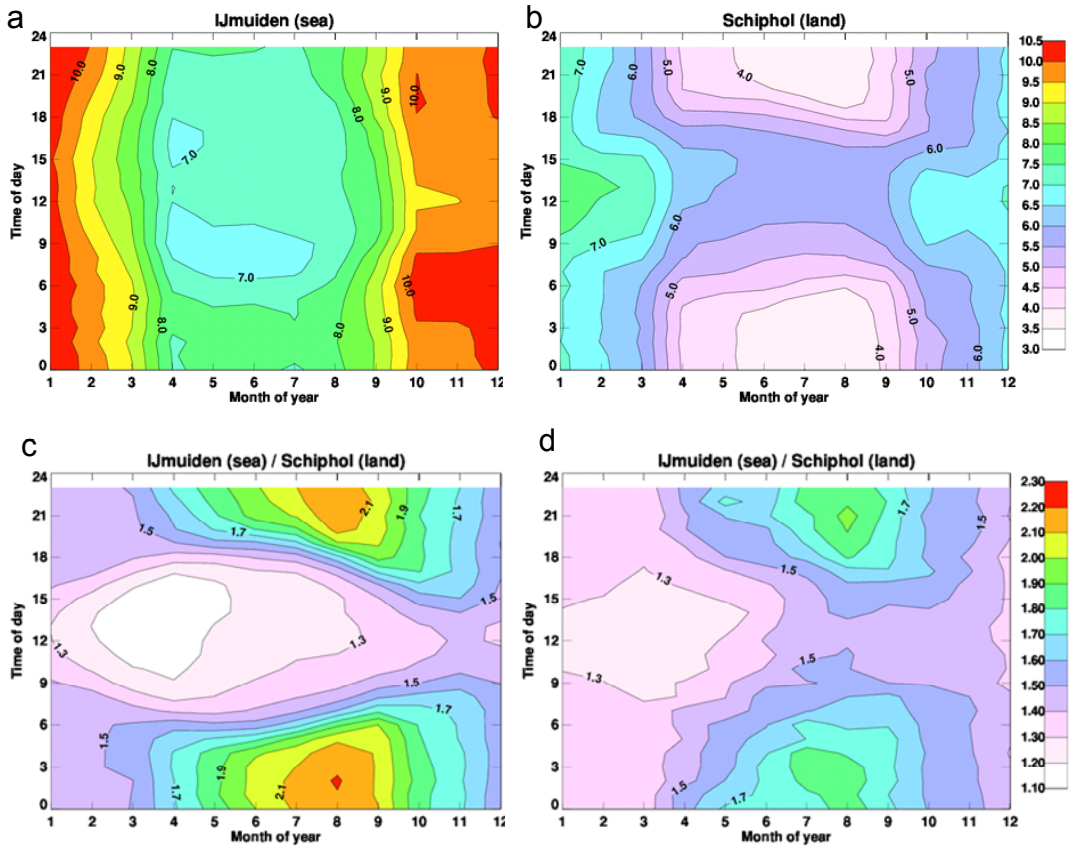

Figure 6.1. Yearly and diurnal cycle of the 10-m wind speed at IJmuiden (a) and Schiphol (b). Yearly and diurnal cycle of the IJmuiden/Schiphol wind speed ratio including all wind speeds (c), and only cases that exceed the 7 Bft threshold value of 13.9 m/s (d). Only westerly winds are included.

6.2 The relation with stability

Sea to land wind speed ratios were calculated using 30 years of hourly observations from the stations IJmuiden and Schiphol. Figure 6.2a presents bin-averages of this sea to land ratio as a function of the observed temperature difference between the air and the sea surface. Only data with onshore flow conditions are included. When the conditions over sea become more stable, the sea to land wind speed ratio decreases. Only data of 7 Bft or higher are shown. Figure 6a shows that even for cases of 9 Bft the sea/land ratio decreases systematically with stability. To quantify the impact of stability, linear best fits and the associated trends are included in Figure 6.2. The numbers indicate that the sea/land wind speed ratio decreases with order 5% for each degree of air-water temperature difference. Comparable results were obtained for other station pairs.

Figure 6.2b shows the wind speed ratio between IJmuiden and Schiphol as diagnosed from HARMONIE output. As in the observations, the ratio between the two stations decreases with increasing temperature difference. The modeled trends are persistently

smaller than the observed ones. One reason for this underestimation is the fact that the impact of stability on the near-surface wind over sea is too small (Figure 4.16).

In this analysis, we neglect the variations of stability over land. Experiments with different selection criteria (for example only including daytime data) show that the magnitude of the observed trends may vary, but that the general pattern of Figure 6.2a remains.

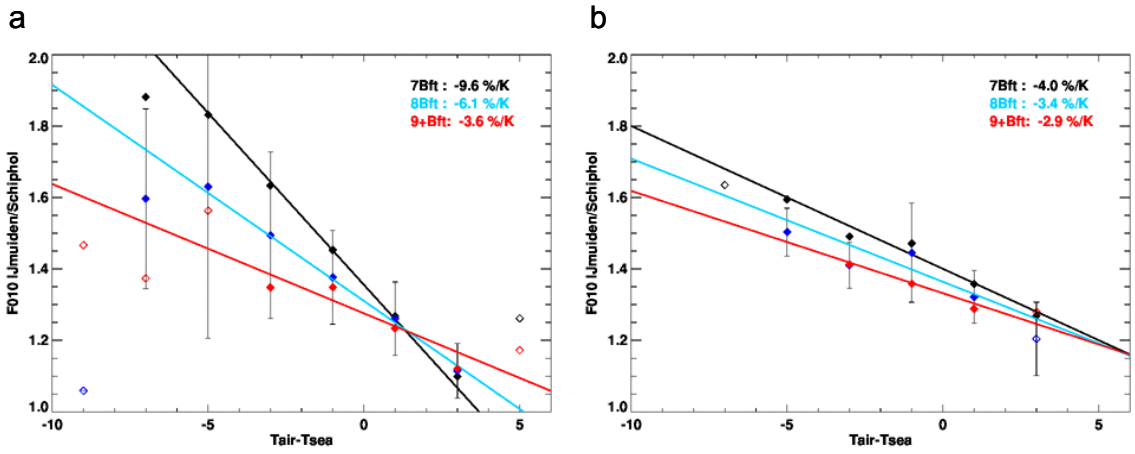

Figure 6.2. Observed (a) and modeled (b) IJmuiden/Schiphol 10-m wind speed ratio as a function of the air-water temperature difference. Data for 7 (black), 8 (blue), and 9 Bft (red) are shown. For the 8 Bft class error bars that indicate one standard deviation are added. Bins with more/less than 10 data points included are indicated with closed/open symbols.

6.3 Comparison between HARMONIE and a two-layer model

For various station combinations, Baas and De Waal (2012) compared water-land speed ratios modelled by HARMONIE versus those obtained from a two-layer model. A summary of their findings is presented here.

Since the work of Wieringa and Rijkoort (1983), the concept of a simple two-layer model (2LM) has frequently been used in the analysis of Dutch wind measurements (e.g. Verkaik *et al.* 2003; Caires *et al.* 2009). Its basic formulas are presented in (Caires *et al.* 2009) and will not be reproduced here. The type of application of the 2LM in this report is rather basic: it consists of the translation of an observed local 10-m wind at a single location (on land) to another single location (having a large area of water in the upwind direction), similar to the analysis reported in Section 5.2 of Caires *et al.* 2009.

Additional assumptions made in the present analysis are:

- Directional roughness length information at the measurement locations is taken from tables applied in earlier SBW studies.
- The 10-m wind speed and direction at the land location are the measured values.

- The wind direction at the water location is assumed to be equal to the wind direction at the land location.
- Only for wind directions at the water location for which the local roughness length in the roughness table is smaller than 0.0002 m, the upwind area is assumed to be water. For other wind directions, a dummy value is attributed to the wind speed at the water location.
- Only at time steps for which all[6] wind speeds exceed a threshold of 10 m/s the water-land wind speed ratio is computed.

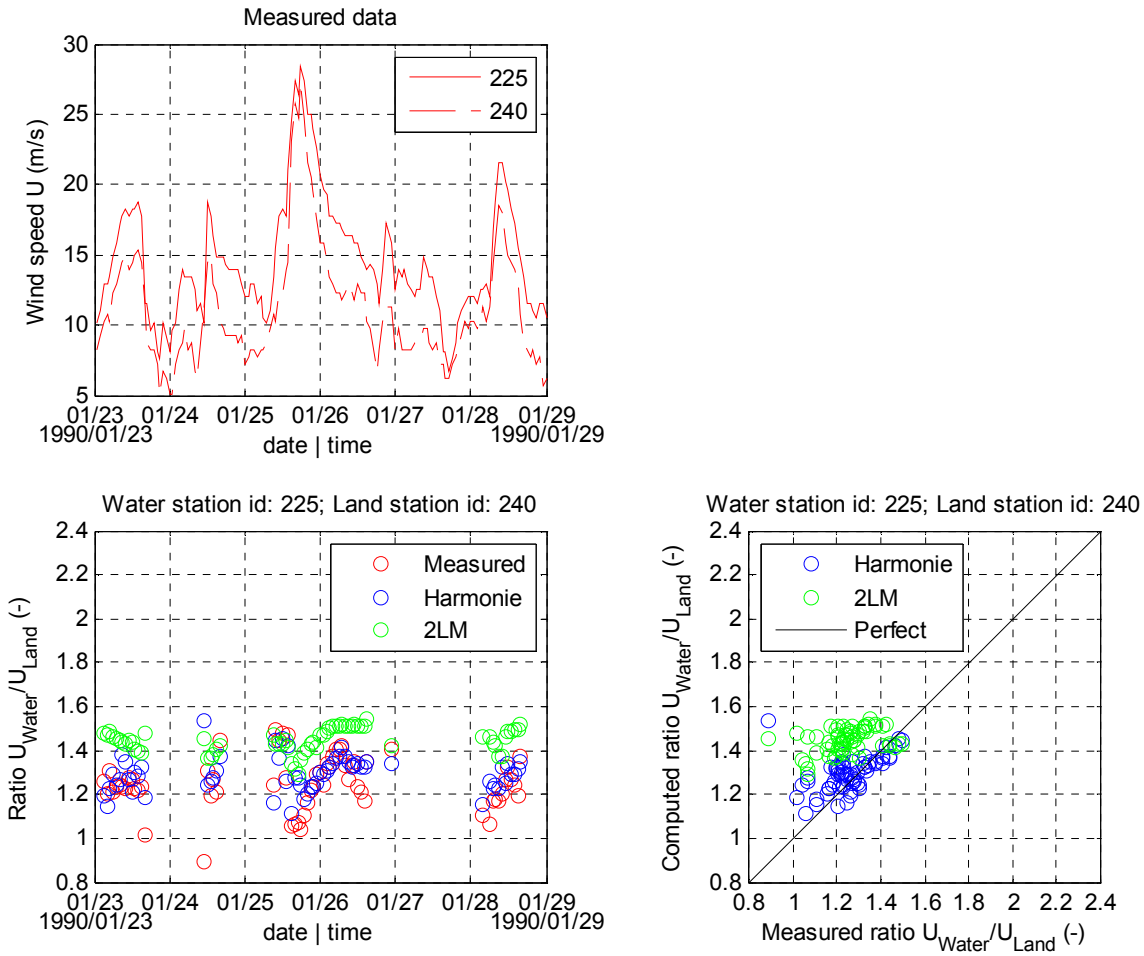

Figure 6.3. Water-land 10-m wind speed ratio for January 1990 for Schiphol (240) and IJmuiden (225).

[6] I.e. at both the land location and the water location, and from measurement, HARMONIE and 2LM results.

As an example, Figure 6.3 shows observed and modelled wind speed ratio's between IJmuiden (225) and Schiphol (240) for the period 23-29 January 1990. The top panel presents time series of observed wind speed for both locations. This indicates the most extreme (and therefore interesting) time windows within the overall time window. Time series of observed and modelled (both by HARMONIE and the 2LM) wind speed ratios are given in the bottom-left panel. The bottom-right panel shows the correlation between the computed and the observed ratios.

The following conclusions can be drawn:

- The measured ratio shows the largest variation, the ratio from 2LM the smallest, and the ratio from HARMONIE lies in between.
- The agreement between HARMONIE and the measurements is better than the agreement between 2LM and the measurements.
- In many cases the 2LM ratios are higher than the HARMONIE ratios

Most of these conclusions are as we expected. The ratios from the 2LM show the effect of difference in roughness only, whereas the ratios from HARMONIE show effects of spatial variation of weather systems and variations in atmospheric stability. Although scatter is rather large, Baas and De Waal show that an evaluation with various other station pairs leads to similar conclusions.

7 Conclusions and recommendations

This report is part of the KNMI-Deltares project 'WTI Wind modelling', which aims to determine a reliable and detailed extreme-wind climatology for The Netherlands (Groeneweg *et al.* 2009). While in the past open-water winds were derived from spatially interpolating sparse point observations, the current project investigates the application of a high-resolution atmospheric model. The HARMONIE model, which has a grid-spacing of 2.5 km, has been selected to perform the simulations.

The present report is the final report of Work Package 1 (WP1) of the Wind Modelling project, summarizing all relevant findings and conclusions of the interim reports that have been published before (Groen and Caires, 2011; Baas and De Waal, 2012; Van den Brink et., 2013, Baas, 2013; Baas and Van den Brink, 2014). WP1 deals with assessing the high-resolution model with specific attention to the spatial and temporal structures of the modelled wind fields.

We rate the overall model results as good. As such, we conclude that, although at some points further evaluation can be done, the model is suitable to be used as it is in Work Packages 2 and 3 of the Wind Modelling project and that it provides a strong basis for further use in the WTI program.

7.1 Conclusions

To assess the quality of the wind fields of the HARMONIE model, simulations of 16 historical storms have been performed. This test-set of storms has been composed in such a way that it contains the most relevant events of the period 1979-2012 from the perspective of the WTI program.

A HARMONIE model environment was set-up that has been used for the simulation of the 16 test-set storms. This model set-up will be used in the remainder of the Wind Modelling project.

Based on a verification with observations, the wind fields produced by the model are realistic, especially over open water. Temporal and spatial characteristics are reproduced well. The added-value of the high-resolution model is most notable in coastal areas and for large inland water bodies like Lake IJssel. Storm surge calculations with the WAQUA model demonstrate the water levels predicted from HARMONIE output are consistently closer to observed water levels than when model output from ERA-Interim is used.

Specific conclusions are listed below following the order of the report.

Temporal evolution

- Temporal correlation between modelled and observed wind speed is 0.95 over sea. Over land values are slightly smaller, differences between stations are small (Section 4.3.2.1).
- Over sea, modelled wind speeds show a positive bias of about 0.5 m/s. For most stations, the rms difference is between 1.5 and 2.0 m/s. These numbers are independent of the wind speed. The bias in wind direction is a few degrees, rms scores range from 15° when all data are taken into account to order 10° for winds of 8Bft and higher. These numbers are rather similar to those derived in operation practice. Note that the observational error is about 1 m/s in the wind speed and 10° in wind direction (Section 4.3.2.1).
- Over land, differences between stations are higher. When all data are considered the wind speed bias is mostly close to zero with rms difference between 1.0 and 1.5 m/s. For wind speeds of 8 Bft and higher generally a negative bias of about 2 m/s is identified with rms differences varying from 1.5 to 4 m/s. This corresponds to an underestimation of the wind speed of about -10% (Section 4.3.2.1).
- There is no trend in the scores for the 16 storms, indicating that the quality of the modelled wind fields is constant over time. For relatively small, quickly developing systems with the centre of low pressure passing close to The Netherlands the difference with observations is largest (Section 4.3.2.2).
- Hour-to-hour variations in the 10-m wind speed are reasonably captured by the model. Extreme changes are clearly underestimated (Section 4.1.2.3).

Spatial patterns

- Spatial correlation between observations valid at the same time amounts 0.87 on average. A comparison with scatterometer data gives a comparable number (Section 4.3.3).
- HARMONIE represents spatial gradients between a selection of stations in 10-m wind speed rather well (Section 4.3.3).
- Modelled extreme geostrophic wind speeds (i.e. pressure gradients) are smaller than observed. This underestimation is uncorrelated with the underestimation of the 10-m wind over land (Section 4.3.3).
- Bias and rms difference scores based on satellite winds over open water from Quikscat agree with scores derived from station observations (Section 4.3.4).

Production runs

- A preliminary analysis of the long-term production runs with station observations shows that these simulation have the same quality as the model simulations of the 16 test-set storms (Section 4.4).

Atmospheric stability

- Vertical profiles as observed along three tall masts (two over open water, one inland) are reproduced satisfactory with HARMONIE. The model tends to underestimate the vertical wind shear (Section 4.5.1).

- A comparison of modelled and observed vertical wind speed ratios indicates that HARMONIE represents the boundary layer in a realistic way. The impact of stably stratified conditions is obviously present, but compared to observations the effect is too low (Section 4.5.2).
- A model sensitivity study indicates that even in storm conditions the 10-m wind over sea may vary by 10% depending on the air – sea temperature difference.

Inland water bodies

- As over sea, the modelled wind speed over Lake IJssel and the Wadden Sea is higher than observed. This conclusion is based on a comparison of model output with data from measuring locations operated by Rijkswaterstaat. Overall, for conditions of 8 Bft and higher, the modelled wind speeds over Lake IJssel are 5-10% higher than observed. For the Wadden Sea the overestimation difference is 0-5%. (Section 4.6.1.1).
- HARMONIE is able to represent the impact of atmospheric stability on the wind patterns over Lake IJssel realistically. However, in comparison with observations the impact of stability is underestimated (Section 4.6.1.2).
- Smaller inland water bodies like the Veluwe Randmeren are not explicitly resolved by HARMONIE. To obtain realistic near-surface winds a correction is needed that compensates for the generally too large roughness length that is used by the model. (Section 4.6.2)

Surface stress and relation between HARMONIE and ERA-Interim

- Differences in the evolution of the storm depressions are small between HARMONIE and ERA-Interim. On average, the minimum surface pressure of the storm depressions is 1.4 hPa lower in HARMONIE than in ERA-Interim. The maximum 10-m wind speed is systematically higher in HARMONIE than in ERA-Interim. The difference increases for higher wind speeds (Section 5.1.1).
- Far from the coast, the 10-m wind speeds in HARMONIE are higher than in ERA-Interim by 0.5-1 m/s. As a consequence of the coarse resolution of ERA-Interim, this difference increases to 3-4 m/s in coastal areas and over Lake IJssel. (Section 5.1.2).
- Differences in surface stress are smaller than differences in wind speed. This is a consequence of the different drag relations that are used in HARMONIE and ERA-Interim, which is demonstrated by introducing the so-called pseudo wind. The pseudo-wind is a translation of a surface stress to a 10-m wind speed using a reference drag relation (Section 5.1.3).
- HARMONIE winds verify better with station observations than ERA-Interim winds, especially for high wind speeds (Section 5.1.4).
- Coastal areas and large inland water bodies like Lake IJssel benefit most from the high-resolution model due to the much better representation in the land-sea mask. In these areas, wind and surface stress values of ERA-Interim become less accurate as a result of the coarse resolution (Section 5.1.5).
- Storm surge predictions from the WAQUA model are closer to observations when HARMONIE surface stress is used than when ERA-Interim surface stress is used (Section 5.2).

Sea to land wind speed ratios

- For westerly winds, the observed wind speed ratio between IJmuiden (sea) and Schiphol (land) show a significant daily and yearly cycle. Around noon, this ratio between the wind speed over sea and over land varies by as much as 25% between its minimum in April and its maximum in November (Section 6.1).
- Both HARMONIE and observations show an increased (decreased) near-surface wind over open water in case cold (warm) air flows over warmer (cooler) water. In this case, the water/land wind speed ratio is increased (reduced) (Section 6.2).
- Observed IJmuiden to Schiphol wind speed ratios were compared to those produced by HARMONIE and by a simple two-layer model (2LM). The agreement between HARMONIE and the measurements is better than the agreement between 2LM and the measurements (Section 6.3).
- In many cases the 2LM ratios are higher than the HARMONIE ratios and too high compared to the observations (Section 6.3).

7.2 Recommendations

To establish the value of the high-resolution model for the determination of the HBCs in more detail, we suggest the following

- The HARMONIE model can be used in Work Packages 2 and 3 of the Wind Modelling project. As it is, it provides a solid basis for further work.
- When using the HARMONIE wind fields to drive hydrodynamical models, special attention should be paid to the consequences of the overestimation of the wind speed over Lake IJssel.
- By means of a statistical upscaling technique, HARMONIE wind fields will be transformed to the normative conditions that are needed for deriving the hydraulic boundary conditions. In the end-phase of the project a comparison of the thus obtained wind fields with those derived from the current practice of interpolating point measurements is needed.
- The underestimation of extreme wind speeds over land remains an intriguing topic for further research. Model development, focusing on the representation of the boundary layer and the air-surface interaction, is needed to better understand the causes of this general model problem.
- In many cases, differences exist in the modelling of the air-sea interaction of hydro-dynamic models and atmospheric models that are used to drive those. This mismatch may lead to ambiguous results. It would be more consistent to drive the hydro-dynamic models with the surface-stress of the atmospheric models rather than with the 10-m wind. In the end, we advocate the use of coupled models in which the interaction between the atmosphere and the water surface is explicitly taken into account.

References

Baas, P., 2013. Evaluation of HARMONIE simulations for 16 historical storms. Avalilable online at http://www.knmi.nl/publications/fulltexts/conceptreport_harmonie_evaluation _20130722.pdf

Baas, P. and H. De Waal, 2012. Interim report on the validation of HARMONIE, Technical Report 1204199-004-HYE-0004 Deltares.

Baas, P. and H. van den Brink, 2014. The added value of the high-resolution HARMONIE model for deriving the HBCs. Available online at publicaties.minienm.nl/download-bijlage/61534/report-dec13-added-value-20140207-final.pdf

Baas P., Bosveld F., and Burgers G. 2014. How atmospheric stability affects the near-surface wind over sea in storm conditions. Submitted to *Wind Energy*.

Barthelmie, R.J., 1999 The effect of atmospheric stability on coastal wind climates. *Meteorol. Appl.*, 6: 39-47.

Beljaars, A.C.M., and A.A.M. Holtslag, 1991. Flux parameterization over land surfaces for atmospheric models. *J. Appl. Meteor.*, 30, 327-341.

Benschop, H., 1996. Windsnelheidsmetingen op zeestations en kuststations: herleiding waarden windsnelheid naar 10-m niveau, KNMI TR-188, 16pp.

Bidlot J.-R., Janssen P, and Abdalla S. 2007. 'Impact of the revised formulation for ocean wave dissipation on the ECMWF operational wave model'. Tech. Memo. 509, ECMWF: Reading, UK.

Bottema, M., 2007. Measured wind-wave climatology Lake IJssel (NL). Main results for the period 1997-2006. Report RWS RIZA 2007.020, July 2007. Available online at: http://english.verkeerenwaterstaat.nl/kennisplein/3/5/359788/Measured_wind-wave_climatology_lake_IJssel_(NL)-main_results_for_the_period1.pdf.

Caires, S., De Waal, H., Groen, G., Wever, N., Geerse, C., 2009. Assessing the uncertainties of using land-based wind observations for determining extreme open-water winds. SBW-Belastingen: Phase 1b of subproject "Wind modelling". Deltares report 1200264-005, October 2009.

Charnock, H., 1955. 'Wind stress on a water surface'. *Q. J. Roy. Met. Soc.*, 81, 639-640.

Coelingh, J.P., A.J.M. Van Wijk, and A.A.M. Holtslag, 1996. Analysis of wind speed observations over the North Sea. *J. Wind Eng. Ind. Aero.*, 61, 51-69.

De Vries, J.W. 2000. `A concise evaluation of water level forecasts from WAQUA/CSM-8', Technical Report memorandum WM-00-01 KNMI.

De Rooy, W.C., Kok, K., 2004. A combined physical-statistical approach for the downscaling of model wind speed. *Weather and Forecasting*, 19, 485-495.

De Waal, H. , 2010. Spatial wind input for HBC production runs. SBW-Belastingen. Phase 3 and conclusions of subproject "Wind modelling". Deltares Report 12000264-005 (Phase 3).

Dee, D.P, *et al.* 2011. The ERA-Interim reanalysis: configuration and performance of the data assimilation system. *Q. J. Roy. Met. Soc.*, 137, 553-597.

Feser, F., B. Rockel, H. von Storch, J. Winterfeldt, and M. Zahn, 2011. Regional Climate Models Add Value to Global Model Data: A Review and Selected Examples. *Bull. Amer. Meteor. Soc.*, 92, 1181–1192.

Frank, H.P., and D. Majewski, 2006. Hindcasts of historic storms with the DWD models GME, LMQ and LMK using ERA-40 reanalysis. *ECMWF Newsletter*, 109, 16-21.

Groen, G. and Caires, S. 2011. 'Selection of historical storms for atmospheric model validation. SBW-HB Wind modelling', Technical Report 1204199-004 KNMI/Deltares.

Groeneweg, J., Burgers, G., Caires, S., and Feijt, A. 2011. 'Plan of approach SBW wind modelling. SBW - Belastingen', Technical Report 1202120-003 Deltares.

Groeneweg, J., Burgers, G., and Caires, S. 2012a. 'Adjusted Planning SBW Wind', Technical report RWS.

Groeneweg, J., S. Caires, and C. Roscoe, 2012b. Temporal and spatial evolution of extreme events. Proceedings of 33rd Conference on Coastal Engineering, Santander, Spain, 2012.

Le Moigne, P., 2012. Surfex scientific documentation. Available online at www.cnrm.meteo.fr/surfex/IMG/pdf/surfex_scidoc_v2.pdf.

Lindenberg, 2011. A verification study and trend analysis of simulated boundary layer wind fields over Europe. PdD thesis, Helmholz-Zentrum Geesthacht, 116pp.

Lopez de la Cruz, J., A. Tijssen, and J. Beckers, 2010. The Evolution of Storms on the Wadden Sea. Deltares Report 120064-004-HYE-0012.

Masson, V. and Y. Seity, 2009. Including atmospheric layers in vegetation and urban offline surface schemes. *J. Appl. Met. Clim.,* 48, 1377–1397.

Paulson, C.A., 1970. The Mathematical Representation of Wind Speed and Temperature Profiles in the Unstable Atmospheric Surface Layer. *J. Appl. Meteor.*, 9, 857–861.

Portabella, M., and A. Stoffelen, 2009. On scatterometer ocean stress. *J. Atm. Ocean Tech.*, 26, 368-382.

Reistad, M., Ø. Breivik, H. Haakenstad, O. J. Aarnes, B. R. Furevik, and J.-R. Bidlot, 2011. A high-resolution hindcast of wind and waves for the North Sea, the Norwegian Sea, and the Barents Sea. *J. Geophys. Res.*, 116, C05019.

Royal Netherlands Meteorological Institute, 2001. Handboek Waarnemingen, http://www.knmi.nl/samenw/hawa/.

Sathe, A., S.E. Gryning, and A. Peña, 2011. Comparison of the atmospheric stability and wind profiles at two wind farm sites over a long marine fetch in the North Sea. *Wind Energy*, 14, 767-780.

Seity, Y., Brousseau, P., Malardel, S., Hello, G., Bénard, P., Bouttier, F., Lac, C., Masson, V., 2011. The AROME-France convective-scale operational model. *Mon. Wea. Rev.*, 139, 976-991.

Tammelin, B. *et al.* 2011. Production of the Finnish wind atlas. *Wind energy*, 16, 19-35.

Van den Brink, H., P. Baas, and G. Burgers, 2013. Towards an approved model set-up for HARMONIE. Available online at htttp://www.knmi.nl/publications/fulltexts/towards_an_approved_model_setup_for_harmonie_sbw_milestone1_final.pdf

Van den Brink, H., 2014. Strategy for the selection of events relevant for the determination of the hydraulic boundary conditions.

Van Wijk, A.J.M., A.C.M. Beljaars, A.A.M. Holtslag, and W.C. Turkenboom, 1990. Evaluation of stability corrections in wind speed profiles over the North Sea. *J. Wind Eng. Ind. Aero.*, 33, 551-566.

Verboom, G.K., de Ronde, J.G., and van Dijk, R.P 1992. `A fine grid tidal flow and storm surge model of the North Sea', *Continental Shelf Research,* 12, 213-233.

Verkaik, J.W., 2001. Documentatie wind metingen in Nederland. KNMI, January 2001.

Verkaik, J., A. Smits, A., and J. Ettema, 2003. Wind Climate Assessment of the Netherlands 2003: Extreme value analysis and spatial interpolation methods for the determination of extreme return levels of wind speed. *KNMI-HYDRA project Phase report 9*. Available online at http://www.knmi.nl/samenw/hydra/documents/phasereports/ph09.pdf.

Verkaik, J.W., 2006. Downscaling of weather model forecasts. *On wind and roughness over land*, PhD thesis, Wageningen University, 69-92.

Vogelzang, J., A. Stoffelen, A. Verhoef, and J. Figa-Saldaña, 2011. On the quality of high-resolution scatterometer winds. *J. Geophys. Res.*, 116, C10033.

Waterwet 2009, www.helpdeskwater.nl/onderwerpen/wetgeving-beleid/waterwet.

Weill, A., Eymard, L., Caniaux, G., Hauser, D., Planton, S., Dupuis, H., Brut, A., Guerin, C., Nacass, P., Butet, A., Cloche, S., Pedreros, R., Durand, P., Bourras, D., Goirdani, H., Lachaud, G., and Bouhours, G. 2003. Toward a better determination of turbulent airsea fluxes from several experiments. *J Climate*, 16, 600–618.

Weisse, R., *et al.* 2009. Regional meteorological-maritime reanalysis and climate change projections. *Bull. Amer. Meteor. Soc.*, 90, 849-860.

Wever, N, Groen, G., 2009. Improving potential wind for extreme wind statistics. KNMI Scientific Report: WR2009-02, March 2009.

Wieringa J, P.J. Rijkoort, 1983. Windklimaat van Nederland. *Staatsuitgeverij*: Den Haag, 263pp.

Winterfeldt, J., and R. Weisse, 2009. Assessment of Value Added for Surface Marine Wind Speed Obtained from Two Regional Climate Models. *Mon. Wea. Rev.*, 137, 2955-2965.

Winterfeldt, J., B. Geyer, and R. Weisse, 2010. Using QuikSCAT in the added value assessment of dynamically downscaled wind speed. *Int. J. Climatol.*, 31, 1028-1039.

APPENDIX A. Overview of KNMI stations

Overview of KNMI observation sites. Columns show station codes, station names, location types (S = open water, C = coast, L = land), measuring heights if different from 10 m, data availability (0 = no data, - = suspicious data, 1 = used data), and the number of storms for which measurements of sufficient quality are available.

				19790214	19830201	19831127	19840114	19890214	19900125	19900226	19901212	19931114	19940128	19960219	20000528	20021027	20061101	20070118	20071109	# storms
391	Arcen	L		0	0	0	0	0	0	0	1	1	1	1	1	1	1	1	1	9
253	AUK-alpha	S	103.3	0	0	1	-	1	-	-	1	1	1	0	1	1	0	0	0	7
380	Beek	L		1	1	1	1	1	1	1	1	1	1	1	1	1	1	1	1	16
249	Berkhout	L		0	0	0	0	0	0	0	0	0	0	0	1	1	1	1	1	5
348	Cabauw	L		0	0	0	0	1	1	1	1	1	1	1	1	1	1	1	1	12
308	Cadzand	C	17.1	1	1	1	1	1	1	1	1	1	1	1	1	1	1	1	1	16
260	De Bilt	L	20	1	1	1	1	1	1	1	1	1	1	1	1	1	1	1	1	16
235	De Kooy	C		1	1	1	1	1	1	1	1	1	1	1	1	1	1	1	1	16
275	Deelen	L		1	1	1	1	1	1	1	1	1	1	1	1	1	1	1	1	16
280	Eelde	L		1	1	1	1	1	1	1	1	1	1	1	1	1	1	1	1	16
370	Eindhoven	L		1	1	1	1	1	1	1	1	1	1	1	1	1	1	1	1	16
377	Ell	L		0	0	0	0	0	0	0	0	0	0	0	1	1	1	1	1	5
321	Europlatform	S	29.1	0	-	-	1	1	1	1	1	1	1	1	1	1	1	1	1	13
206	F16-A	S	75.5	0	0	0	0	0	0	0	0	0	0	0	0	0	0	1	1	2
239	F3	S	59.2	0	0	0	0	0	0	0	0	0	1	1	1	1	1	1	1	7
350	Gilze-Rijen	L		1	1	1	1	1	1	1	1	1	1	1	1	1	1	1	1	16
315	Hansweert	C	16	0	0	0	0	0	0	0	0	0	0	0	1	1	1	1	1	5
278	Heino	L		0	0	0	0	0	0	0	0	1	1	1	1	1	1	1	1	8
356	Herwijnen	L		0	0	0	0	0	1	1	1	1	1	1	1	1	1	1	1	11
330	Hoek van Holland	C	16.6	0	1	1	1	1	1	1	1	1	1	1	1	1	1	1	1	15
311	Hoofdplaat	S	16.5	0	0	0	0	0	0	0	0	0	0	0	1	1	1	1	1	5
279	Hoogeveen	L		0	0	0	0	0	1	1	1	1	1	1	1	1	1	1	1	11
251	Hoorn Terschelling	C		0	0	0	0	0	0	0	0	0	0	1	1	1	1	1	1	6
258	Houtribdijk	S	17.25	0	0	0	0	0	0	0	0	0	0	0	0	0	0	0	1	1
285	Huibertgat	S	18	0	1	1	1	1	1	1	1	1	1	1	1	1	1	1	1	15
283	Hupsel	L		0	0	0	0	0	1	1	1	1	1	1	1	1	1	1	1	11
209	IJmond	S	16.5	0	0	0	0	0	0	0	0	0	0	0	0	1	1	1	1	4
225	IJmuiden	C	18.5	0	1	1	1	1	1	1	1	1	1	1	1	1	1	1	1	15
252	K13	S	73.8	0	-	-	-	1	1	1	1	1	1	1	1	1	1	1	1	12
277	Lauwersoog	C		0	1	1	1	1	1	1	1	1	1	1	1	1	1	1	1	15
270	Leeuwarden	L		0	1	1	1	1	1	1	1	1	1	1	1	1	1	1	1	15
269	Lelystad	C		0	0	0	0	0	1	1	1	1	1	1	1	1	1	1	1	11
320	Lichteiland Goeree	S	38.3	0	-	-	-	1	-	-	1	1	1	1	1	1	1	1	1	10
273	Marknesse	L		0	0	0	0	1	1	1	1	1	1	1	1	1	1	1	1	12
254	Meetpost Noordwijk	S	27.6	0	1	1	1	0	0	1	1	1	1	1	1	1	0	0	0	10
286	Nieuw Beerta	L		0	0	0	0	0	1	1	1	1	1	1	1	1	1	1	1	11
312	Oosterschelde	S	16.5	0	1	1	1	1	1	1	1	1	1	1	1	1	1	1	1	15
343	Rotterdam Geulhaven	L		0	1	1	1	1	1	1	1	1	1	1	1	1	1	1	1	15
902	RWS-FL2	S		0	0	0	0	0	0	0	0	0	0	0	0	1	1	1	0	3
926	RWS-FL26	S		0	0	0	0	0	0	0	0	0	0	0	0	1	1	1	0	3
937	RWS-FL37	S		0	0	0	0	0	0	0	0	0	0	0	0	0	1	1	0	2
929	RWS-SL29	S		0	0	0	0	0	0	0	0	0	0	0	1	1	1	1	0	4
316	Schaar	C	16.5	0	1	1	1	1	1	1	1	1	1	1	1	1	1	1	1	15
240	Schiphol	L		1	1	1	1	1	1	1	1	1	1	1	1	1	1	1	1	16
265	Soesterberg	L		1	1	1	1	1	1	1	1	1	1	1	1	1	1	1	1	16
324	Stavenisse	C	16.5	0	0	0	0	0	0	0	0	0	0	0	1	1	0	1	1	4
267	Stavoren-AWS	C		0	0	0	0	0	0	0	1	1	1	1	1	1	1	1	1	9
229	Texelhors	C		-	1	1	1	1	1	1	1	1	1	1	0	1	1	1	1	14
331	Tholen	C	16.5	0	1	1	1	1	1	1	1	1	1	1	1	1	1	1	1	15
290	Twenthe	L		1	1	1	1	1	1	1	1	1	1	1	1	1	1	1	1	16
210	Valkenburg	C		1	1	1	1	1	1	1	1	1	1	1	1	1	1	1	1	16
313	Vlakte van de Raan	S	16.5	0	0	0	0	0	0	0	0	0	0	0	1	1	1	1	1	5
242	Vlieland	C		0	1	1	1	1	0	0	0	0	0	1	1	1	1	1	1	10
310	Vlissingen	C	27	1	1	1	1	1	1	1	1	1	1	1	1	1	1	1	1	16
375	Volkel	L		1	1	1	1	1	1	1	1	1	1	1	1	1	1	1	1	16
248	Wijdenes	C		0	0	0	0	0	0	0	0	0	0	1	1	1	1	1	1	6
323	Wilhelminadorp	C		0	0	0	0	0	1	1	1	1	1	1	1	1	1	1	1	11
340	Woensdrecht	L		0	0	0	0	0	0	0	0	0	0	1	1	1	1	1	1	6
344	Zestienhoven	L		1	1	1	1	1	1	1	1	1	1	1	1	1	1	1	1	16
	# stations per storm			15	27	28	28	32	35	36	40	41	42	45	52	56	54	56	53	

APPENDIX B. Applicability of the Benschop correction

The Benschop correction transforms the observed wind at the measurement height to the reference 10-m level using a logarithmic wind profile and the local roughness. As already indicated by Benschop (1996), this procedure is strictly speaking only justified in neutral conditions. Especially in stably stratified conditions large deviations from the assumed logarithmic wind profile may occur. On the other hand, the frequency of (near) neutral conditions increases rapidly for increasing wind speed, as demonstrated by Barthelmie (1999) and Sathe *et al.* (2011). Still, Baas et al (2014) show that even in high-wind conditions stability cannot be a priori neglected, especially over sea.

In this APPENDIX we investigate if the application of the Benschop correction is justified for our purpose using selected locations with non-standard measuring heights. We determine if the bias and rms differences between model and observations is sensitive to the way the observations are converted to the 10-m level. Therefore, a correction procedure has been formulated that does include the impact of stability. It is essentially the same method as used by Van Wijk *et al.* (1990).

According to Monin-Obukhov Similarity Theory the dimensional wind and temperature gradients are universal functions of the z/L, where z is the height above the surface and *L* is the Obukhov length. The dimensional gradients for wind and temperature are given by

$$\frac{kz}{u_*}\frac{\partial U}{\partial z} = \phi_m\left(z/L\right) \text{ and} \tag{B1}$$

$$\frac{kz}{\theta_*}\frac{\partial \theta}{\partial z} = \phi_h\left(z/L\right), \tag{B2}$$

respectively. Here *U* and *θ* are the wind speed and the potential temperature, u_* and θ_* are the friction velocity and the temperature scale, *k* is the Von Kármán constant, taken as 0.4. The Obukhov length is defined as

$$L = -\frac{\theta}{kg}\frac{u_*^2}{\theta_*}, \tag{B3}$$

where g is the acceleration of gravity. The gradient functions (B1) and (B2) can be integrated to give the profile functions that give the mean quantities as a function of height:

$$U\left(z\right) = \left(u_*/k\right)\left(\ln\left(z/z_0\right) - \psi_m\left(z/L\right)\right) \tag{B4}$$

$$\theta\left(z\right) = T_{sea} + \left(\theta_*/k\right)\left(\ln\left(z/z_0\right) - \psi_h\left(z/L\right)\right). \tag{B5}$$

Here z_0 is the roughness length, which is taken as 0.0016 m for both momentum and heat. The profile functions ψ are an integrated for of the gradient functions ϕ. Here we use the formulation of Beljaars and Holtslag (1991) for stable conditions and the formulation of

Paulson (1970) for unstable conditions. By rewriting Eq. B4, the wind speed at a specific height, z_2 can be calculated from a given the wind speed at height z_1:

$$U_2 = U_1 \left[\ln\left(\frac{z_2}{z_0}\right) - \psi_m\left(\frac{z_2}{L}\right) \right] \Big/ \left[\ln\left(\frac{z_1}{z_0}\right) - \psi_m\left(\frac{z_1}{L}\right) \right]. \qquad \text{(B6)}$$

Input variables for this procedure are the observation height, z_1, of the observed wind speed, U_1, the air temperature, T_{air} and the sea surface temperature, T_{sea}. To apply Eq. B6 an estimate of L is required. Therefore an iterative procedure is used that calculates u_* and θ_* from a first estimate of L using Eqs. B4 and B5. With these values L can be recomputed according to Eq. B3. Subsequently, this new value of L can be used to calculate improved estimates of u_* and θ_*. After only 4 or 5 iterations the value of L converges to the required accuracy. Ones L is known, the wind speed at 10 m (z_2) can be calculated from the wind speed at measuring height (z_1) using Eq. B6.

The impact of the Benschop correction is tested for the platforms K13 and Europlatform. The observation height of these stations is 73.8 and 29.1 m, respectively. For these stations, Table B.1 gives scores for three different comparison methods:

A Modelled 10 m wind vs Benschop corrected observations,
B Modelled 10 m wind vs observations corrected to 10 m following Eq B6,
C Modelled wind at measurement height vs uncorrected observations.

The results indicate that differences between methods A and B are small. This indicates that using the Benschop correction is justified for calculating overall bias and rms scores. Table B.1 also demonstrates that a comparison at measuring height (method C) cannot be used to assess the quality of the modelled 10 m wind. For all three station a significant low bias is identified, which increases for increasing measurement height. This is because the model's turbulence scheme has the tendency produce too well-mixed profiles in neutral and unstable conditions. This phenomenon is further discussed in Section 4.5.

Table B.1. Model scores for K13 and Europlatform for different comparison methods.

	Bias		Rms difference		Scatter index		Corr. Coeff.	
	K13	Epl	K13	Epl	K13	Epl	K13	Epl
A	0,361	0,142	1,366	1,275	0,108	0,103	0,96	0,96
B	0,321	0,088	1,397	1,303	0,111	0,105	0,957	0,958
C	-0,653	-0,445	1,686	1,473	0,109	0,106	0,963	0,96

For various wind speed classes, Figure B.1 considers the model bias for different bins of T_{air}-T_{sea}. In the left panels the default Benschop correction is applied (method A), in the right panels the correction including stability (method B). Including stability causes a tilting

of the data points with the stable data moving upwards and the unstable data moving downwards. This explains why the overall statistics are insensitive to which method is applied. The model bias does not change significantly with stability. The fact that a small positive trend is visible when stability is included in the conversion of the observations (right panels) indicates that the stability correction in the model is not strong enough. This corresponds to the results presented in Section 4.5.

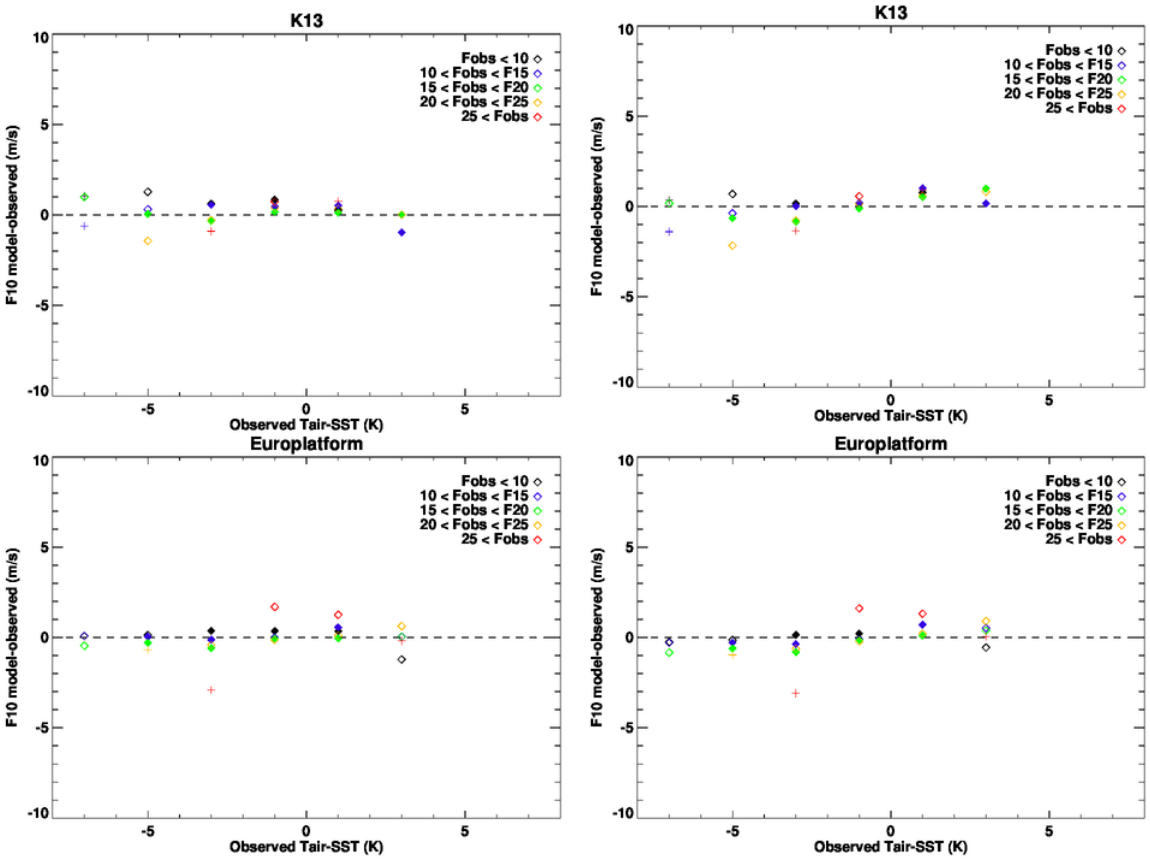

Figure B.1. Model bias for K13 and Europlatform as a function of the air-sea temperature difference. In the left panels the default Benschop correction is applied, in the right panels the impact of stability is included in the transformation from observation height to the 10m level. Color indicate different wind speed classes. The plus symbols represent 1-5 data point, the open diamonds 5-50 datapoints, and the closed diamonds more than 50 data points.

Given the above results, we conclude that for our purposes application of the Benschop correction is justified. Associated errors are smaller or comparable in size to the errors in the observations.

APPENDIX C. Lake IJssel and Wadden Sea scatter plots

Figure C.1 show scatter plots for a number of observation location in Lake IJssel and the Wadden Sea.

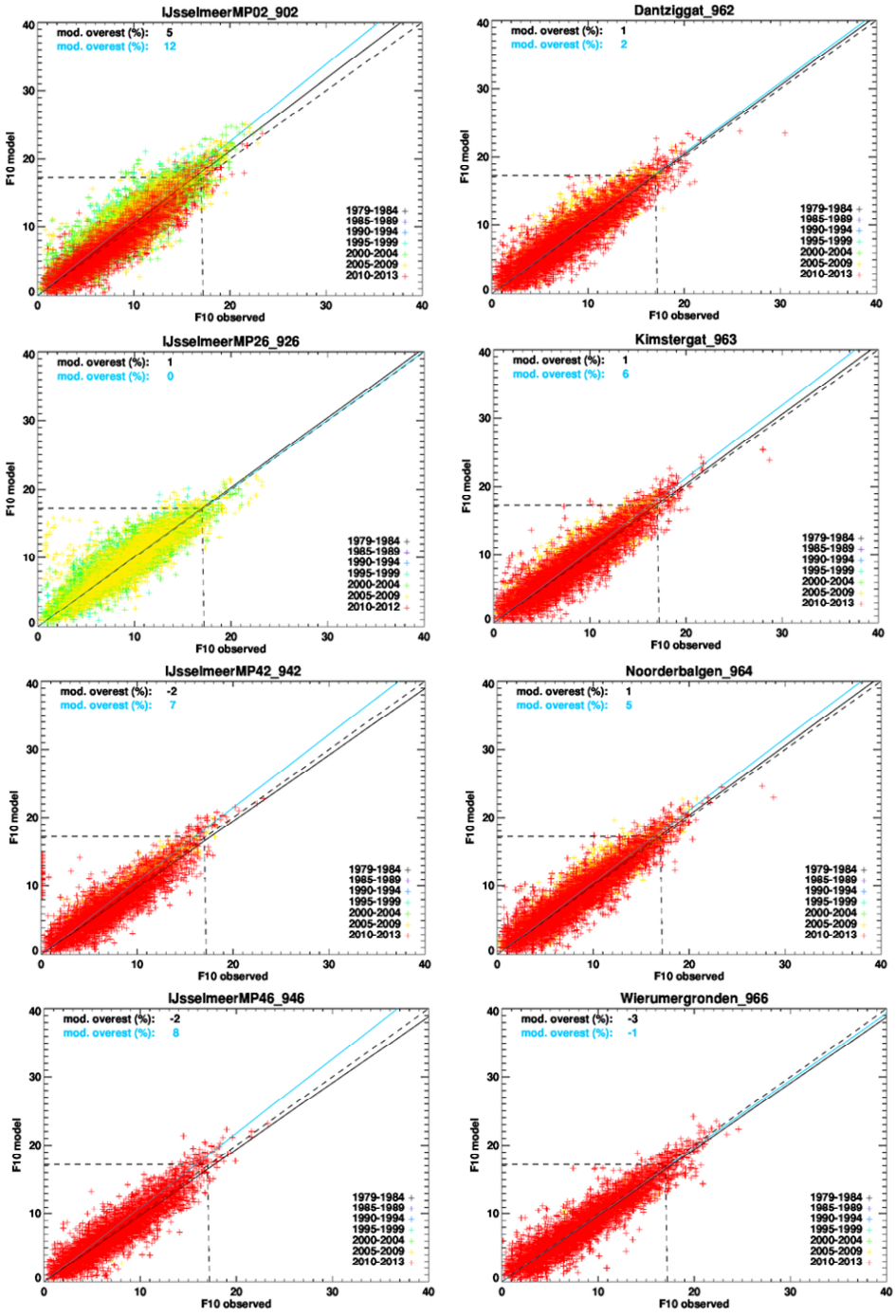

Figure C.1. Modelled versus observed wind speed for station in Lake IJssel (left panels) and the Wadden Sea (right). Station locations can be found in Figure 4.2. For each location the overestimation of the model is given in %. The black number refers to all data, the blue number to those cases in which the 8 Bft threshold (indicated by the dashed lines) in either the observations or the model is exceeded.

APPENDIX D. Scatter plots of the 17 maximum surges

Figure D.1 shows the modelled maximum skew surge against the observed skew surge. The results of WAQUA (8km) driven by HARMONIE are indicated in blue, and the results for ERA-Interim/ERA40 in red. See also Table 5.1 for the corresponding statistical quantities.

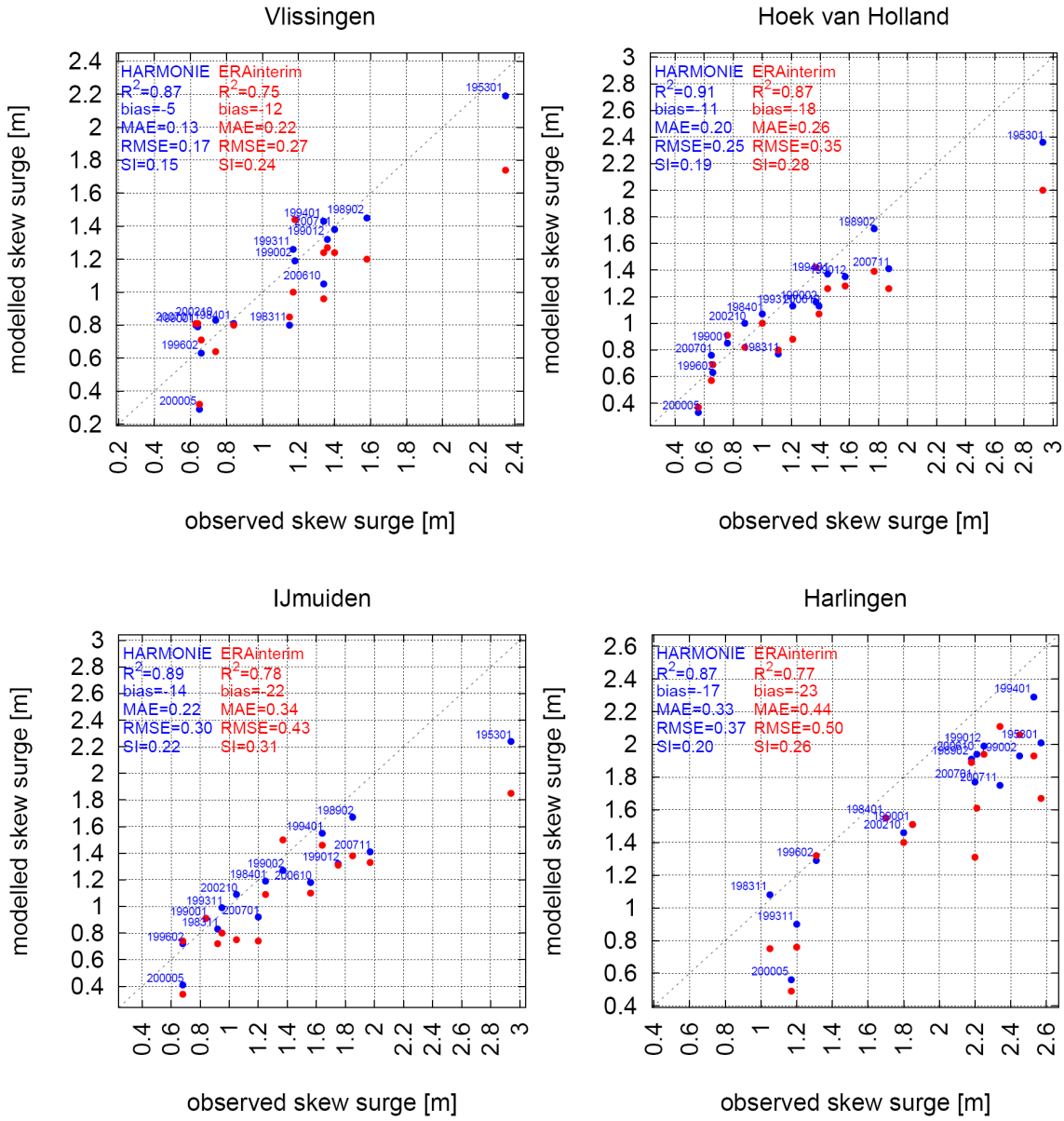

Figure D.1. Scatter plot of the maximum skew surge at several coastal stations for the 17 events as modeled by HARMONIE (blue) and ERA (red).

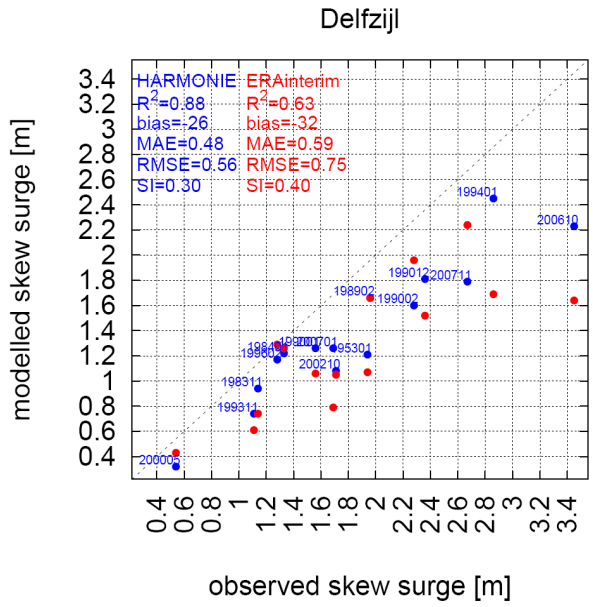

Figure D.1. (Continued)

A complete list of all KNMI-publications (1854 – present) can be found on our website

www.knmi.nl/knmi-library/knmipub_en.html

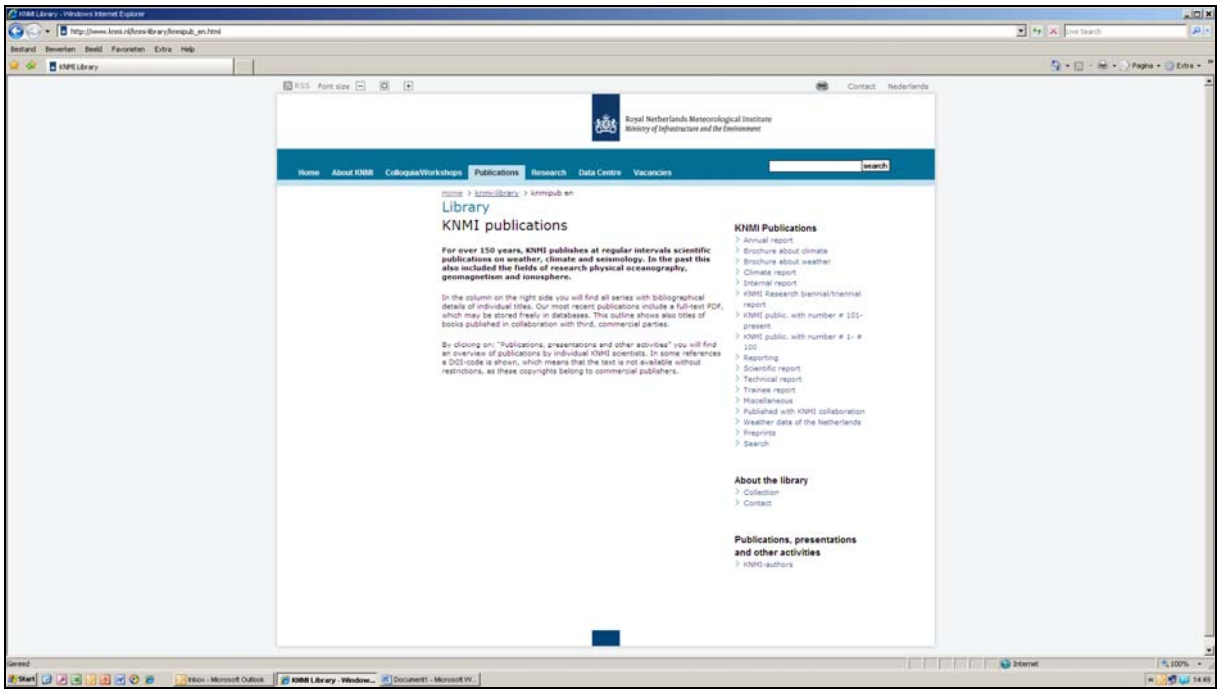

The most recent reports are available as a PDF on this site.